Aerodynamic Study of Tall Buildings Under Wind Load

A REPORT SUBMITTED

IN PARTIAL FULFILLMENT OF THE REQUIREMENTS

FOR THE AWARD OF THE DEGREE OF

MASTER OF TECHNOLOGY

IN

CIVIL ENGINEERING

Submitted By

Kunwar Navodit Srivastava

2K19/STE/501

UNDER THE SUPERVISION OF

DR. RITU RAJ

CIVIL ENGINEERING DEPARTMENT

DELHI TECHNOLOGICAL UNIVERSITY

(Formerly Delhi College of Engineering)

Bawana Road, Delhi-110042

CANDIDATE DECLARATION

I, "**Kunwar Navodit Srivastava"** student of M. Tech Structural Engineering, DTU hereby certify that the project dissertation which is being presented in the thesis entitled **"Aerodynamic Study of Tall Buildings under Wind Load"** in partial fulfilment of the requirement for the award of the Master in Technology and is submitted to the Department of Civil Engineering, Delhi Technological University, Delhi, is original and not copied from any source without proper citation. This work has never before been used to give a degree, diploma, associateship, fellowship, or other equivalent title or recognition.

Place**:** Delhi

Date: 27/05/2021

Kunwar Navodit Srivastava

(2K19/STE/501)

navodit

CIVIL ENGINEERING DEPARTMENT

DELHI TECHNOLOGICAL UNIVERSITY

(Formerly Delhi College of Engineering)

Bawana Road Delhi-110042

CERTIFICATE

I hereby certify that the Project Dissertation titled "Aerodynamic Study of Tall Buildings Under Wind Load" which is submitted by Kunwar Navodit Srivastava (2K19/STE/501) Civil Engineering Department, Delhi Technological University, Delhi in partial fulfilment of the requirement for the award of the degree of Master of Technology, is a record of the project work carried out by the student under my supervision. To the best of my knowledge, this work has never before been submitted to give a degree, diploma, associateship, fellowship, or other equivalent title or recognition.

Place: Delhi

Dr. RITU RAJ

Supervisor

Assistant Professor

Department of Civil Engineering

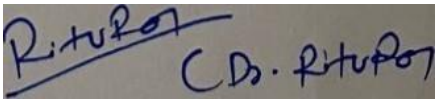

ABSTRACT

In Design of high-rise structures, Wind is considered as one of the important horizontal forces that have significant impact on the response of building. Due to rise in population, the demand for tall buildings is increasing day by day. Wind Load on such structures are calculated using pressure coefficients and force coefficients which are available in various international codes and standards. However, these international codes and standards give information about regular shape buildings such as square, rectangle, circular or octagonal. With the technological advancement, composite plan shape buildings such as square and circular, circular and hexagonal and square and octagonal etc. have been considered by many architects keeping in view of aesthetics of Building. The wind flow around a tall building with composite plan shapes having different height ratio variation differs from what we get in regular shape analysis. Since, data is not available regarding such buildings, the need to carry wind tunnel testing or CFD become important for analyzing wind effect on such buildings. CFD (Computation Fluid Dynamics) for determining wind responses is becoming immensely popular. It has expanded as a tool to replace wind tunnel testing as it is quicker, less expansive and give more information and control to designers.

In the present research study, two building plan shape triangle and circle has been considered with different height ratio. The building selected to carry out the numerical analysis are uniform and composite plan tall buildings. The length of equilateral triangle is taken as 40m and height being 200m. For composite plan shape building only height ratio is changed keeping the same dimensions. The prototype building is considered to be located in terrain category 2 as per IS-875 Part 3. Assumption is made that the variation for wind speed with height follows the power law with power law coefficient taken as 0.147.

CFD analysis is carried out in ANSYS CFX taking 1:200 scaled down model of tall buildings. In total, 5 models have been considered and pressure is evaluated taking various points on the building. Each model is analyzed for different angle of wind incidence namely 0, 60, 120 and 180 degrees. The result obtained for the uniform shape cross section building has been compared with the wind tunnel testing results available in various literatures.

ACKNOWLEDGEMENT

I would like to express my gratitude to my mentor, Dr. RITURAJ who gave me the opportunity to carry out this wonderful project on the topic "Aerodynamic Study of Tall Buildings Under Wind Load" which helped me in boosting my technical knowledge and experimental skills. His directions and support were the basic essence of motivation for me.

I feel of paucity of words to express our thanks to the honourable Head of Department of Civil Engineering, Dr. V.K Minocha, for allowing me to utilize the department facilities and have been a constant source of motivation during the course of project.

I express my deepest sense of gratitude towards the Professors of Civil Engineering Department who helped me in formulating the problem statement and clarifying our doubts regarding the learning about the tall buildings.

At last, I would like to thank to PhD scholar Rahul Kumar Meena and my colleagues who helped me by actively participating in discussions and giving their valuable feedbacks. Their presence and support were invaluable. Finally, we would like to thank our parents for their undying support, motivation and providing me the golden opportunity to study in this prestigious institution.

Signature: navodit

Name: Kunwar Navodit Srivastava

Roll Number: 2K19/STE/501

Date: 27/05/2021

Table of Contents

CHAPTER 1 INTRODUCTION……1

1.1 General 1

1.2 Types of Wind 2

1.3 CFD (Computational fluid dynamics) 2

1.4 Factors Affecting Wind Loads 3

1.5 Objectives and Scope 3

1.6 Organization of the Thesis 3

CHAPTER 2 LITERATURE REVIEW……....4

2.1 GENERAL 4

2.2 Codal Provision 5

2.3 Research papers and their summaries as a source of information 6

CHAPTER 3 RESEARCH METHDOLOGY……..……11

CHAPTER 4 NUMERICAL SIMULATION USING ANSYS……...12

4.1 Model Scale 12

4.2 CFD Validation 14

4.3 Governing Equations 20

CHAPTER 5 RESULTS AND DiSCUSSIONS……21

5.1 Pressure Distribution 21

5.2 Velocity Distribution 53

5.3 Vertical Centerline Pressure Coefficients 59

5.4 Pressure Coefficient……... 84

CHAPTER 6 CONCLUSION……77

7 REFERENCES……78

List Of Figures

Figure 4-1 Different faces of the model with direction of wind 14
Figure 4-2 Velocity Profile 15
Figure 4-3 Turbulence Intensity 15
Figure 4-4 Domain 16
Figure 4-5 Domain (virtual wind tunnel) 16
Figure 4-6 Model 1 75% Triangle & 25% Circle 17
Figure 4-7 Model 2 50% Triangle 50% Circle 17
Figure 4-8 Model 3 25% Triangle & 75% Circle 18
Figure 4-9 Model 100% Triangle 18
Figure 4-10 Domain Meshing 19
Figure 5-1 Contour Plots for different faces at 0- degree of incidence for Model 1 24
Figure 5-2 Contour Plots for different faces at 60- degree of incidence for Model 1 26
Figure 5-3 Contour Plots for different faces at 120- degree of incidence for Model 1 28
Figure 5-4Contour Plots for different faces at 180- degree of incidence for Model 1 30
Figure 5-5Contour Plots for different faces at 0- degree of incidence for Model 2 33
Figure 5-6Contour Plots for different faces at 60- degree of incidence for Model 2 35
Figure 5-7Contour Plots for different faces at 120- degree of incidence for Model 2 37
Figure 5-8Contour Plots for different faces at 180- degree of incidence for Model 2 39
Figure 5-9Contour Plots for different faces at 0- degree of incidence for Model 3 41
Figure 5-10Contour Plots for different faces at 60- degree of incidence for Model 3 42
Figure 5-11Contour Plots for different faces at 120- degree of incidence for Model 3 44
Figure 5-12Contour Plots for different faces at 180- degree of incidence for Model 3 46
Figure 5-13Contour Plots for different faces at 0- degree of incidence for Model 4 48
Figure 5-14Contour Plots for different faces at 60- degree of incidence for Model 4 50
Figure 5-15Contour Plots for different faces at 120- degree of incidence for Model 4 51
Figure 5-16Contour Plots for different faces at 180- degree of incidence for Model 4 52
Figure 5-17Velocity Streamline Plots for different faces at different degree of incidence for Model 1 54
Figure 5-18Velocity Streamline Plots for different faces at different degree of incidence for Model 2 55

Figure 5-19Velocity Streamline Plots for different faces at different degree of incidence for Model 3 57
Figure 5-20Velocity Streamline Plots for different faces at different degree of incidence for Model 4 58
Figure 5-21Pressure Variation along Centerline for face A for all degrees AOA of model 1 59
Figure 5-22Pressure Variation along Centerline for face B for all degrees AOA of model 1.60
Figure 5-23Pressure Variation along Centerline for face C for all degrees AOA of model....60
Figure 5-24Pressure Variation along Centerline for face A for all degrees AOA of model 1 61
Figure 5-25Pressure Variation along Centerline for face B for all degrees AOA of model 1.62
Figure 5-26Pressure Variation along Centerline for face C for all degrees AOA of model 1.62
Figure 5-27Pressure Variation along Centerline for face D for all degrees AOA of model 1 63
Figure 5-28Pressure Variation along Centerline for face A for all degrees AOA of model 2 64
Figure 5-29Pressure Variation along Centerline for face B for all degrees AOA of model 2.64
Figure 5-30Pressure Variation along Centerline for face C for all degrees AOA of model 2.65
Figure 5-31Pressure Variation along Centerline for face A for all degrees AOA of model 2 66
Figure 5-32Pressure Variation along Centerline for face B for all degrees AOA of model 2.67
Figure 5-33Pressure Variation along Centerline for face C for all degrees AOA of model 2.67
Figure 5-34Pressure Variation along Centerline for face D for all degrees AOA of model 2 68
Figure 5-35Pressure Variation along Centerline for face A for all degrees AOA of model 3 69
Figure 5-36Pressure Variation along Centerline for face B for all degrees AOA of model....69
Figure 5-37Pressure Variation along Centerline for face C for all degrees AOA of model 3.70
Figure 5-38Pressure Variation along Centerline for face A for all degrees AOA of model 3 71
Figure 5-39Pressure Variation along Centerline for face B for all degrees AOA of model 3.71
Figure 5-40Pressure Variation along Centerline for face B for all degrees AOA of model 3.72
Figure 5-41Pressure Variation along Centerline for face B for all degrees AOA of model 3.72
Figure 5-42Pressure Variation along Centerline for face A for all degrees AOA of model 4 73
Figure 5-43Pressure Variation along Centerline for face B for all degrees AOA of model 4.74
Figure 5-44Pressure Variation along Centerline for face C for all degrees AOA of model 4.74

List Of Tables

Table 4-1 Prototype and Model Dimension.....12
Table 4-2 Value of Cp for different codes.....14
Table 5-1 Cp for different faces for different triangular models at different angle of incidence 75
Table 5-2 Cp for different faces for different circular models at different angle of incidence ……. 85

CHAPTER 1

INTRODUCTION

1.1 General

Tall Buildings have always fascinated humans having unique appeal and pride associated with them. Due to increasing population and scarcity of land the demand for Tall Buildings have increased day by day. With the development of new better construction techniques, better materials and structural systems, these buildings have proven to be the safe and economical structural solution to problem of spacious designs.

In design of tall structures, wind loading is one of the prime important lateral loads that needs to be considered while designing. In general, occupant comfort needs to be considered along with structural safety. Wind is a time varying force having two components, a mean and a fluctuating component. Wind is a complicated phenomenon having eddies of varied size add rotating properties. Due to these eddies wind is turbulent and gusty in nature. Wind Loading initially was viewed as estimating the dynamic pressure of wind at the structure and then just multiply it by some Shape factor and area of a structure to obtain the wind force. However later it was realized that wind dynamic in nature and dynamic responses such as galloping, flutter, vortex excitement, ovalling etc. need to be examined too. The shape of buildings is a well-known subject in aerodynamics optimization that has a significant impact on the behavior of high structures under wind loads. Wind response can be reduced by optimizing the geometry of supertall structures for aerodynamics during the design stage.

Wind is a phenomenon in which the motion of individual particles is so unpredictable that statistical distributions of velocity rather than simple averages must be considered. Although each has its own local impact, the total wind force is equal to the sum of windward pressure and leeward suction. In order to get complete wind analysis, one need to determine the wind climate, influence of terrain and topography, aerodynamic shape of a structure and dynamic effects. Various international codes and standards such as ASCE 7-10: Minimum design loads for buildings and other structures, IS-875 Part 3 : Code of practice for design loads (other than earthquake) for buildings and structures), BS 6399-2:1997 loading for buildings code of practice for Wind loads British standards, EN 1991-1-4: Eurocode : Actions on Structure Part 1-4: General Actions-Wind Actions,2010 estimates the pressure coefficients and force

coefficients which are used for computing wind loads on buildings subjected to wind loads. Very Limited Information for uniform plan shaped buildings with different aspect ratio are available in these standards. The Indian code suggests pressure coefficients for different plan shape like square, rectangle etc. at 0-degree and 90-degree angle of wind incidence. The wind pressure of tall building not only influenced by building geometry and wind incidence but also depend upon height ratio between the plan shapes However, these codes do not provide information regarding wind load acting on composite plan shaped buildings. Also, available information does not include wind pressure coefficient (Cp) or wind force coefficient (Cf) for the buildings where cross-sectional shape change with height. For such buildings wind tunnel testing have been proven to be the efficient and practical approach to study the response of buildings and structures under wind load. Recent Studies have also shown the use of CFD to carry out investigation for wind load pressure distribution and computation of pressure and force coefficients.

1.2 Types of Wind

In India in general wind is considered as the mix of following:

a). Typical cyclone

b). Monsoon

c). Local Thunder storms

d). Extra tropical cyclone and pressure system

1.3 CFD (Computational fluid dynamics)

Computational fluid dynamics involves numerical approach and algorithms to solve and analyze problems that involves fluid flow. CFD analysis is widely employed in aerodynamics and hydrodynamics where pressure and velocities are the parameters. CFD analysis can save a lot of time and are cheaper as compared to conventional testing.

All of the relevant parameters may be analyzed and monitored at the same time in CFD, with great time and spatial resolution. Because CFD analysis approximates a genuine physical solution, it cannot totally replace actual testing.

The steps of CFD analysis include the following:

1. PRE-PROCESSING

2. SOLVING

3. POST PROCESSING

Compared to wind tunnel testing, CFD has the following advantages:

1. Comprehensive domain analysis
2. Simple alternative analysis
3. Improved visualisation of outcomes
4. Cost-effective

1.4 Factors Affecting Wind Loads

Wind Load are strongly influenced by the geometry of the building like aspect ratio, openings, projections, roof pitch slope, angle of wind incidence, wind flow characteristics etc. Aspect ratio for the building

1.5 Objectives and Scope

- The present study focuses on studying buildings having uniform varying cross section along the height.
- Different angle of attack for wind have been considered in this study.
- To investigate the mean wind pressure coefficient on different faces of building using CFD technique.
- To plot pressure contours for different faces of building considering different angle of attack.

1.6 Organization of the Thesis

The thesis is presented in six chapters. Chapter 1 discusses the introduction and general overview for wind loading. Chapter 2 give a brief discussion on literature carried out in this field by various researchers. Codal provisions and standards have also been discussed in this chapter. Chapter 3 discusses research methodology. Chapter 4 deals with the details of prototype and modelling. Chapter 5 deals with the results of CFD study on building models with varying plan shapes. Chapter 6 summarizes the conclusion of the study.

CHAPTER 2

LITERATURE REVIEW

2.1 GENERAL

Several scholars have derived a plethora of useful data by assuming that wind pressure acts in a static fashion since the 1960s. The results of wind tunnel testing at a constant steady velocity were estimated using this method.

Tall structure design has a long and illustrious history. Architects and structural engineers have worked together for generations to design taller structures. Today's skyscrapers are the result of continuous research, invention, and discovery. In the twentieth and twenty-first centuries, urbanization fueled the development of tall buildings, which grew in height as demand grew. The world's tallest structure prior to the eighteenth century was a church. Chicago pioneered a new style of structure that relied on iron or steel to support the structure's weight in the nineteenth century. In 1885, the 42-meter-high Home Insurance Building in Chicago became the world's first skyscraper. Following that, a growing number of tall buildings were built, including the Empire State Building (102 floors), which was completed in 1931.Following that, with the rapid growth of construction technology and the development of computer modelling techniques, an increasing number of tall buildings were built around the world.

As the building becomes taller, cross sections should be carefully chosen, keeping in mind the demand for serviceability and functionality, as new lateral forces are created by unintentional deflections. In most cases, wind load, rather than seismic loading, is the dominant load in tall structure lateral stability system design. Tall buildings have a longer natural period, resulting in a smaller earthquake response than low-rise buildings. This may or may not be the case, depending on the region.

2.2 Codal Provision

1. **British Standard (IIS EN 199h14, 2005)**

   This code of practise establishes guidelines for determining natural wind activities in the structural design of buildings and civil engineering projects for each load scenario. This rule of practice applies to constructions and buildings up to a certain height. Bridges having a span of no more than 200 meters, as well as structures over 200 meters in height. This code also aims to predict normal wind behaviors on land-based structures. Their constituents There is no information on wind for irregular cross-sectional forms. Dispersion of pressure This criterion also applies to information about different skews wind directions.

2. **American Standard (ASCE4, 2002)**

   ASCE-7 is a comprehensive guide on wind loads on low-rise buildings with diverse roof types. Low-rise buildings with varying aspect ratios are also covered by this standard. However, data on wind loads on high-rise structures of varied cross-sectional forms is few. No information is available in the event of skew wind.

3. **Australia and New Zealand Standard (AS/NZS-1 170-2, 2011)**

   Structures that match the following characteristics are covered by this code of practice: I roof span of less than 100 meters and a height of less than or equal to 200 meters. This code includes wind loads on structures other than offshore constructions, such as bridges and transmission towers. There is no information in this code of practice about cross-sectional shapes other than square and rectangular. There is very little information about the pressure distribution when a building is impacted by a skew wind angle.

4. **Indian Standard (875, part-3, 2015)**

   Wind loads must be addressed while designing buildings, structures, and components, according to IS: 875 (Part-3). This code generates a single wind map with the greatest wind speed in metres per second (peak gust speed averaged over a brief time interval of roughly 3 seconds duration).The wind speeds were determined for a 50-year return period using the most recent wind data. The fundamental wind speed was adjusted using modification parameters to account for geography, local topography, structure size, and

other aspects. For a variety of clad and unclad buildings, as well as specific structural elements, force and pressure coefficients were provided. Force coefficients (drag coefficients) were determined for frames, lattice towers, walls, and hoardings.

2.3 Research papers and their summaries as a source of information

A. Biswarup Bhattacharyya and Sujit Kumar Daluis (Experimental and Numerical Study of Wind-Pressure Distribution on Irregular-Plan-Shaped Building)

In this work, they presented a detailed analysis of an E-plan-shaped building that is asymmetrical across both plan axes when exposed to wind stimulation. The wind angle of incidence ranged from 0 to 330 degrees, with a 30-degree gap in between. This study is done numerically in a wind tunnel using the computational fluid dynamics (CFD) technique. The numerical study employs the k-epsilon and shear stress transport (SST) k-models. They also investigated a symmetrical E-plan shaped building with the same cross section area, looking for the most favorable and negative effects. As a result of a minor aerodynamic change, mean pressure coefficients have changed. At skew wind angles, when the wind flow is not perpendicular to the building axis, the greatest positive mean Cp was recorded on some building faces; however, the maximum negative mean Cp was observed at a significantly lesser number of skew wind angles. This is due to asymmetry in the plan shape around both axes.

B. Najah Assainar and Sujit Kumar Dalui (Aerodynamic analysis of pentagon-shaped tall buildings)

This research study uses computational fluid dynamics (CFD) simulation with the software package ANSYS CFX to analyses the efficiency of aerodynamic modifications made to a pentagonal-plan shaped model. Setback and tapering

aerodynamic shapes, as well as corner alterations like chamfered, recessed, and rounded, are investigated.

The chamfered model, according to the data, is the most successful corner change in terms of pressure and force coefficients, as well as dynamic performance. The tapered model was also found to be superior than the other aerodynamic forms at reducing pressure and force coefficients during static analysis. With the exception of peak frequency, which was better predicted by the setback model, the dynamic analysis indicated a similar trend.

C. R. Sheng and L. Perret (Wind tunnel investigation of wind impacts on a high-rise building at a scale of 1:300)

The goal of this study is to evaluate the unstable properties wind tunnel tests on a high-rise structure with a well-defined atmospheric boundary layer at a 1:300 scale of global and local wind loads, as well as their connections with the atmospheric boundary layer. Wind data such as mean velocity profile, turbulence intensity, and power spectrum of the fluctuation are used to investigate the power spectrum of the fluctuation for global and local wind loads. The findings reveal that upstream flow or shear layers that occur at the building's upstream corners, or both, influence wall-pressure pressures on the tower, depending on the location.

D. Suresh K Nagar and Ritu Raj (Experimental study of wind-induced pressures on tall buildings of various shapes)

Wind tunnel testing is used to evaluate the mean wind pressure coefficients of square and H-plan shaped tall buildings in this paper. The experiment was carried out for a variety of wind direction angles ranging from 0 to 30, 60, and 90 degrees, as well as for a variety of equivalent building interference situations. The interfering factor was computed to study the interference effects. Full obstruction, half blockage, and no blockage were all considered as interference circumstances.

Non-dimensional interference factors (IF) are used to demonstrate interference effects and reflect the aerodynamic stresses on a plan-shaped big building with interference from surrounding plan-shaped buildings. They hypothesized that when the wind

incidence angle increases up to 60 degrees, the value of the mean wind pressure coefficient falls. After a further increase in wind incidence, suction begins.

E. M. Pavani and G. Nagesh Kumar (Shear Wall Analysis and Design Optimization in Case of High-Rise Buildings Using Etabs)

They built a shear wall and optimized it using the software ETabs for this study. Shear walls are placed in such a way that they can withstand lateral forces in the event of a collapse. According to Indian standards, zone III is present throughout the building. The following are a list of in this project, we used optimization techniques. The shear wall's size is consistent. The results are then analyzed, and the failed shear wall is identified. Dimensions are increased to resist the entire structure; in this way, the optimization was repeated a number of times until the entire structure became stable to resist the forces; and finally, the optimization was completed until the entire structure was stable enough to withstand the forces.

F. Kwok and Bailey's (Effects of Aerodynamic Modifications of Building Shapes on Wind Induced Response of Tall Buildings)

Kwok and Bailey (1987), Kwok et al (1988), and Kwok (1988) conducted wind tunnel Wind induced vibrations in tall structures are investigated using tests that include aerodynamic devices, building edge layout, and through building opening. The dynamic along wind and crosswind responses of the rectangular cross-section CAARC Standard Tall Building were considerably reduced when horizontal slots, slotted corners, and chamfered corners were used.

G. (A Critical Review of Wind Load on High-Rise Buildings with Different Configurations) A.K. Roy is the author of this piece.

The wind effects on structural frames with different plan forms and outcomes were described in this work. The wind load is calculated using basic wind speed, as well as other factors such as topography, terrain, and building usage, as well as the risk factor for that specific region, with respect to permissible drifts of different buildings.

They conclude that the Wind Pressure Coefficient is highest in square plan shapes and lowest in circular plan shapes of tall buildings, and that the octagonal plan form of a tall building with a sharp windward edge is more successful than the hexagonal plan shape of a tall building with a sharp windward edge in reducing wind pressure coefficient. For maximum mean overturning moment coefficients, tapered models, such as 4-Tapered and Setback Models, provide superior aerodynamic behaviours in the along wind direction, whereas corner modification models provide better aerodynamic behaviours in the across wind direction.

H. A. Mukherjee and A. K. Bairagi (Wind pressure and velocity pattern around 'N' plan form tall structure)

The wind pressure and velocity pattern around 'N' shaped tall structures were researched by Mukherjee et al. (2017). The focus of the paper is on applying k-methods to determine the wind pressure coefficient and wind velocity analyses of the building.

I. J. A. Amin and A. K. Ahuja (Experimental Study of Wind Pressures on Irregular Plan Shape Buildings, 2008).

This study presents the results of wind tunnel testing on a 1:5000 scaled-down model with the same plan area and height but different plan forms ("L" and "T"). The mean, maximum, minimum, and r.m.s. values of pressure coefficients are determined when wind pressure swings at pressure locations on all surfaces.

They discovered that there is a considerable difference in pressure along the height and breadth of different faces of the models, and that changing the plan dimensions has a major impact on the wind pressure distributions on different faces of the models.

J. Patrick Kastner and Timur Dogan (Streamlining meshing approaches for annual urban CFD simulations, 2020)

They calculated the time savings methods that might be used, as well as particular mesh parameters, in order to lead the recommended strategy. In this article, they created a circular mesh for urban wind simulations. They compared the box-shaped computational domain to the cylindrical simulation domain and discovered that the

box-shaped approach is advantageous if no yearly wind analysis is required. A simulation domain that is cylindrical is more likely to outperform one that is box-shaped.

K. Pal Supriya and Ritu Raj (Comparative research of wind induced mutual interference effects on square and fish plan form tall buildings, 2021)

On twin Square and Fish-plan form building models with equal volume, wind-induced mutual interference effects were explored. They determined the most effective condition by examining the maximum efficiency of both shapes in terms of induced wind pressure and base shear.

L. Jörg Franke and Charles K. (Recommendations on the use of CFD in wind engineering)

With a focus on statistically steady wind simulation, this paper analyses the outcomes of published simulations and gives recommendations for the use of CFD in wind engineering jobs. This work summarized the data for mean velocities and turbulence in the created environment from statistically steady RANS simulations available in the literature to give recommendations on how to use CWE properly for that goal.

M. M. Mallick, A. Mohanta, A. Kumar, and V. Raj (Modeling of Wind Pressure Coefficients on C-Shaped Building Models)

Monalisa Mallick et al. (2018) used ANSYS Fluent to simulate the structure geometry, orientation, aspect ratios, and wind angle of attack all had a substantial impact on the pressure on the building, according to the wind pressure coefficient on C-shaped building models.

CHAPTER 3

Research Methodology

DESIGN WIND PRESSURE

As per IS-875 Part 3,

[Design Velocity] = V_b*K_1*K_2*K_3*K_4

Where, V_b=Basic Wind velocity

K_1= Probability Factor/Risk Coefficient

K_2=Terrain and Height Factor

K_3=Topography Factor

K_4=Importance factor of the cyclonic region

Design wind pressure is given as:

$$\mathbf{P_d=0.6\ [V_z]\text{^}2}$$

The mean pressure coefficient '$C_{p\ mean}$' is calculated from the equation given below:

$$\mathbf{C_{p\ mean}} = \frac{(\mathbf{p}-\mathbf{p_o})}{\frac{1}{2}\rho \mathbf{U_H}^2}$$

where p is the pressure at point on surface,

p_o is the reference height static pressure,

ρ is the air density

U_H is mean wind velocity at the building reference height.

CHAPTER 4

Numerical simulation using ANSYS

4.1 Model Scale

In this study, two different composite building plan shapes, triangle and circle are considered with different height ratios. The sides of triangle and total height of buildings are 40m and 100m respectively. The following dimensions are considered for all models with only height ratio changed. The prototype building has been considered to be situated at in Terrain Category-2. The free mean wind velocity is taken as 10m/s and each model is studied at various wind incidence angle of 0°, 60°, 120°, 180°. The wind profile boundary layer is governed by power law equation with power law index coefficient as 0.147.

Table 4-1 Prototype and Model Dimension

Parameter	Prototype Dimension(m)	ANSYS Model Dimension(mm)	Scale of Model
Length	40	200	1:200
Height	100	500	

The following geometrical parameters are considered in this study,

1. Wind Incidence Angle (0°, 60°,120°, 180°)
2. Cross section combination of Triangle and Circle along height.
3. Height of Building (75% Triangle & 25% Circle, 50% Triangle & 50% Circle, 25% Triangle & 75% Circle and 100% triangle)

This study also has been validated with wind pressure of an isolated square the wind effects of typical plan shape buildings were compared to those of plan shape tall buildings using CFD simulation. Indian code IS: 875 (Part- 3), 2015.

MEAN WIND PROFILE WITH HEIGHT

Due to the roughness of earth surface, there acts a drag force on wind flow near the ground. This effect gradually decreases as the height increases and at a certain gradient level (around 400m), this drag-force becomes negligible. The vertical profile of wind speed is determined by the degree of surface roughness and drag induced by surrounding projections that impede wind flow. The drag effects decrease at a certain height, and the related velocity is called gradient velocity. The height up-to which wind speed is influenced by topography is called atmospheric boundary layer.

POWER LAW

As per Power Law, the wind speed profile within the atmospheric boundary layer is given by:

$$\frac{V}{Vo} = \left[\left(\frac{Z}{Zo}\right) \wedge \left(\frac{1}{alpha}\right)\right]$$

Where, V = velocity of wind at height Z

Vo = gradient velocity of wind at reference height Zo

Z = height above ground

Zo = Nominal height of Boundary layer (also called gradient height)

alpha = power law coefficient.

LOGARITHMIC LAW

$$u = \frac{1}{k} u_* \ln \frac{Z}{Z_0}$$

where u is the wind speed at height Z above ground,

k is the von Karman constant equal to 0.4 (approximately)

and Zo is the ground roughness.

u_* is shear velocity which is defined as:

$$u_* = \sqrt{\frac{\tau_0}{\rho}}$$

where τ_0 is the stress of wind at ground level and ρ is the air density.

4.2 CFD Validation

The validity of the ANSYS CFX software is validated before beginning the numerical study of the building. A square plan shaped building with dimensions of 150 mm x 150 mm and a height of 500 mm (i.e., aspect ratio 1:5) is analysed in the domain under uniform wind flow using the k-model with ANSYS CFX.

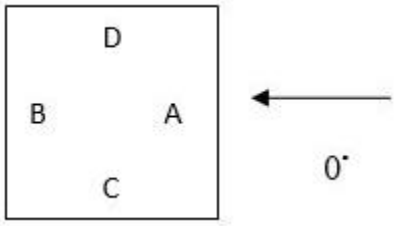

Figure 4-1 Different faces of the model with direction of wind

At the inlet, a uniform wind flow of 10 m/s is given. As previously stated, the domain is built according to Revuz et al (2010). The ANSYS CFX programme determines the face average values of coefficient of pressure, which are then compared to wind action codes from various regions.

Table 4-2 Value of Cp for different codes

Wind loading code	**Face- A**	**Face-B**	**Face-C**	**Face-D**
By ANSYS CFX	0.9	-0.46	-0.67	-0.68
ASCE 7-10	0.8	-0.5	-0.7	-0.7
AS/NZS-1170.2(2002)	0.8	-0.5	-0.65	-0.65
IS: 875 (part3) (2015)	0.8	-0.25	-0.8	-0.8

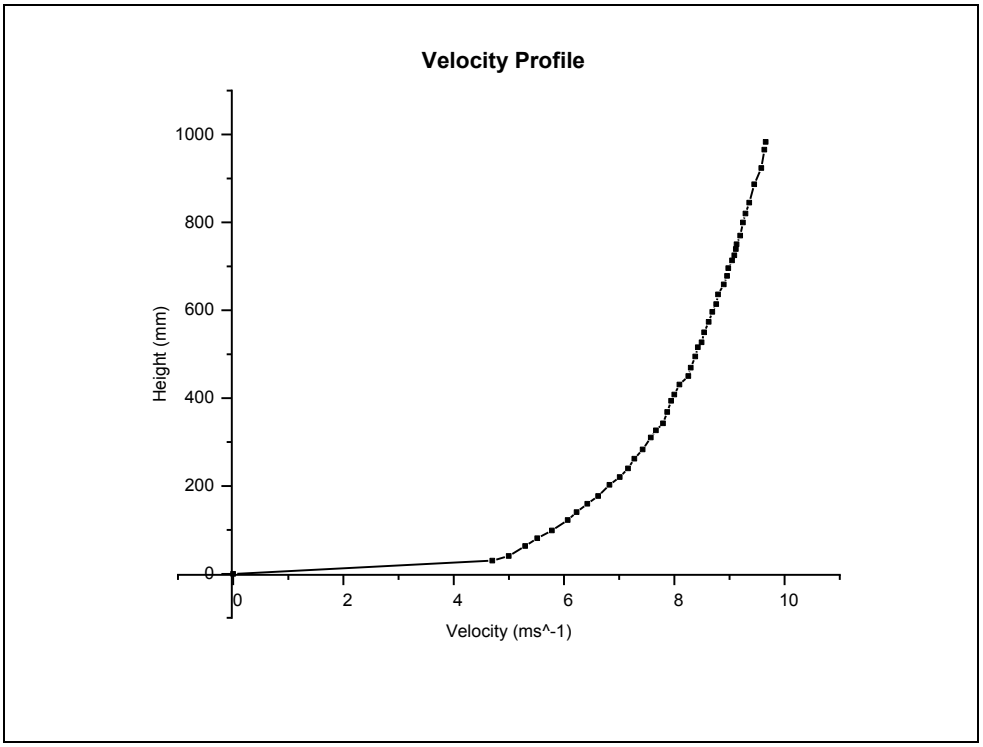

Figure 4-2 Velocity Profile

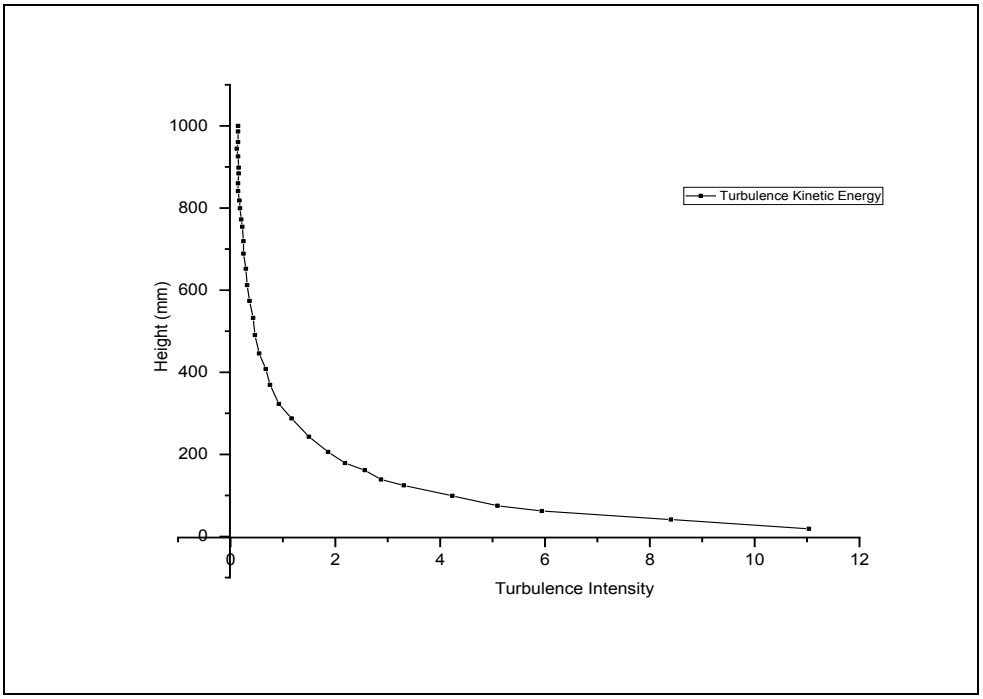

Figure 4-3 Turbulence Intensity

Domain

In case of high-rise buildings, domain size is mainly governed by height of the building such that a large number of cell count could be formed and out of them, many being used up in the region far away from wake region.

Domain size selected in modeling is defined as per frank et al (2004), The domain's inlet and outlet distances from the building position are calculated as 5H and 15H, respectively. The top clearance and side aspect are also calculated as 5H, where H is the building's height. The domain configurations are represented graphically. in Fig.

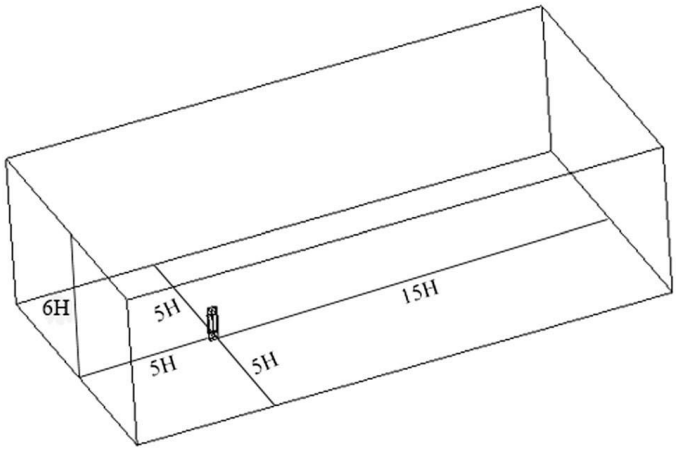

Figure 4-4 Domain

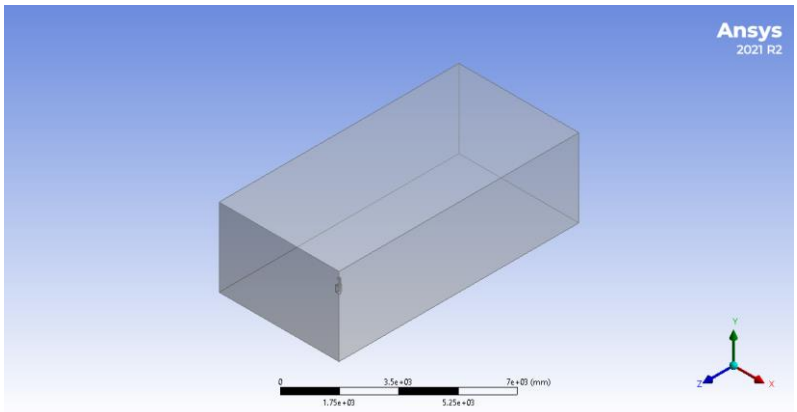

Figure 4-5 Domain (virtual wind tunnel)

Models:

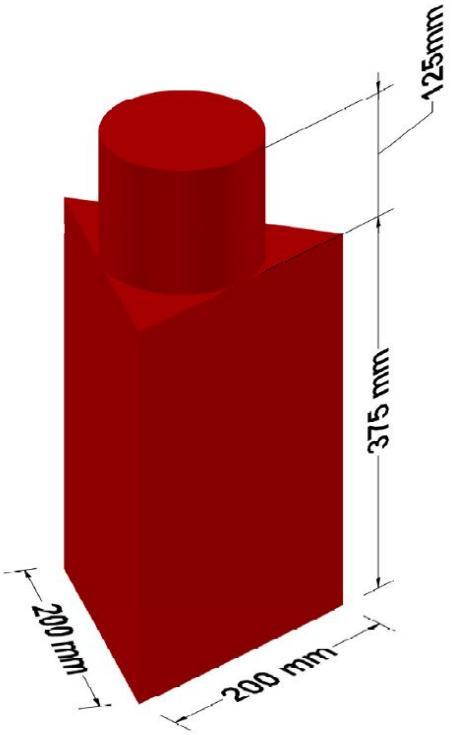

Figure 4-6 Model 1 75% Triangle & 25% Circle

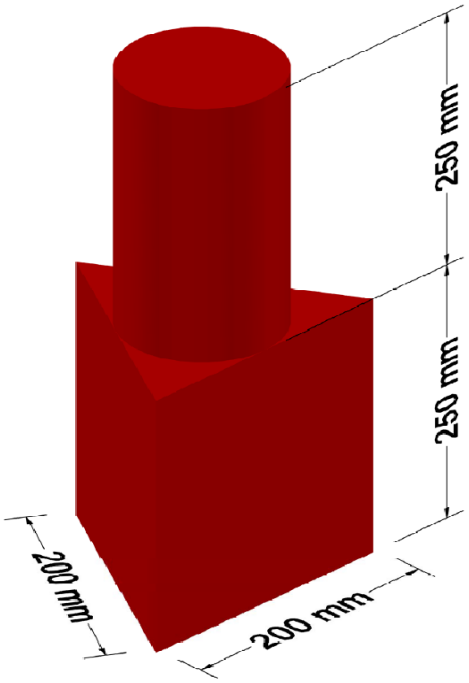

Figure 4-7 Model 2 50% Triangle 50% Circle

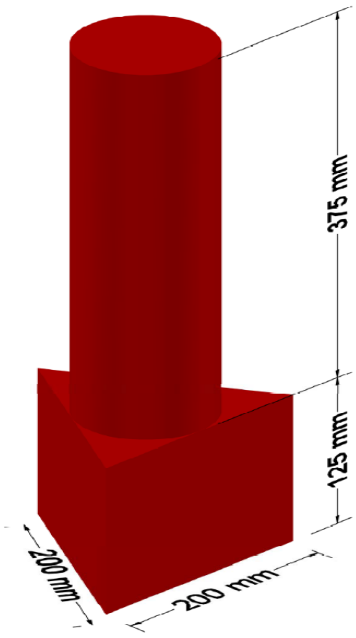

Figure 4-8 Model 3 25% Triangle & 75% Circle

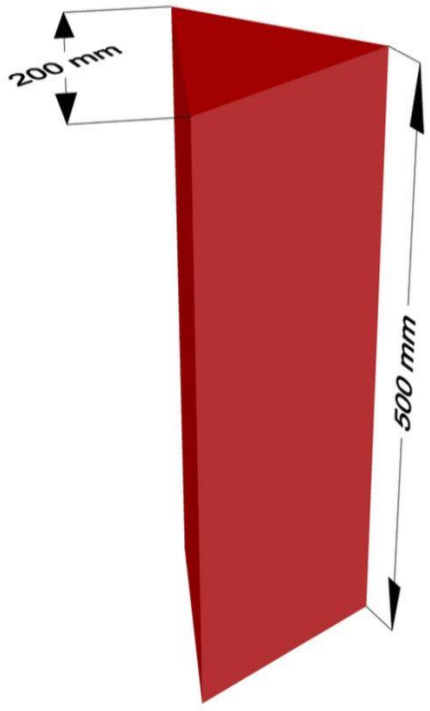

Figure 4-9 Model 100% Triangle

MESHING

Meshing is a step in the engineering simulation process that involves breaking down complex geometries into simple parts that can be used as discrete local approximations of a wider domain.

Meshing influences the accuracy, convergence and speed of the simulation. Finer the mesh, better the accuracy.

Types of Mesh

A. Tetrahedron Meshing
B. Pyramid Meshing
C. Hexahedron Meshing
D. Polyhedron Meshing
E. Prism Meshing

The meshing in domain is done by tetrahedral mesh elements. Meshing near the buildings are made comparatively finer for enhancing the accuracy of results. The velocity at the inlet is taken as 10 m/s. No slip condition is defined for side walls and ground.

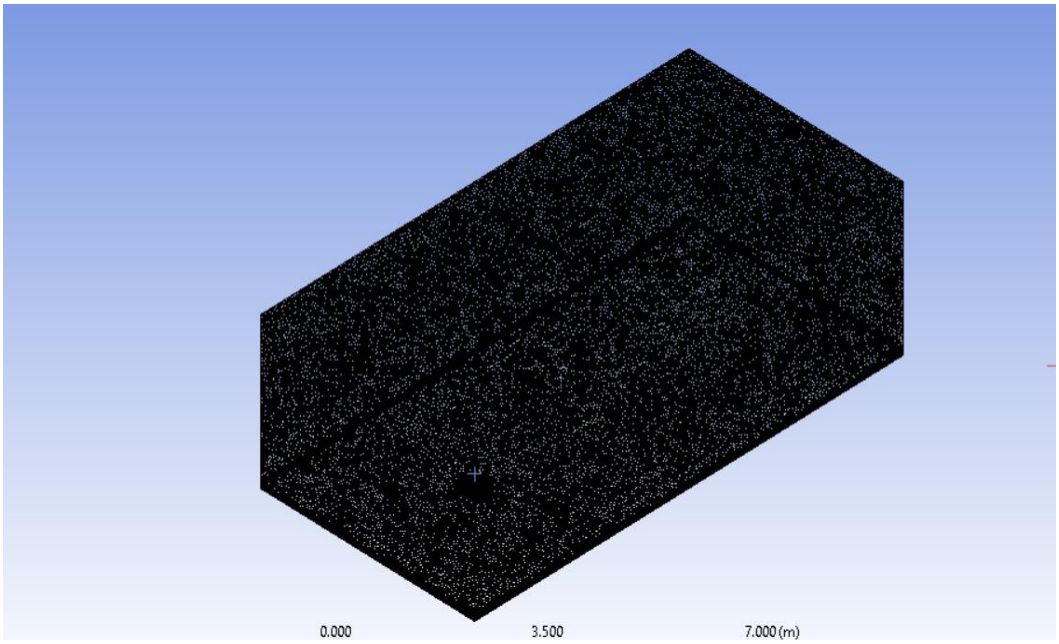

Figure 4-10 Domain Meshing

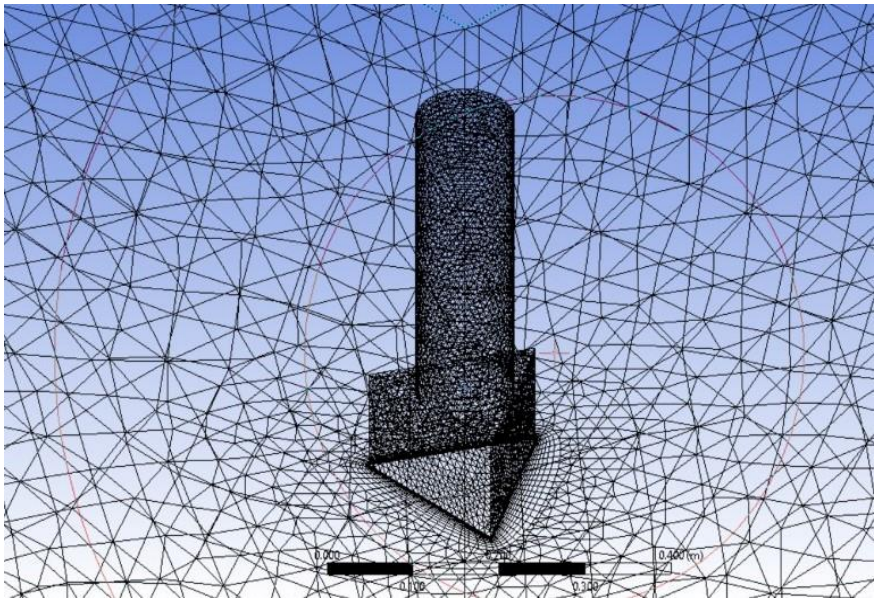

Figure 4-11 Building Meshing

4.3 Governing Equations

K-ε turbulence model is used to simulate mean flow characteristics for model. This model uses two equation model by means of two transport equations. The k-ε model uses the gradient diffusion hypothesis to relate the Reynold stresses to the mean velocity gradients and turbulent viscosity. Here, k is turbulence kinetic energy and is defined as the variance of fluctuations in velocity and Ɛ is the turbulence eddy dissipation (the rate at which the velocity fluctuation dissipates).

For a turbulence model used, instantaneous velocity can be written as the summation of time averaged mean velocity and a time varying fluctuating component given as below:

$$u_i = U_i + u_i'$$

where, u_i = instantaneous velocity

U_i = time averaged mean velocity

u_i' = fluctuating component of velocity

As per Reynold's Average Navier Stokes Equation (RANS) equation:

$$\frac{\partial}{\partial x_i}(\rho U_i) = 0$$

where, ρ = density of fluid

and conservation of momentum equation can be written as,

$$\frac{\partial}{\partial x_j}(\rho U_i U_j) = -\frac{\partial P}{\partial x_i} + \frac{\partial}{\partial x_f}\left[\mu\left(\frac{\partial U_i}{\partial x_j} + \frac{\partial U_f}{\partial x_i}\right)\right] + \frac{\partial}{\partial x_j}\left(-\rho\overline{u_i' u_j'}\right)$$

CHAPTER 5

Results and Discussions

The external pressure coefficient is calculated by using the expression,

$$C_{pe} = \frac{P}{0.6 \times V_z^2}$$

5.1 Pressure Distribution

The pressure variation at various faces of Buildings are as shown using contour plots.

MODEL 1

1. Model- 1 (375 triangle 125 circle)

- The pressure contours for different faces at various angle of incidence depicts the pressure distribution on faces and are shown in figures.
- Initially, at 0 degree of incidence face A shows a positive pressure being the windward face of the triangular building whereas face B and C depicts a negative pressure distribution being the leeward and side wall face of the building.
- Similarly, at 0 degree of incidence face A shows a positive pressure being the windward face of the circular building whereas the building's leeward and side wall faces represent a negative pressure distribution (facing B, C, and D).

- As the angle of incidence changes to the pressure distribution changes and so the pressure coefficient.
- For 60° and 120° angle of incidence, positive pressure distribution at face A become slightly less compared to what in case of 0° along with suction pressure increase at face C in triangular building and face D in circular and a comparable change can be viewed from the pressure coefficient data so obtained as a result.
- For 180° angle of incidence, face C in triangular building and face D in circular building become windward and similar contour plot pattern as of face A when angle of attack was 0° can be seen.

1. zero-degree Contour Plots

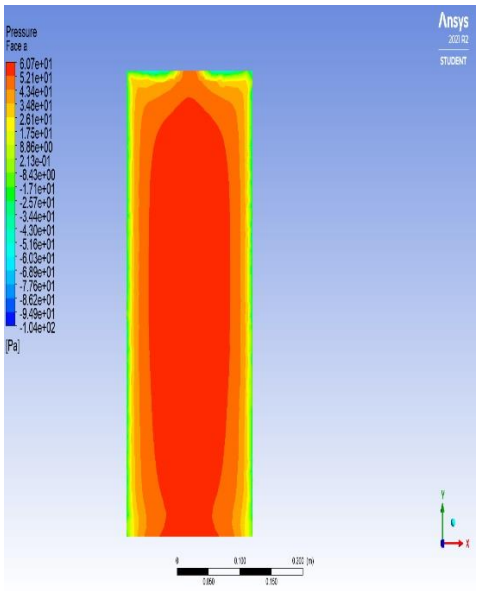

Triangle Face A

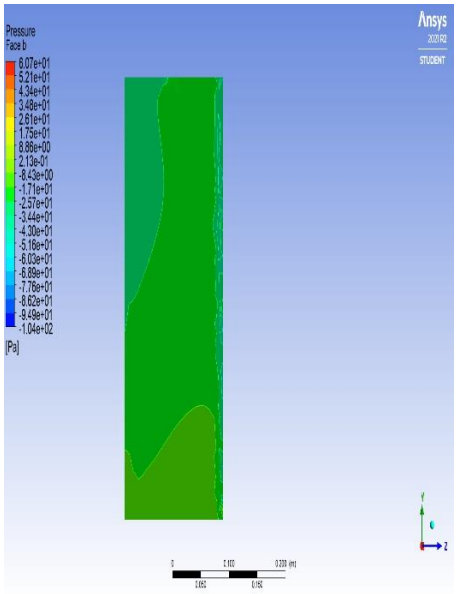

Triangle Face B

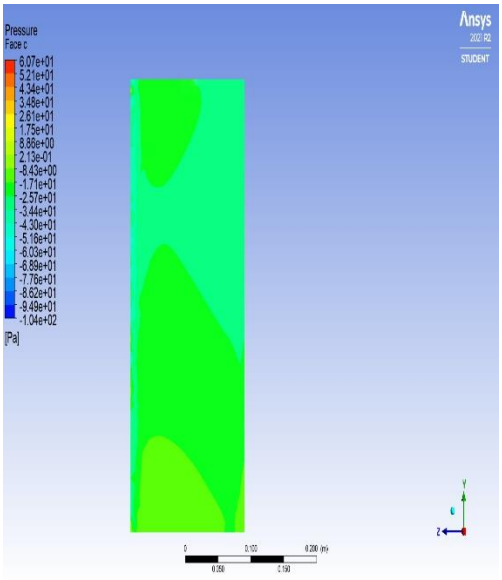

Triangle Face C

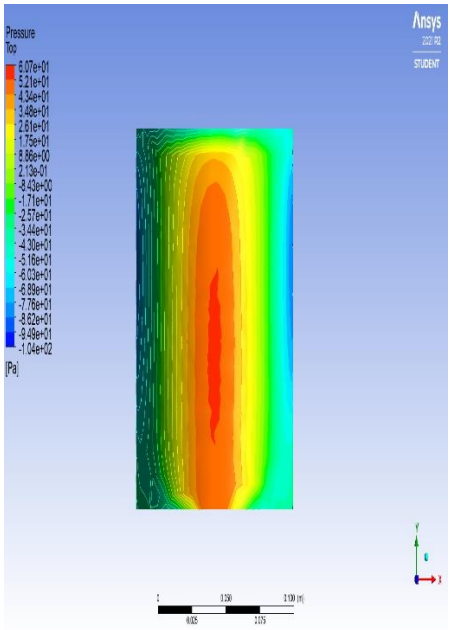

Circle Face A

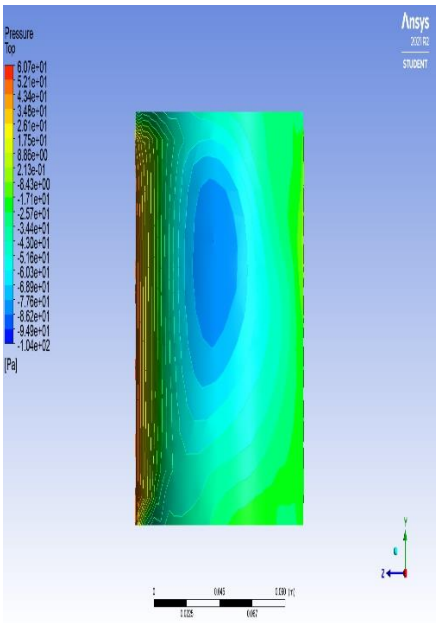

Circle Face B

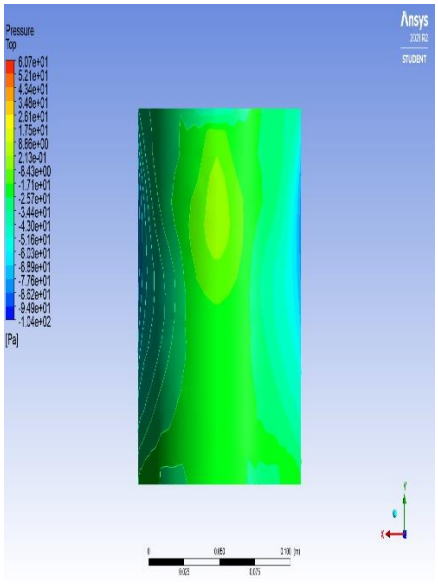

Circle Face C

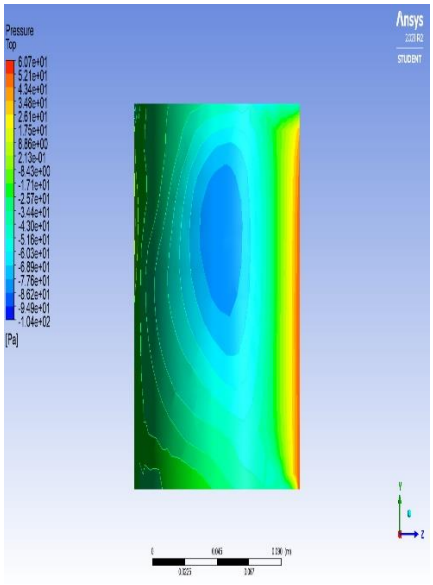

Circle Face D

Figure 5-1 Contour Plots for different faces at 0- degree of incidence for Model 1

2. sixty-degree contour plot

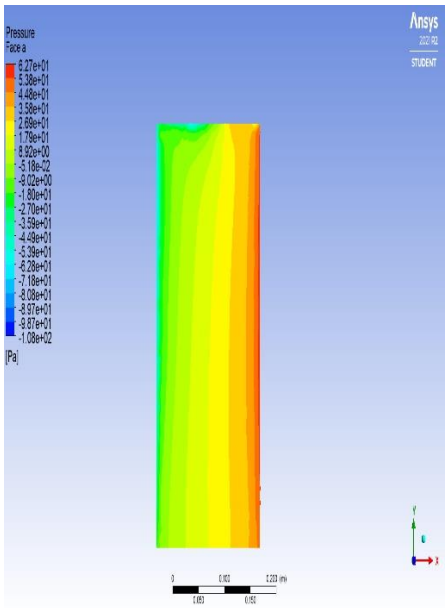

Triangle Face A

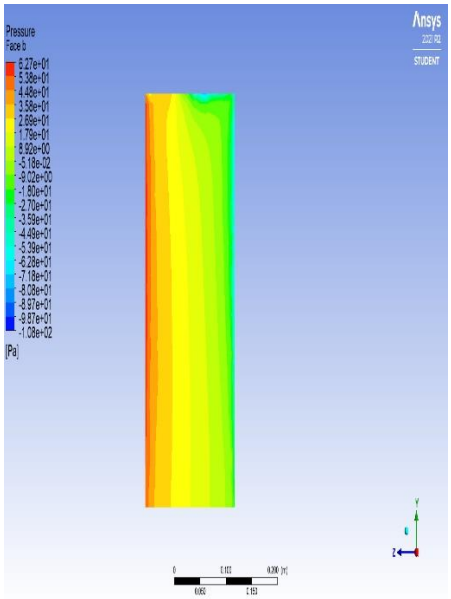

Triangle Face B

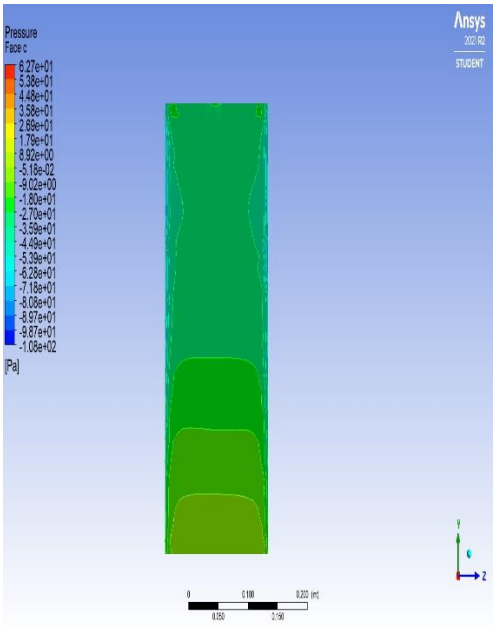

Triangle Face C

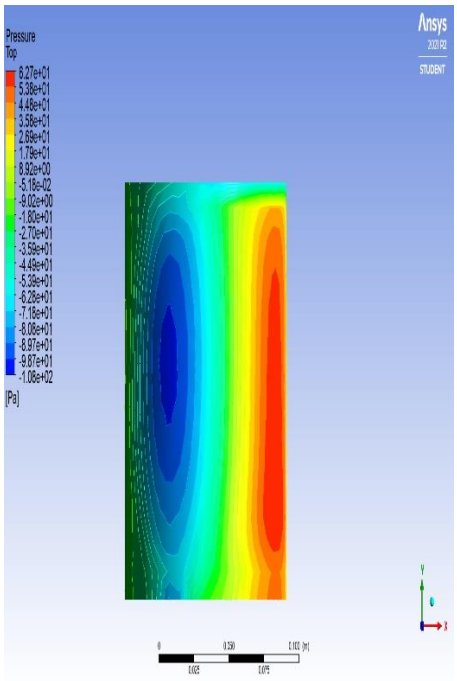

Circle Face A

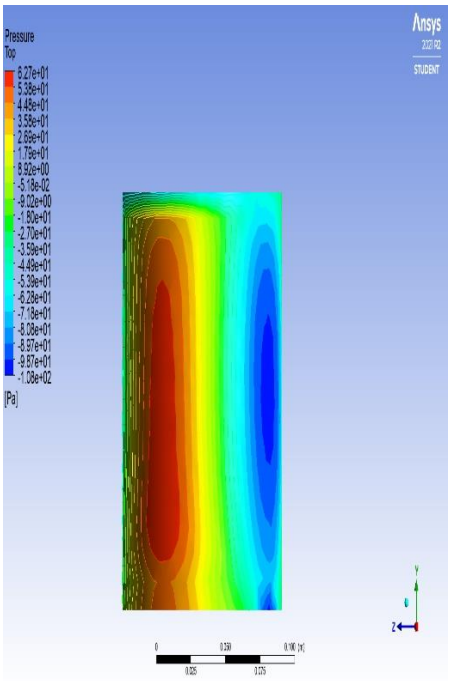

Circle Face B

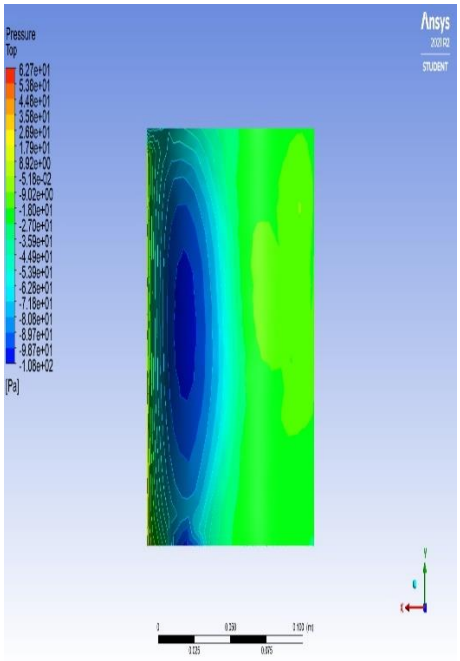

Circle Face C

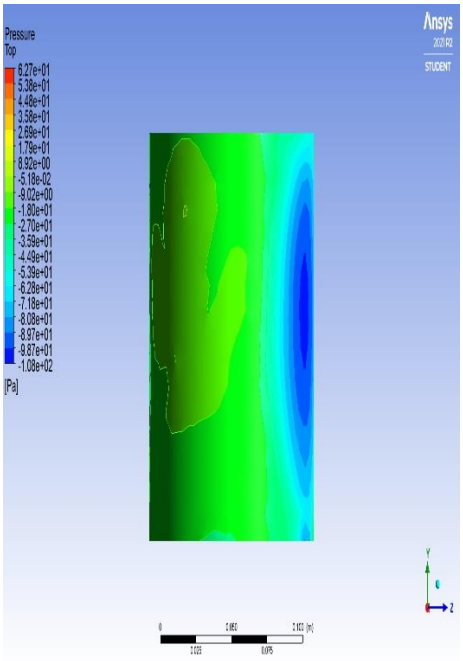

Circle Face D

Figure 5-2 Contour Plots for different faces at 60- degree of incidence for Model 1

3. One twenty-degree contour plot

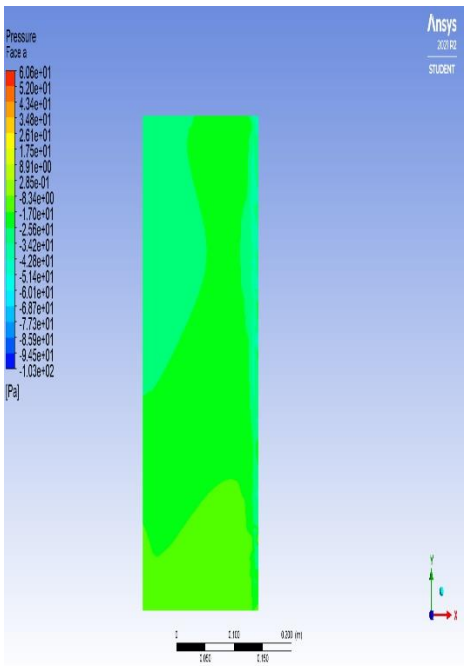

Triangle Face A

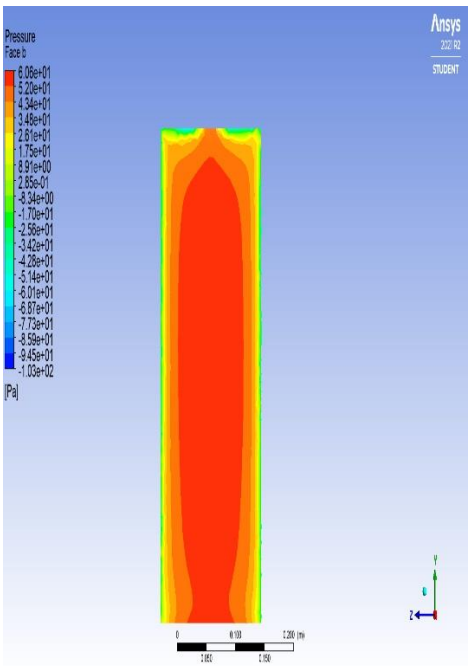

Triangle Face B

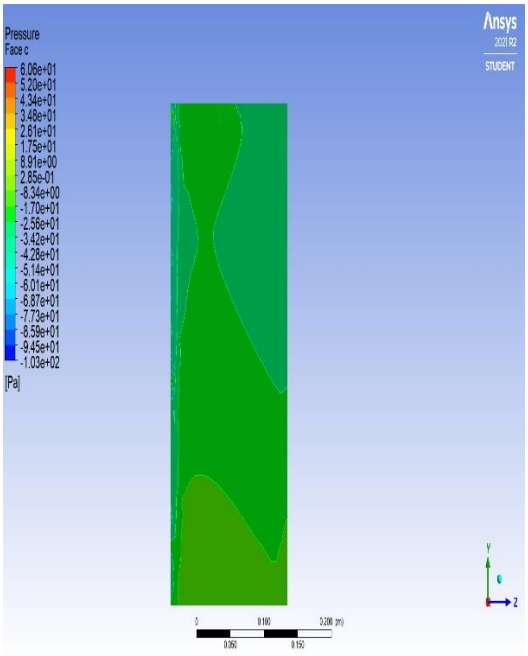

Triangle Face C

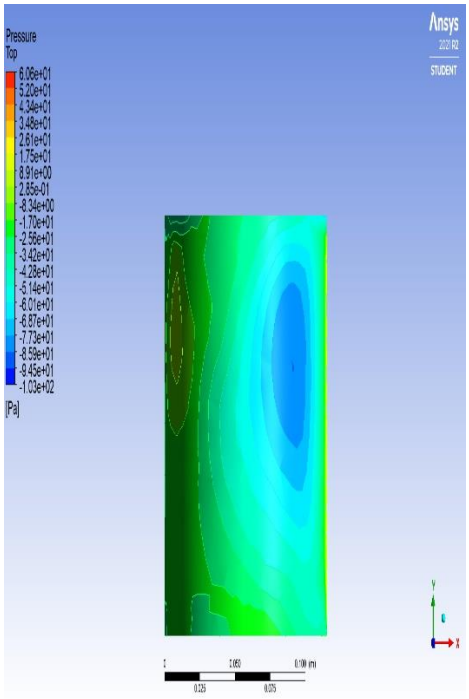

Circle Face A

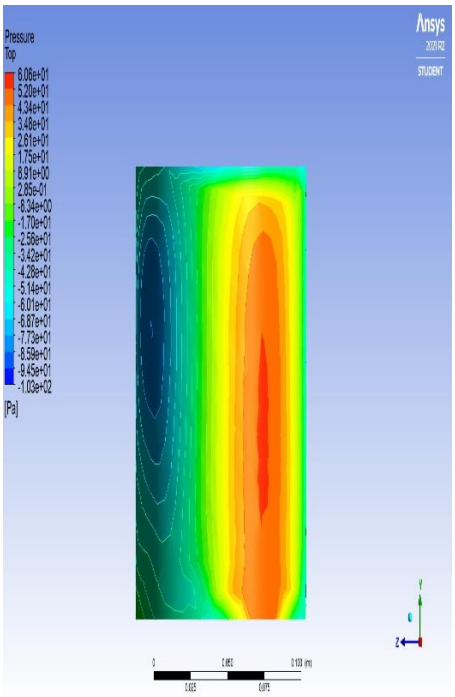

Circle Face B

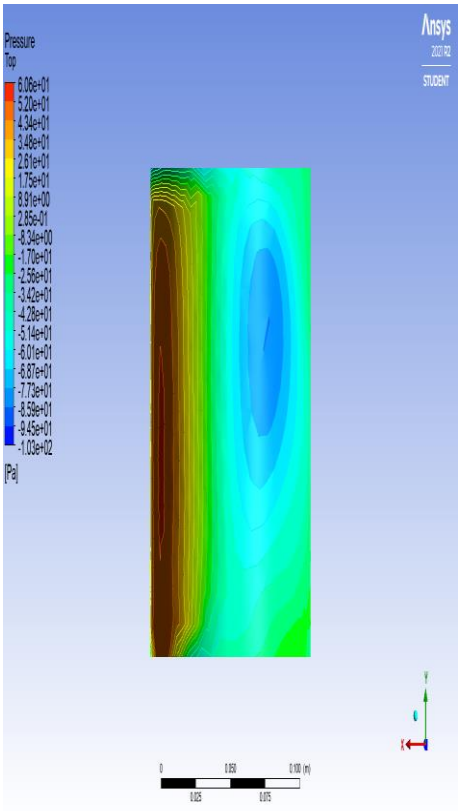

Circle Face C

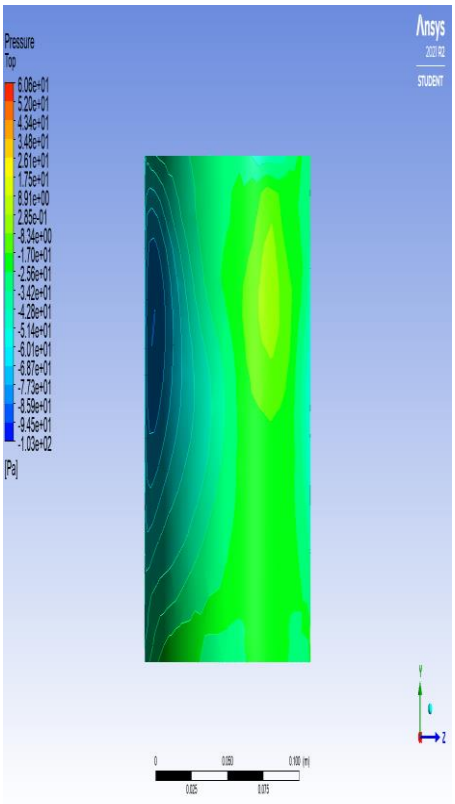

Circle Face D

Figure 5-3 Contour Plots for different faces at 120- degree of incidence for Model 1

4. One eighty-degree contour plot

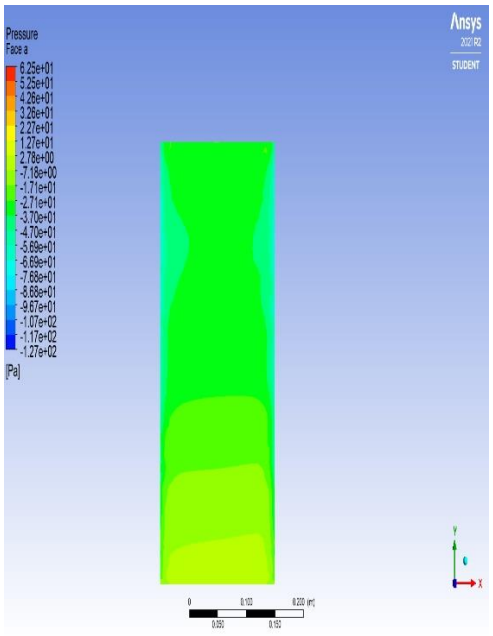

Triangle Face A

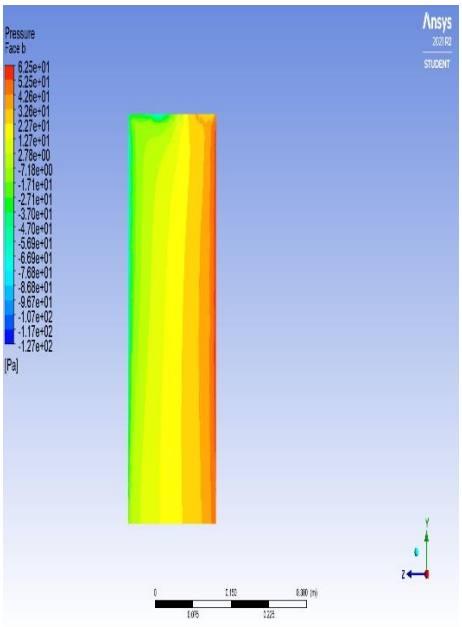

Triangle Face B

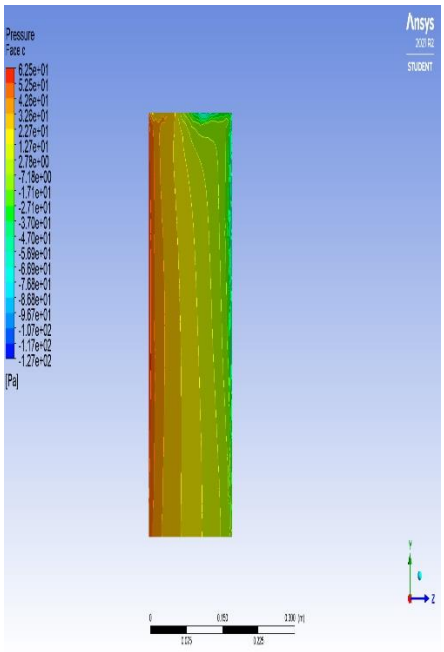

Triangle Face C

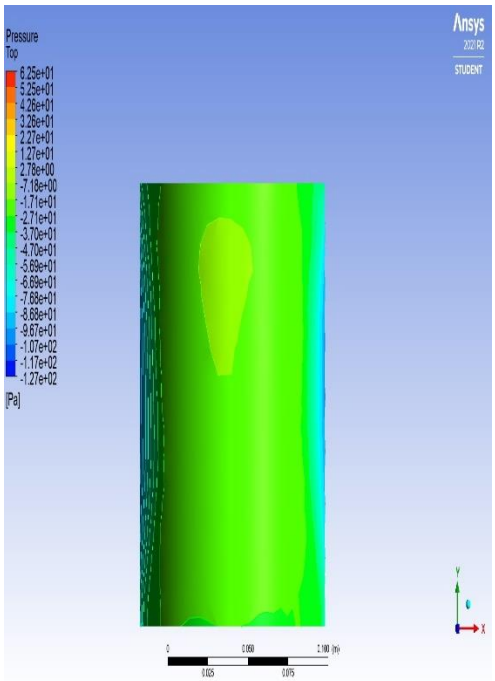

Circle Face A

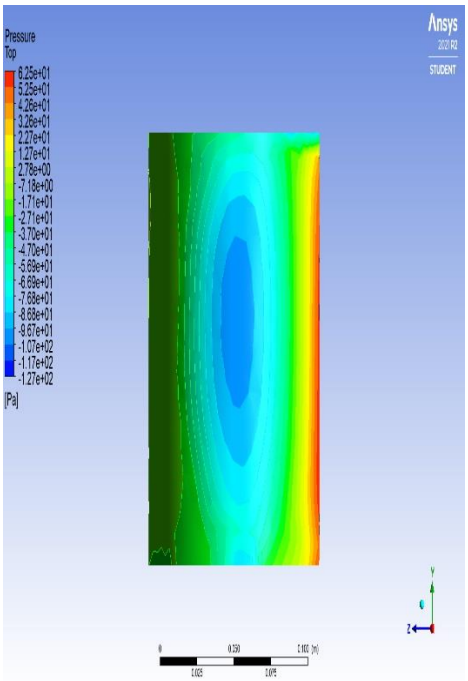

Circle Face B

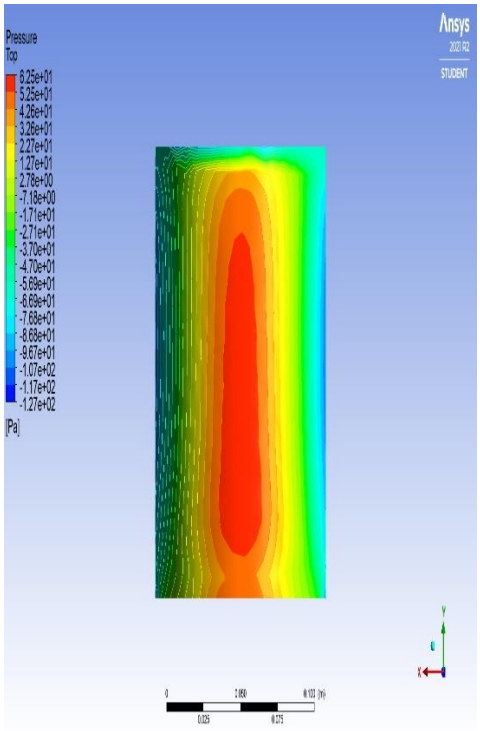

Circle Face C

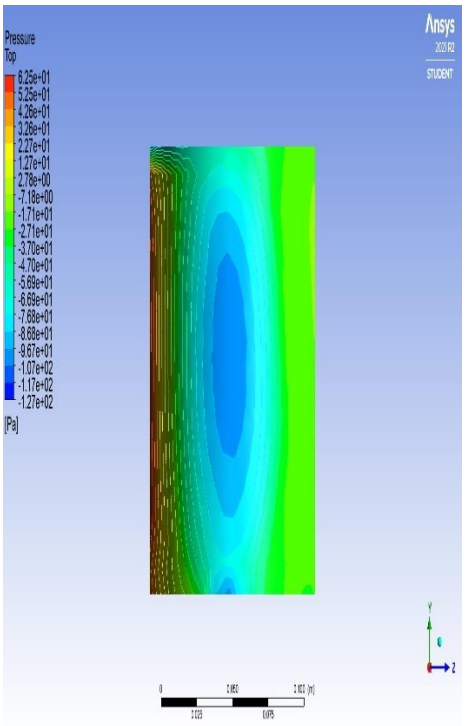

Circle Face D

Figure 5-4 Contour Plots for different faces at 180- degree of incidence for Model 1

MODEL 2

Model- 2 (250 triangle 250 circle)

- Figures 5-5 to 5-8 exhibit the pressure distribution on different faces at varying angles of incidence.
- Initially, at 0 degree of incidence face A shows a positive pressure being the windward face of the triangular building whereas face B and C depicts a negative pressure distribution being the leeward and side wall face of the building.
- Similarly, at 0 degree of incidence face A shows a positive pressure being the windward face of the circular building whereas The building's leeward and side wall faces represent a negative pressure distribution (facing B, C, and D).
- As the angle of incidence changes to the pressure distribution changes and so the pressure coefficient.
- For 60° and 120° angle of incidence, positive pressure distribution at face A become slightly less compared to what in case of 0° along with suction pressure increase at face

C in triangular building and face D in circular and a comparable change can be viewed from the pressure coefficient data so obtained as a result.

- For 180° angle of incidence, face C in triangular building and face D in circular building become windward and similar contour plot pattern as of face A when angle of attack was 0° can be seen.

1. Zero-degree contour plot

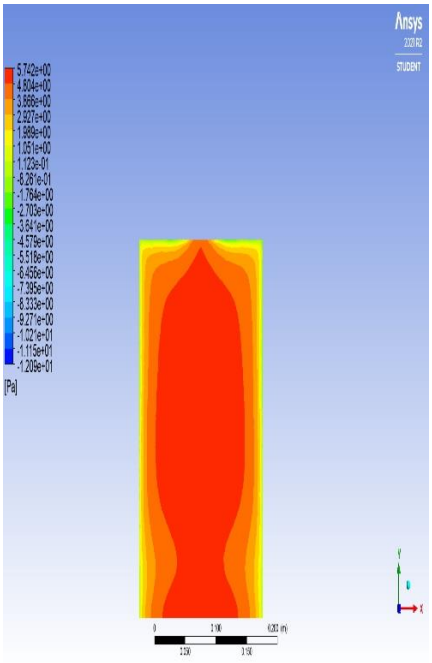

Triangle Face A

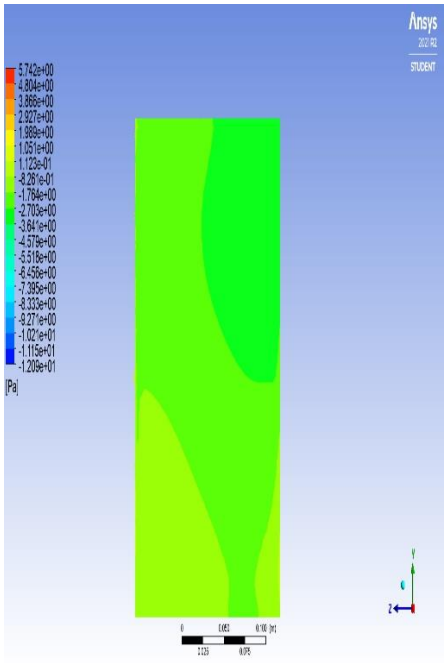

Triangle Face B

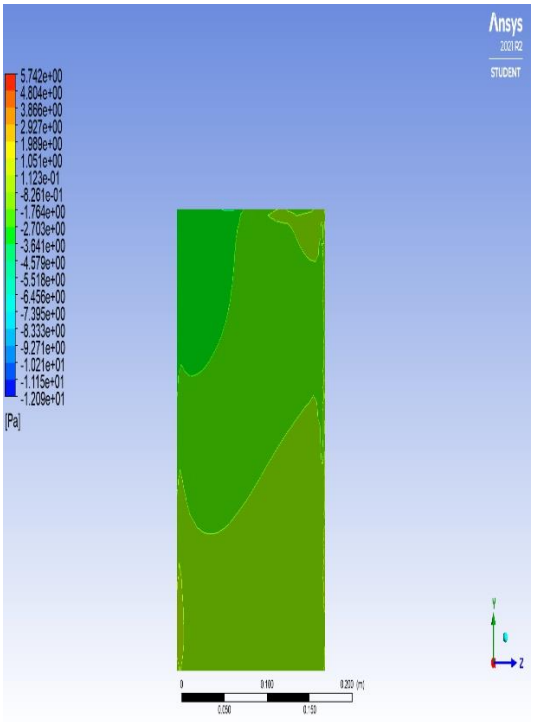

Triangle Face C

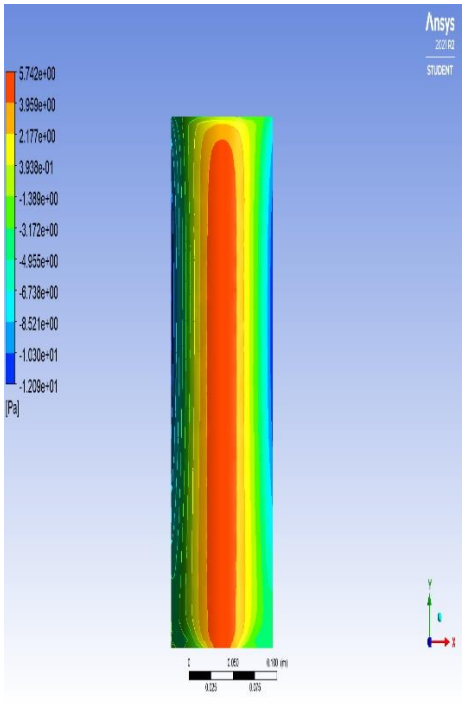

Circle Face A

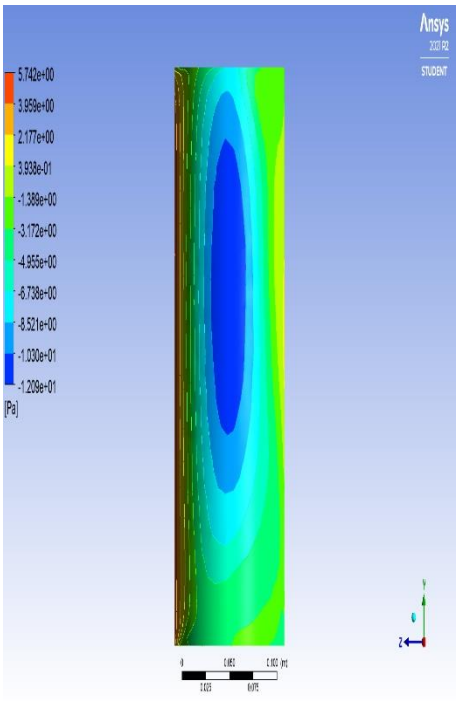

Circle Face B

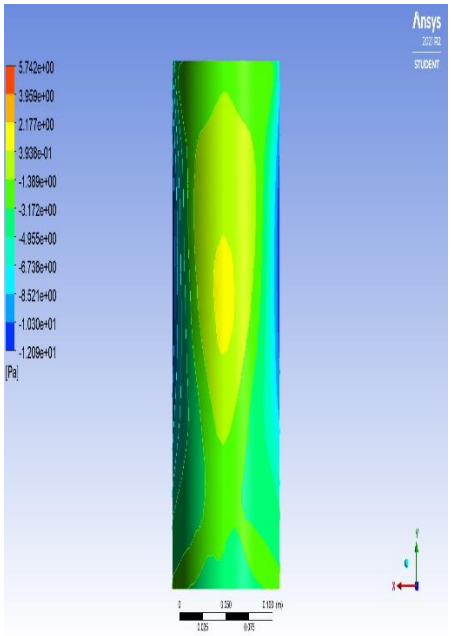

Circle Face C

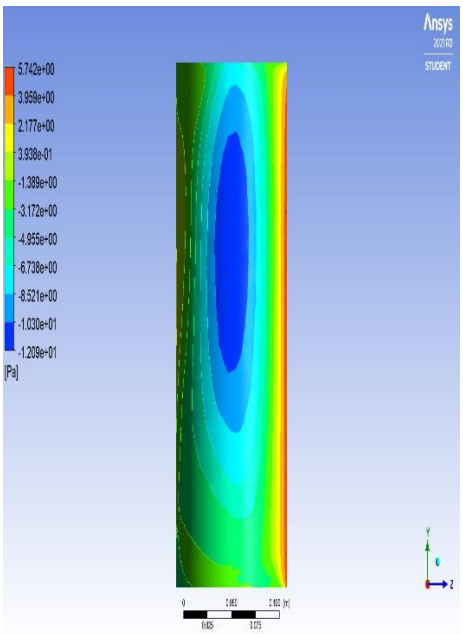

Circle Face D

Figure 5-5 Contour Plots for different faces at 0- degree of incidence for Model 2

2. Sixty-degree contour plot

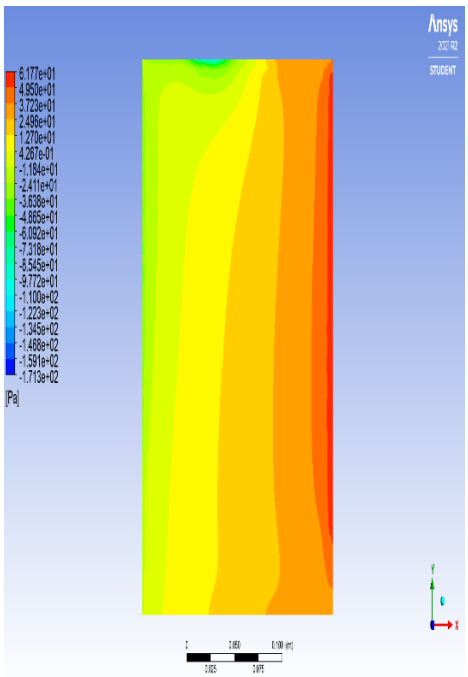

Triangle Face A

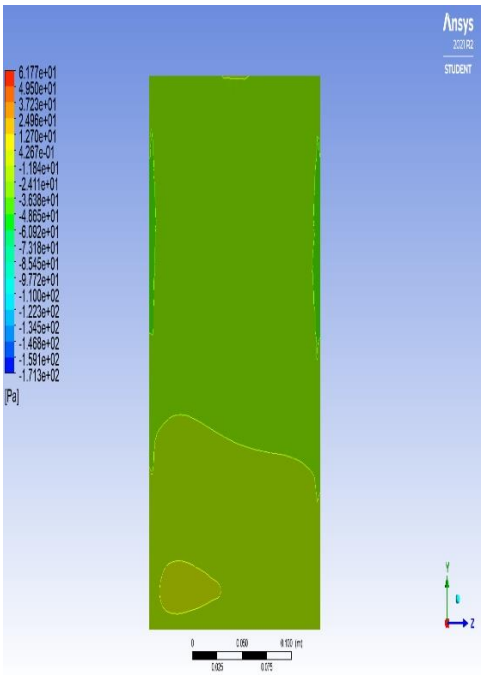

Triangle Face B

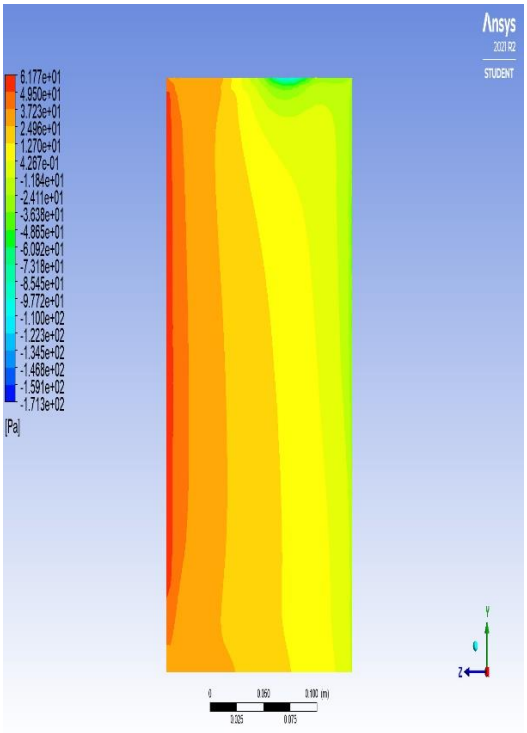

Triangle Face C

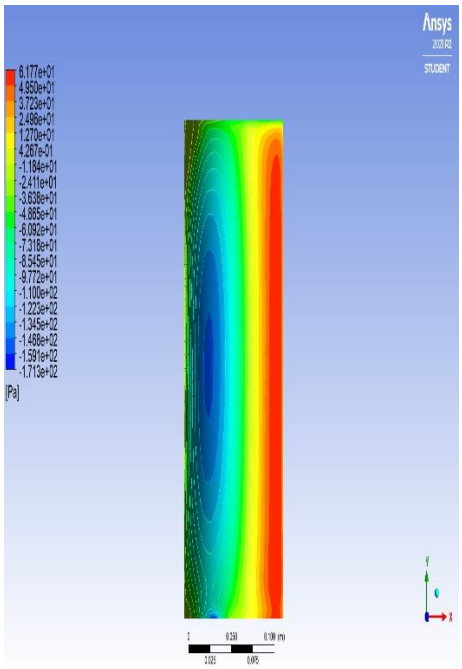

Circle Face A

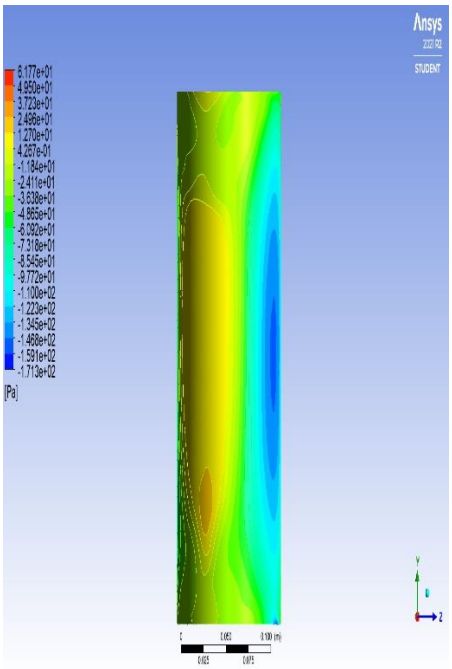

Circle Face B

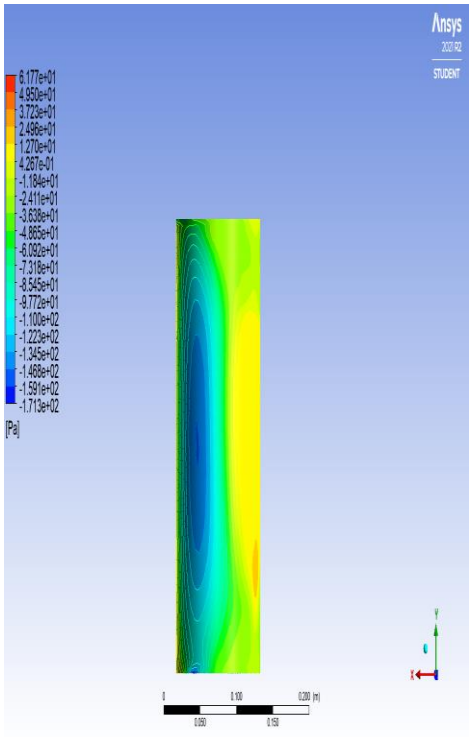

Circle Face C

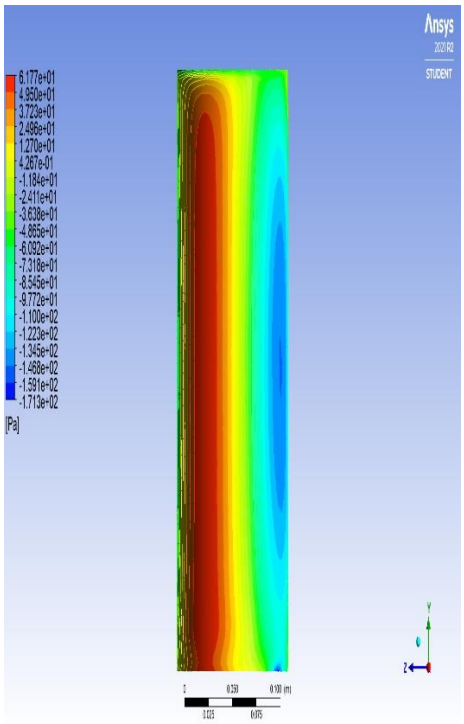

Circle Face D

Figure 5-6 Contour Plots for different faces at 60- degree of incidence for Model 2

3. One twenty contour plot

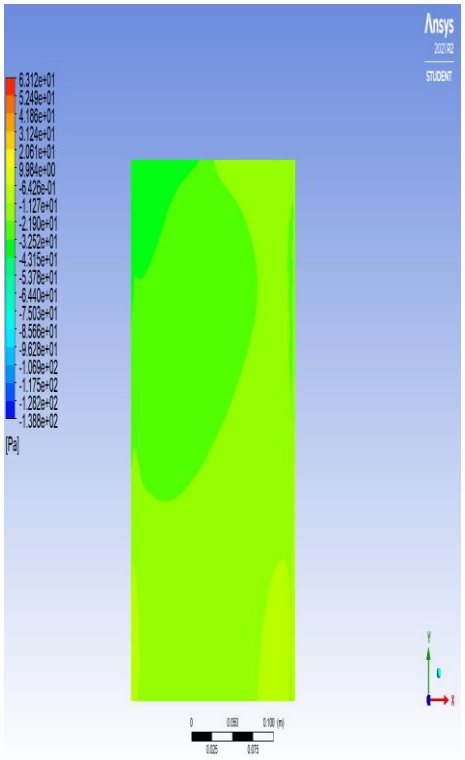

Triangle Face A

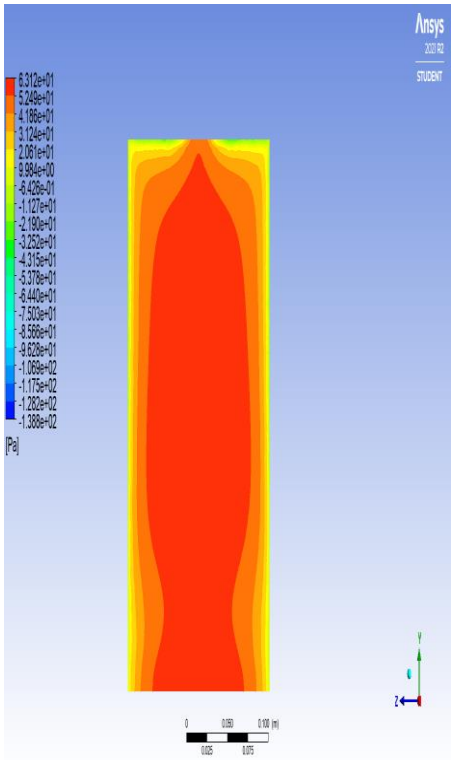

Triangle Face B

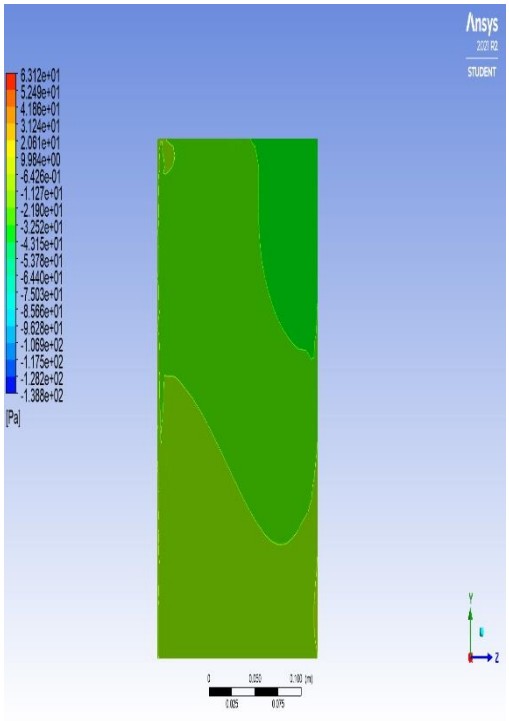

Triangle Face C

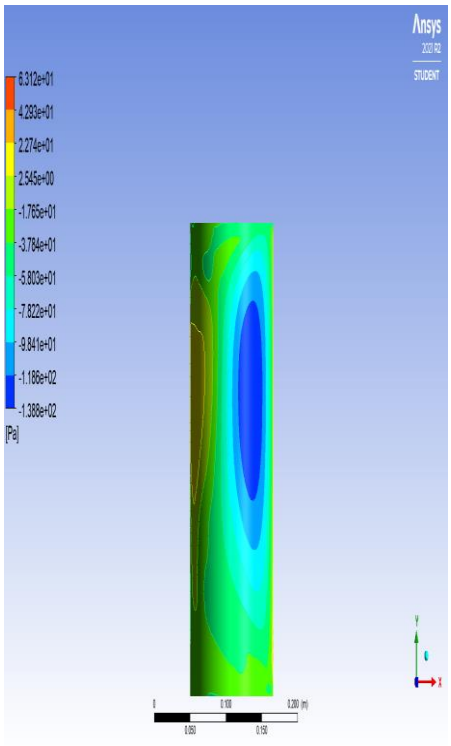

Circle Face A

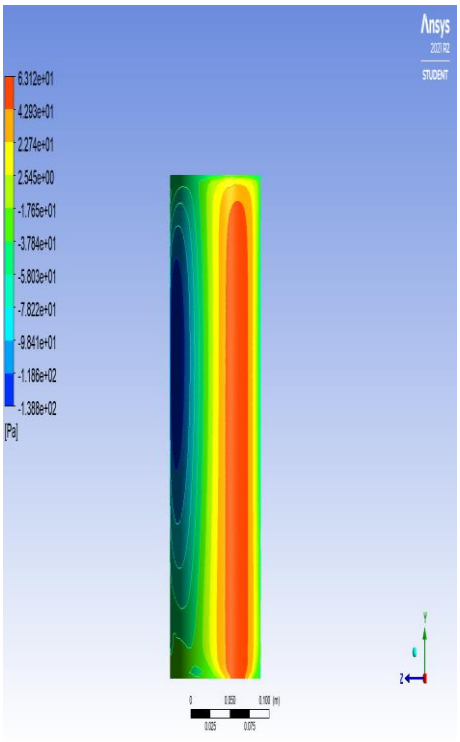

Circle Face B

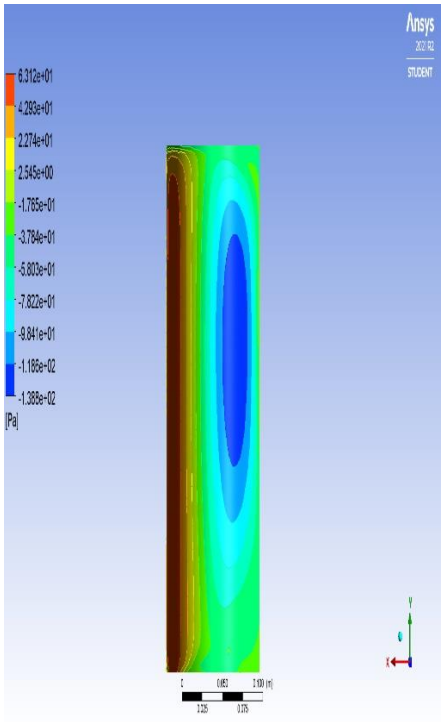

Circle Face C

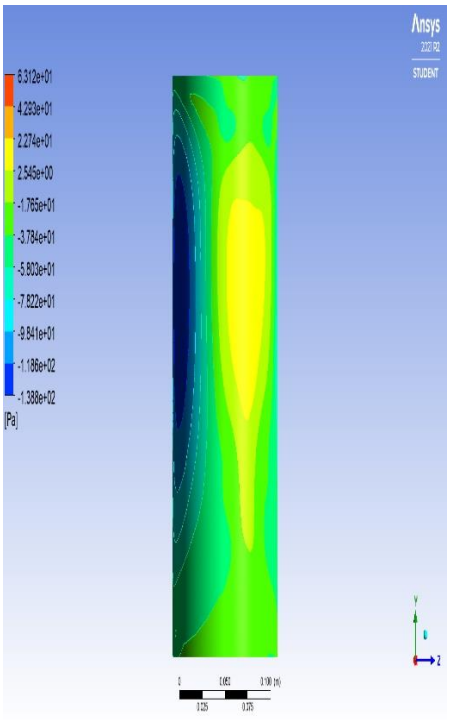

Circle Face D

Figure 5-7 Contour Plots for different faces at 120- degree of incidence for Model 2

4. One eighty contour plot

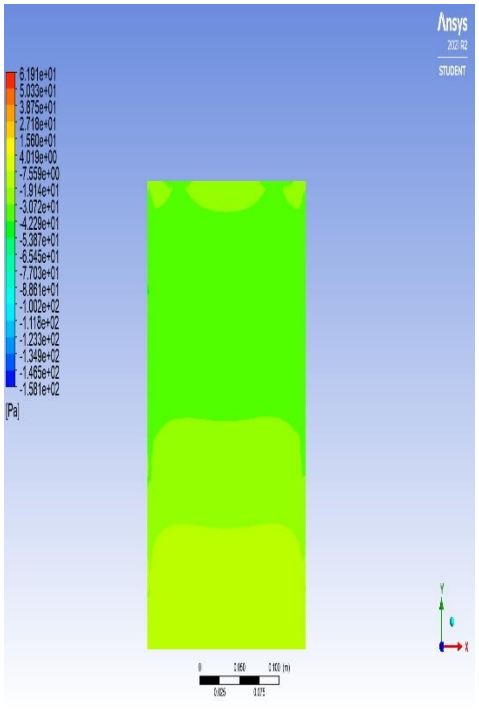

Triangle Face A

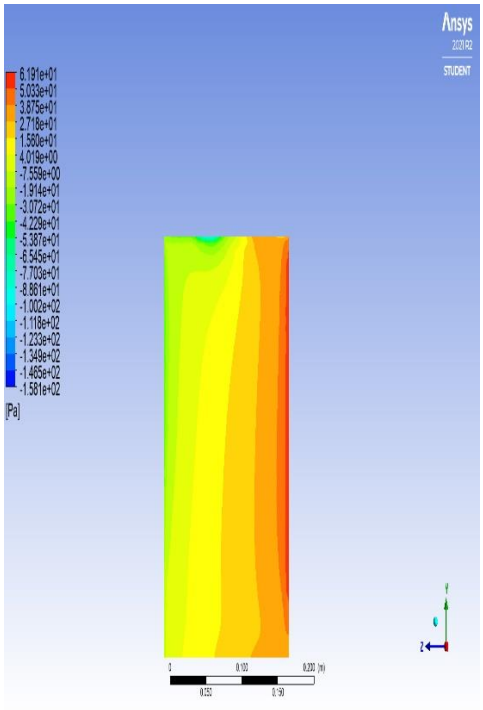

Triangle Face B

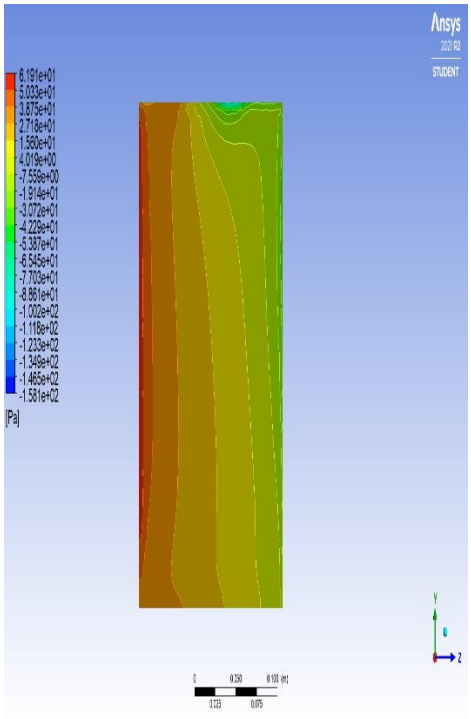

Triangle Face C

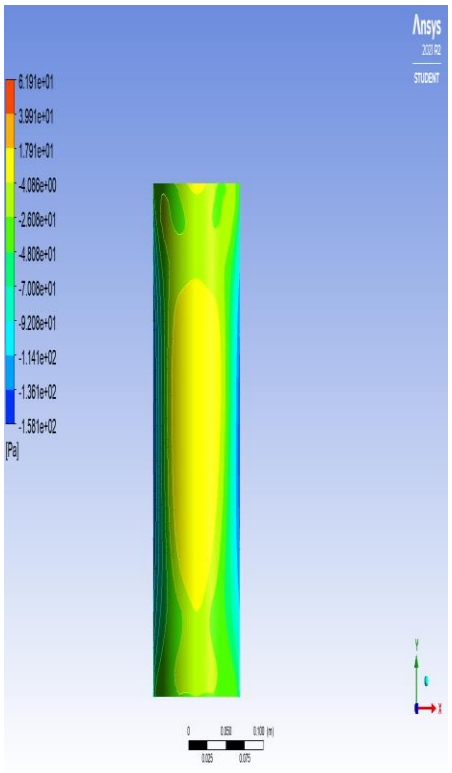

Circle Face A

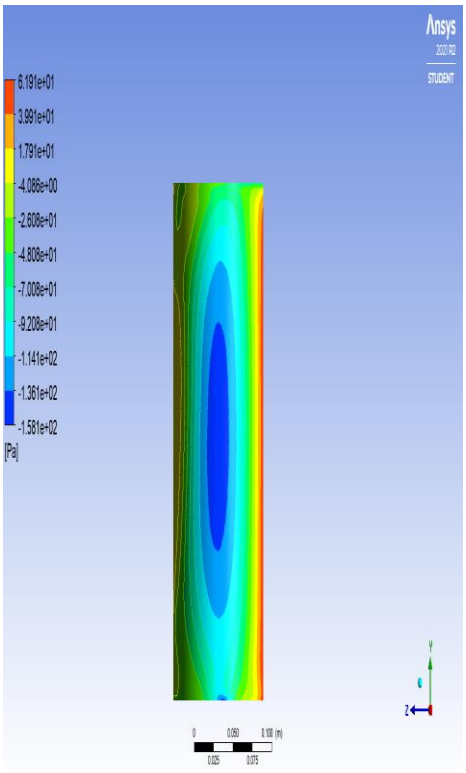

Circle Face B

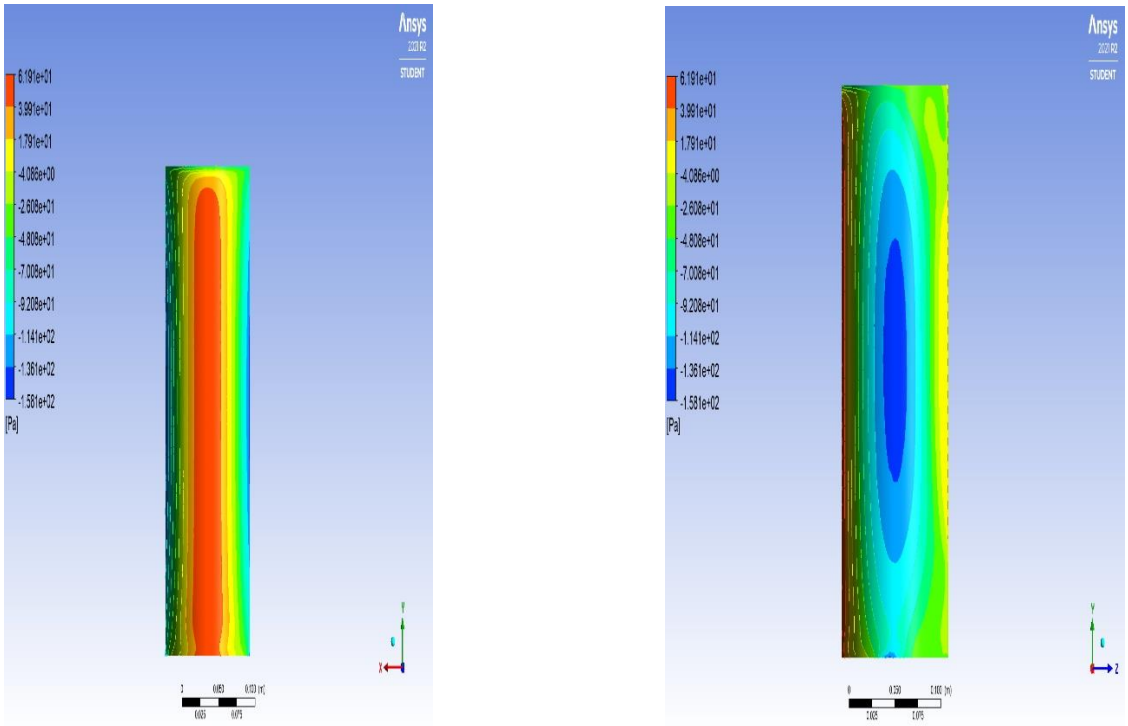

Circle Face C Circle Face D

Figure 5-8 Contour Plots for different faces at 180- degree of incidence for Model *2*

MODEL 3 (125 triangle 375 circle)

- The pressure contours for different faces at various angles of incidence are depicted in fig. 5-9 to 5-12 and illustrated the pressure distribution on faces.
- At 60° and 120° angles of incidence, positive pressure distribution at face A is slightly less than at 0°, while suction pressure increases at face C in triangular building, resulting in an equivalent change in the pressure coefficient data obtained as a result.
- Similarly at 60° and 120° angles of incidence, positive pressure distribution at face A is slightly less than at 0°, while suction pressure increases at face D in circular building, resulting in an equivalent change in the pressure coefficient data obtained as a result.
- When the angle of incidence is 180°, face C becomes windward in triangular building and face D becomes windward in circular building and the contour plot pattern is similar to that of face A when angle of attack was 0°.

1. Zero-degree contour plot

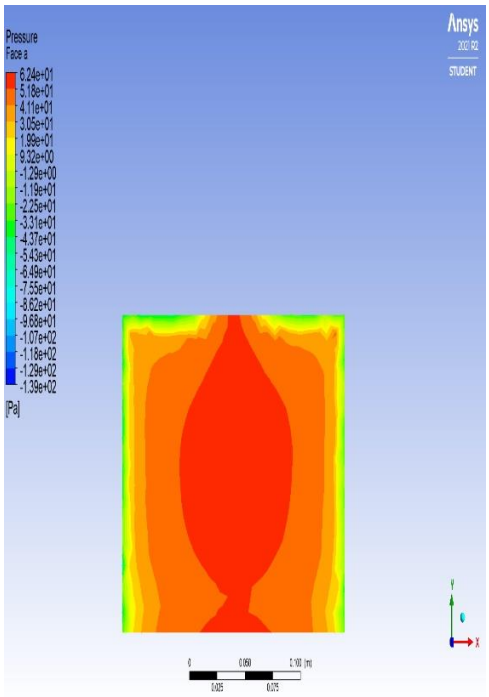

Triangle Face A

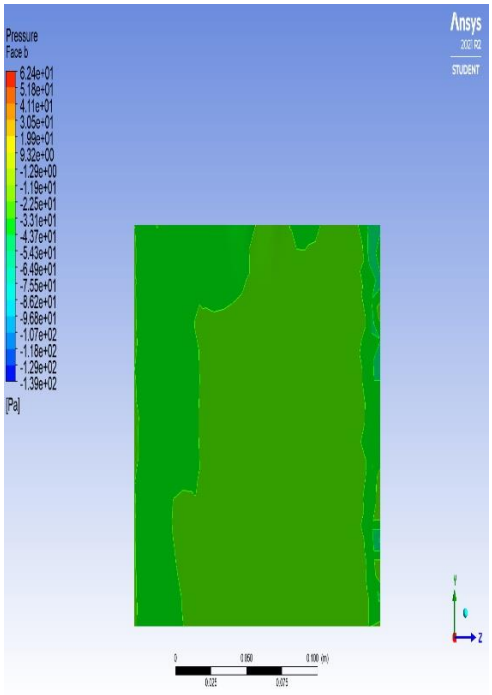

Triangle Face B

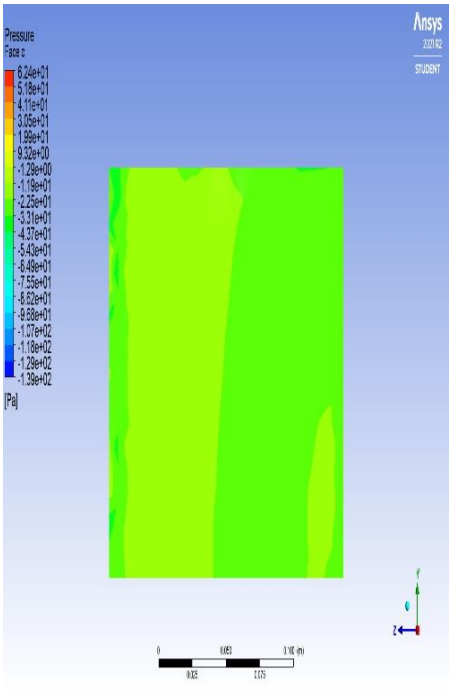

Triangle Face C

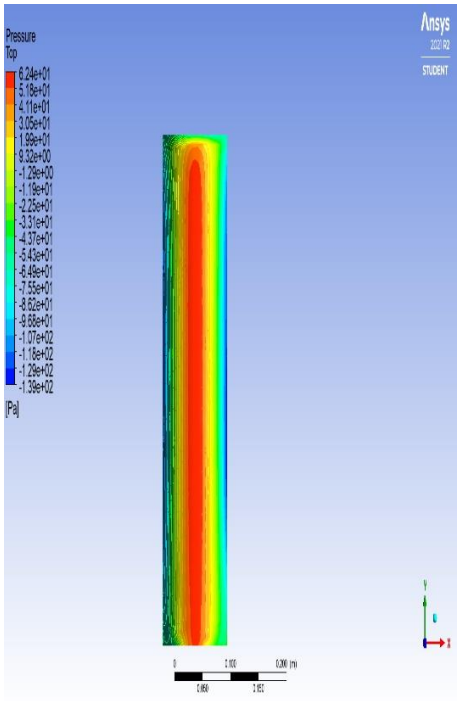

Circle Face A

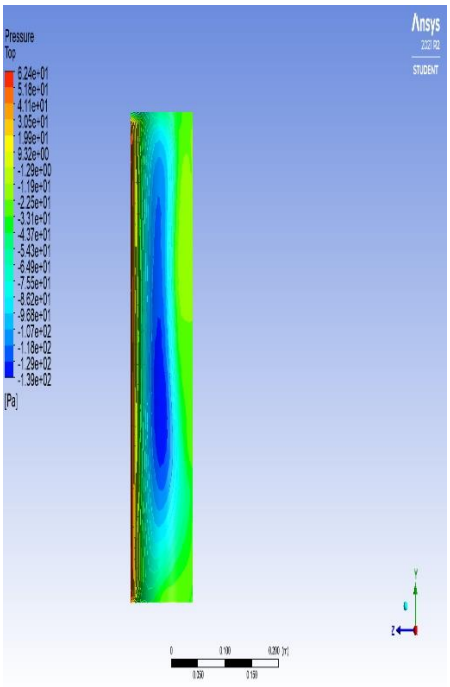

Circle Face B

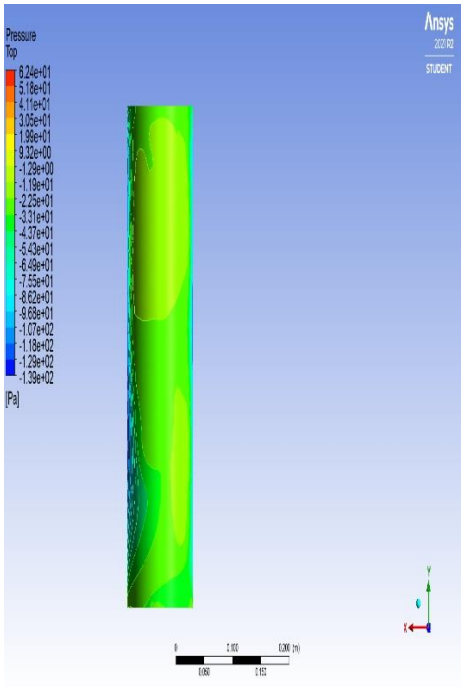

Circle Face C

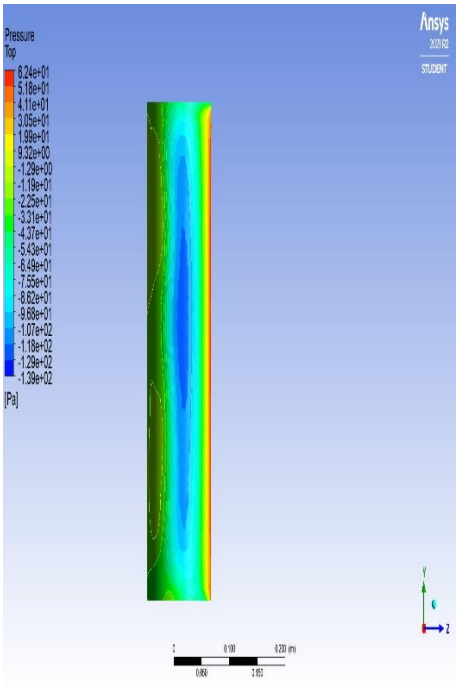

Circle Face D

Figure 5-9 Contour Plots for different faces at 0- degree of incidence for Model 3

2. Sixty -degree contour plot

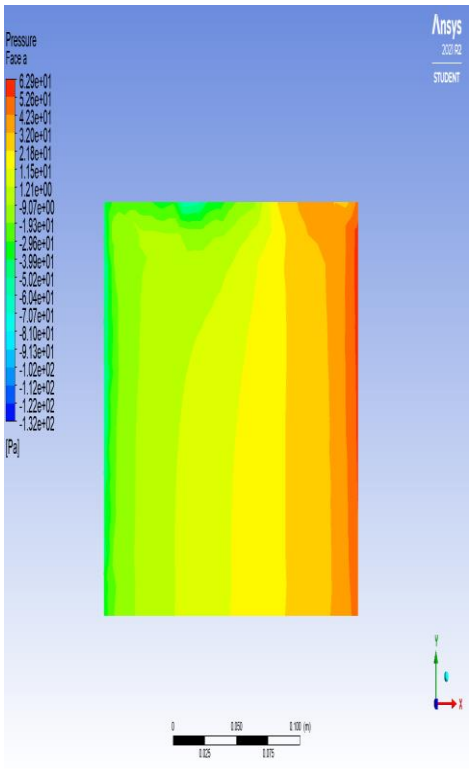

Triangle Face A

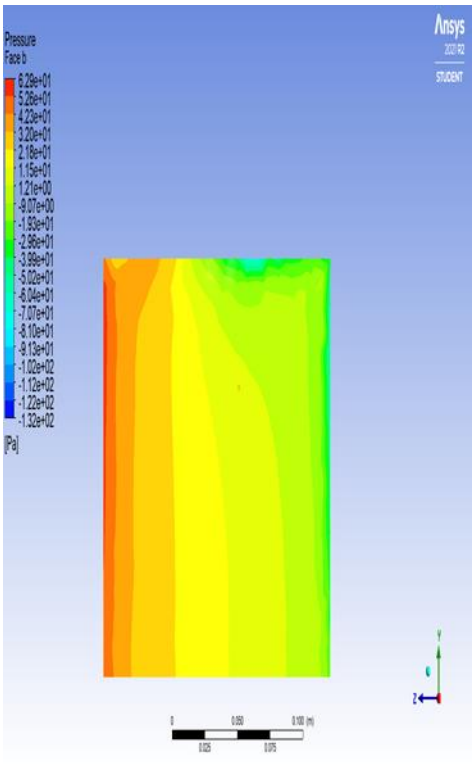

Triangle Face B

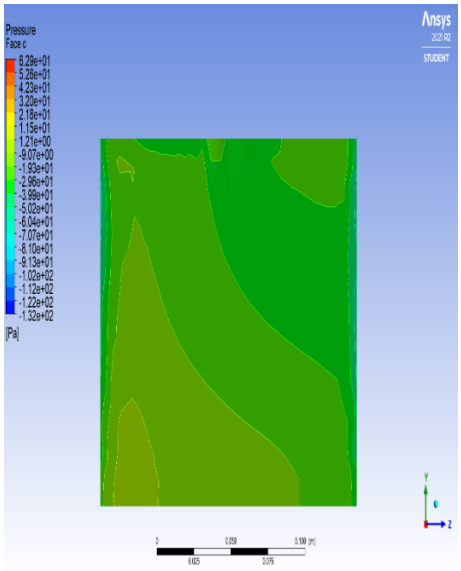

Triangle Face C

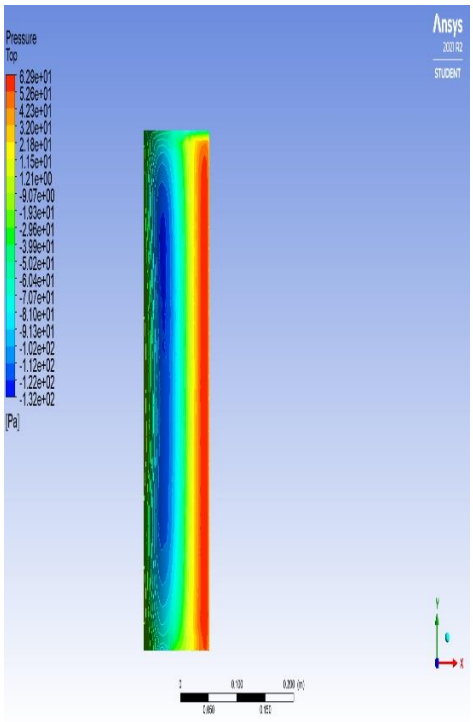

Circle Face A

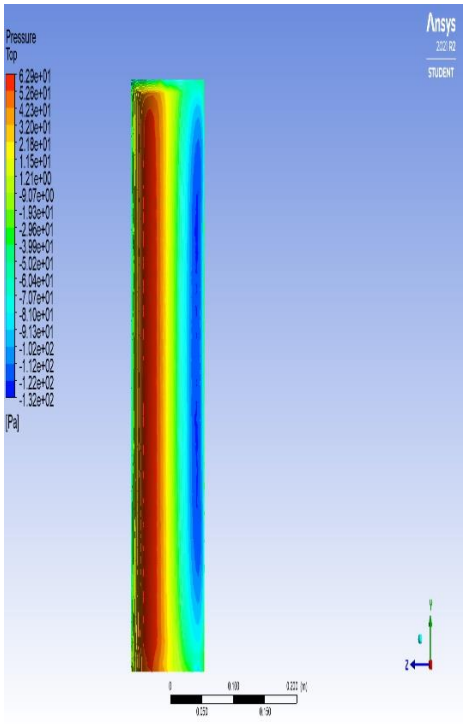

Circle Face B

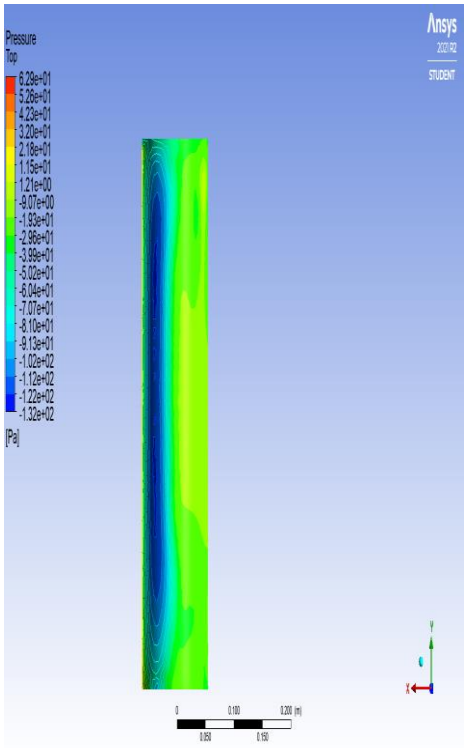

Circle Face C

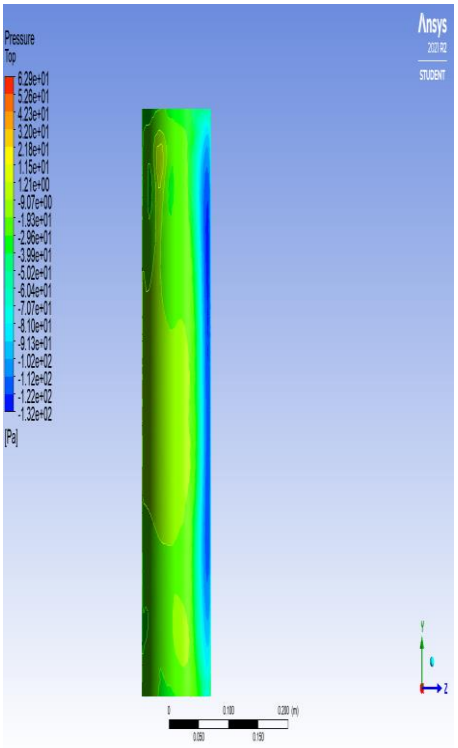

Circle Face D

Figure 5-10 Contour Plots for different faces at 60- degree of incidence for Model 3

3. One twenty-degree contour plot

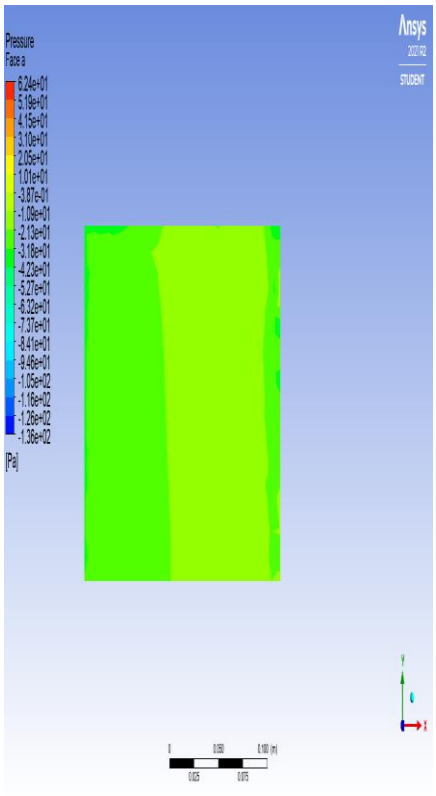

Triangle Face A

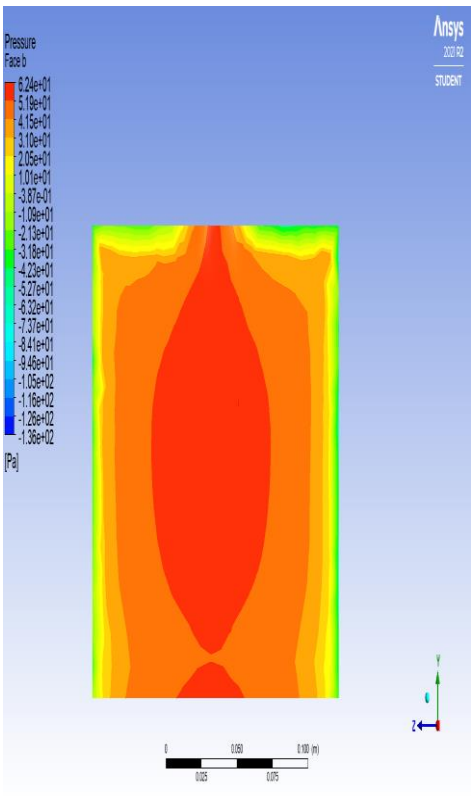

Triangle Face B

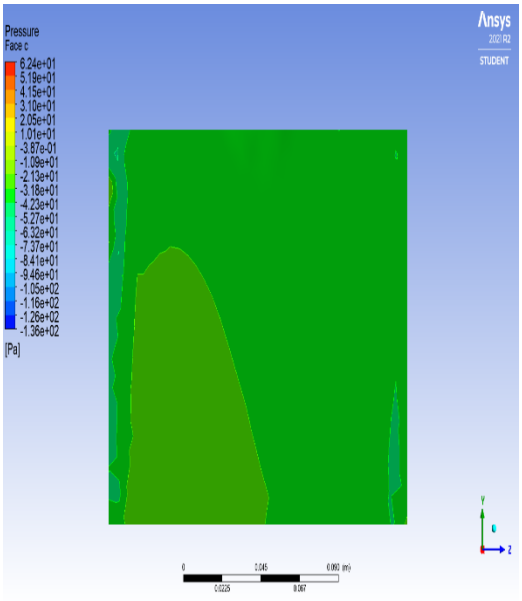

Triangle Face C

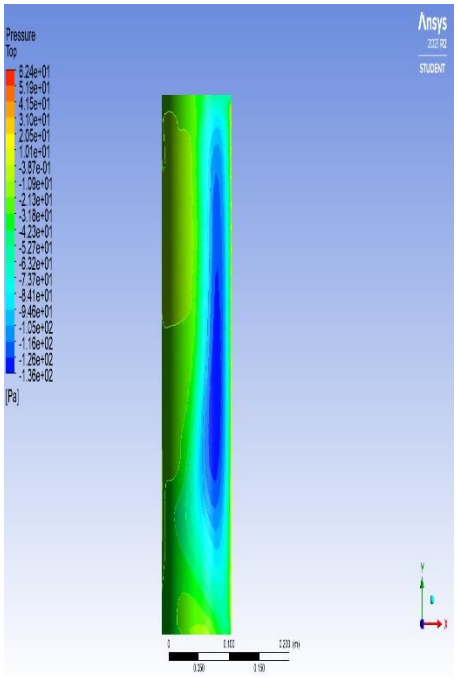

Circle Face A

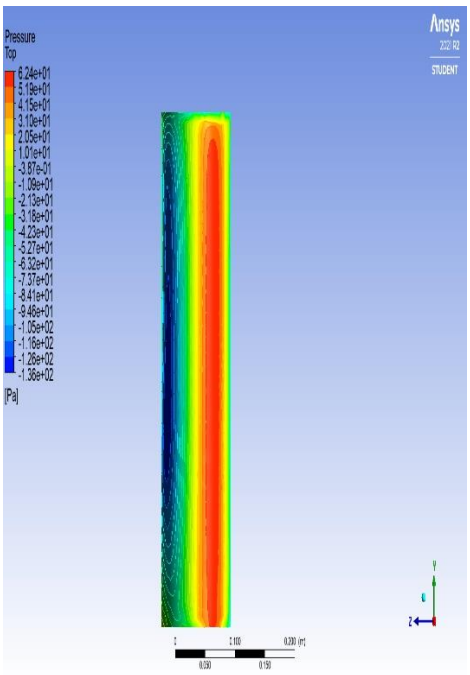

Circle Face B

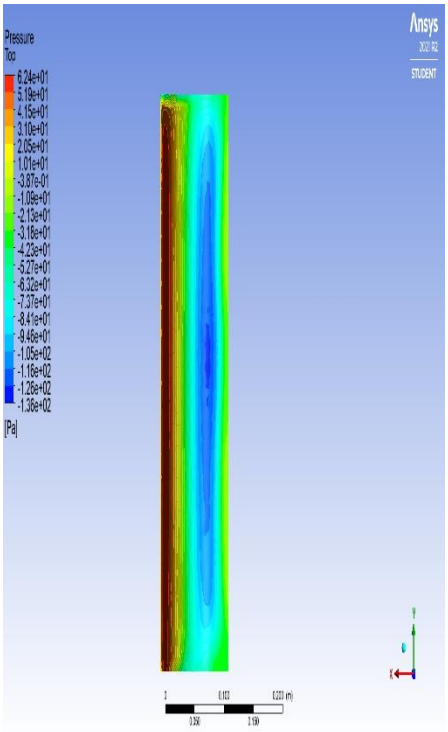

Circle Face C

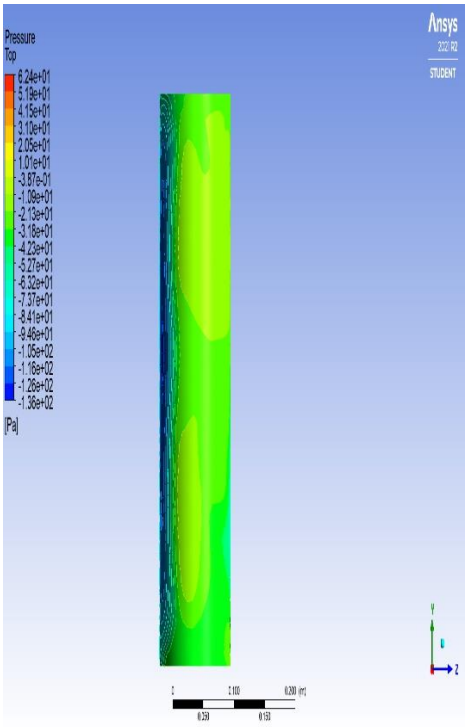

Circle Face D

Figure 5-11 Contour Plots for different faces at 120- degree of incidence for Model 3

4. One eighty-degree contour plot

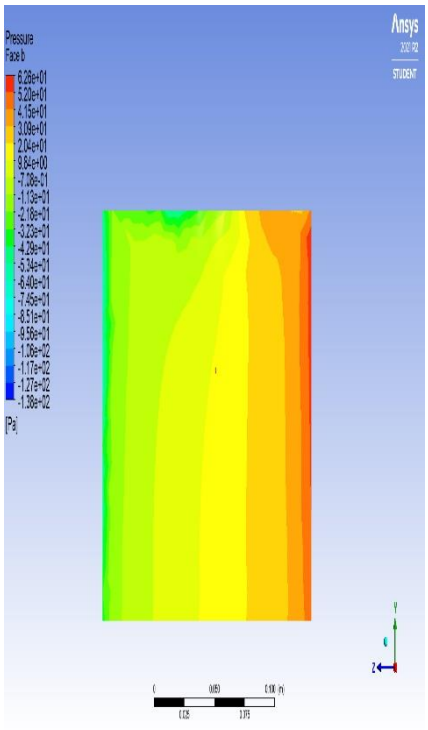

Triangle Face C

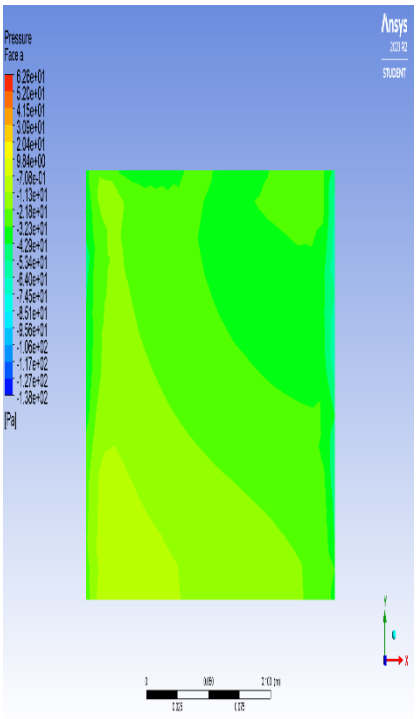

Triangle Face B

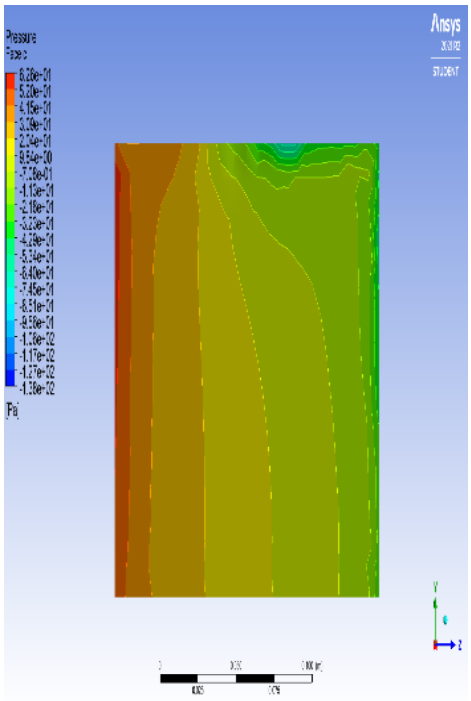

Triangle Face C

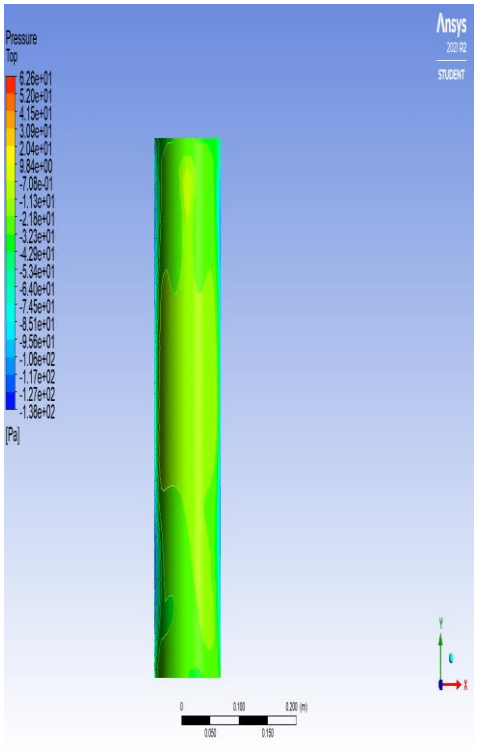

Circle Face A

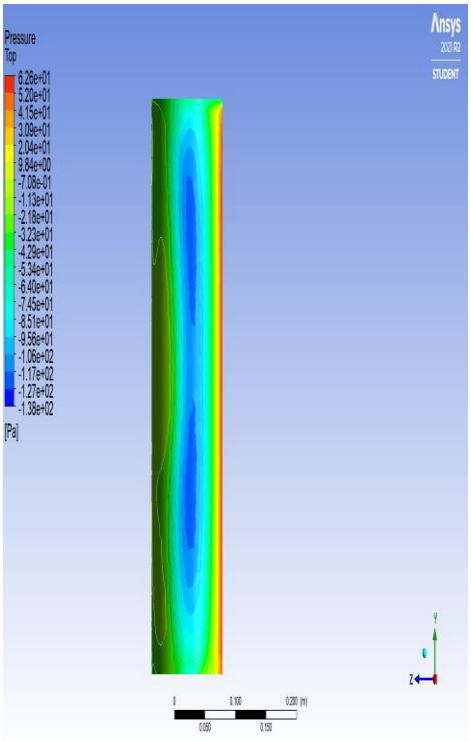

Circle Face B

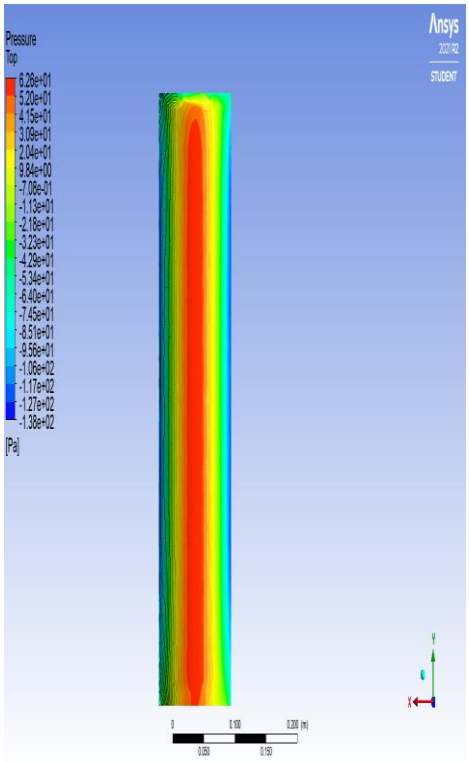

Circle Face C

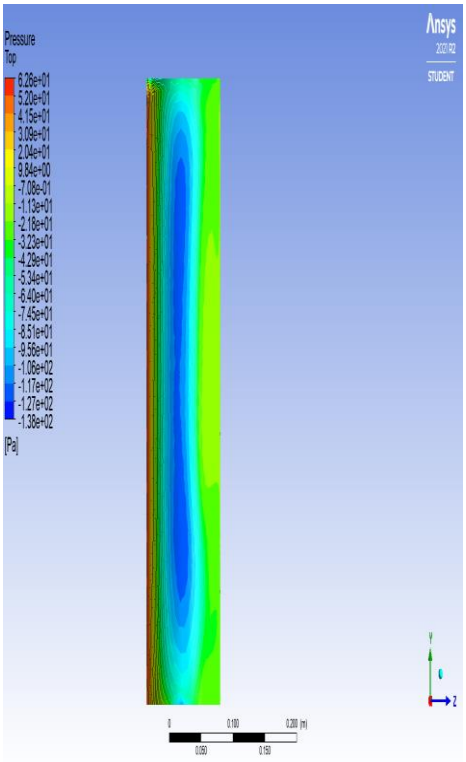

Circle Face D

Figure 5-12 Contour Plots for different faces at 180- degree of incidence for Model

MODEL 4

Model- 4 (500 triangle)

- The pressure contours for different faces at various angles of incidence are depicted in fig. 5-13 to 5-16 and illustrated the pressure distribution on faces.
- Initially, at 0 degree of incidence face A shows a positive pressure being the windward face of the triangular building whereas face B and C depicts a negative pressure distribution being the leeward and side wall face of the building.
- At 60° and 120° angles of incidence, positive pressure distribution at face A is slightly less than at 0°, while suction pressure increases at face C in triangular building, resulting in an equivalent change in the pressure coefficient data obtained as a result.
- When the angle of incidence is 180°, face C becomes windward in triangular building and the contour plot pattern is similar to that of face A when angle of attack was 0°.

1. zero-degree contour plot

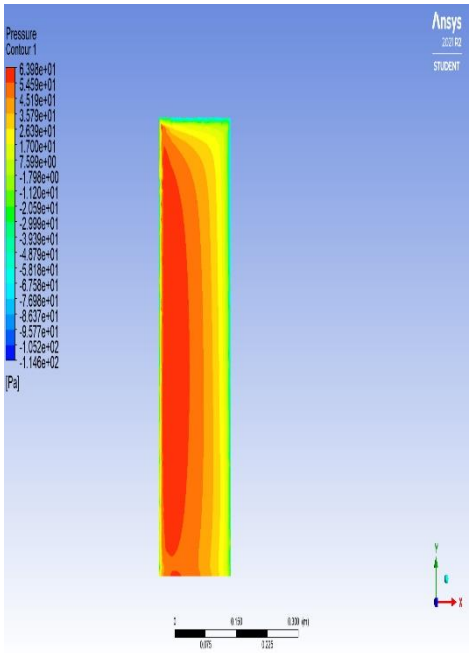

Triangle Face A

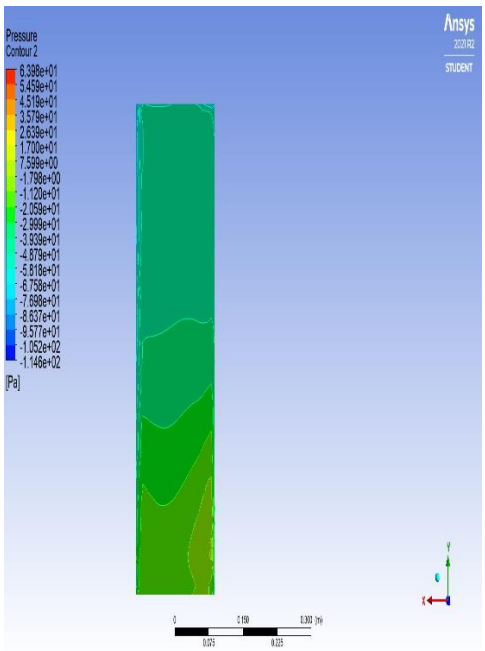

Triangle Face B

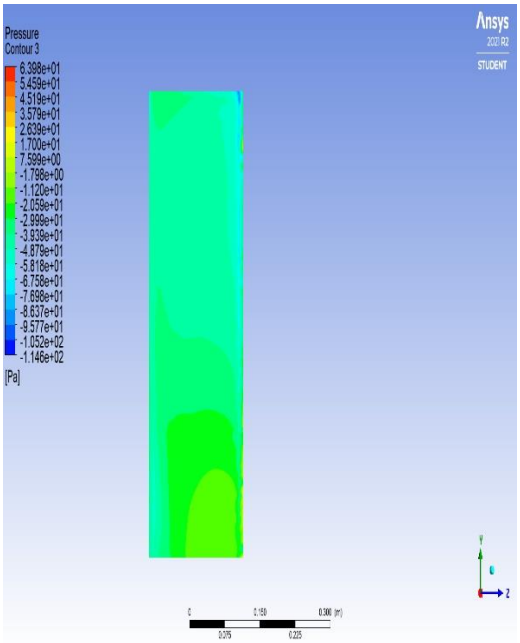

Triangle Face C

Figure 5-13 Contour Plots for different faces at 0- degree of incidence for Model 4

2. sixty-degree contour plot

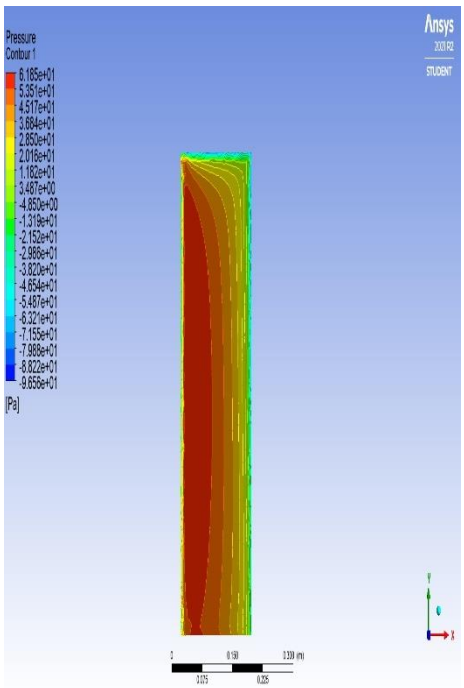

Triangle Face A

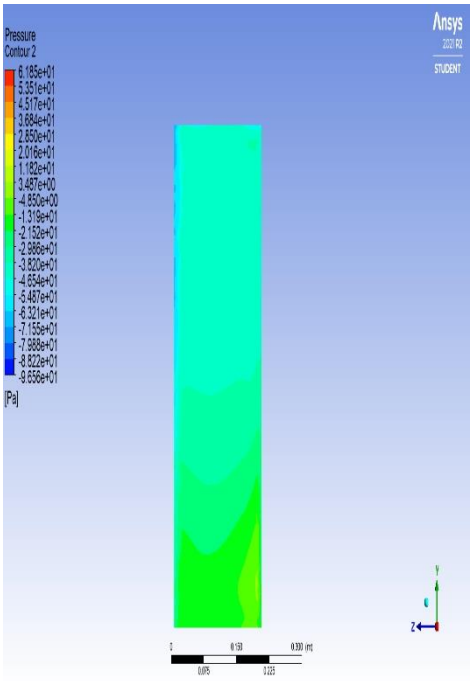

Triangle Face B

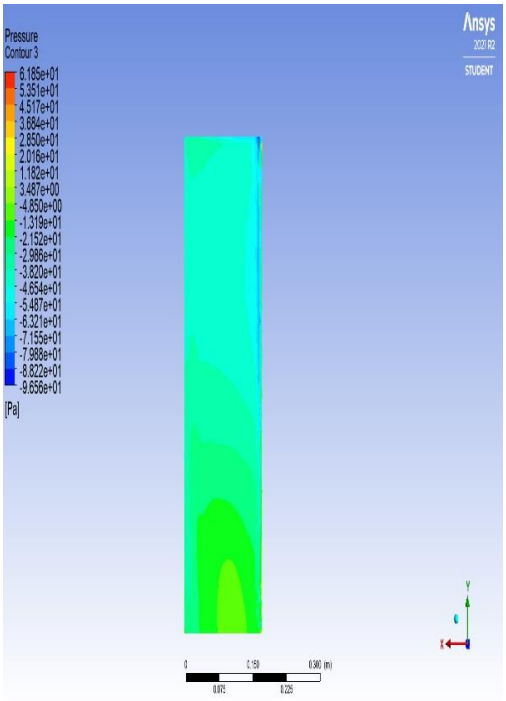

Triangle Face C

Figure 5-14 Contour Plots for different faces at 60- degree of incidence for Model 4

3. One twenty-degree contour plot

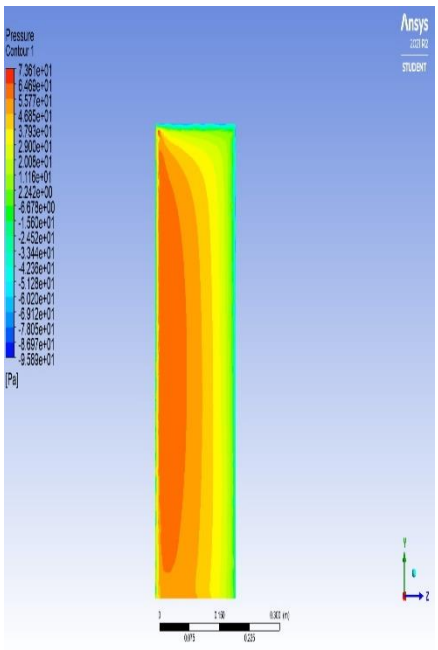

Triangle Face A

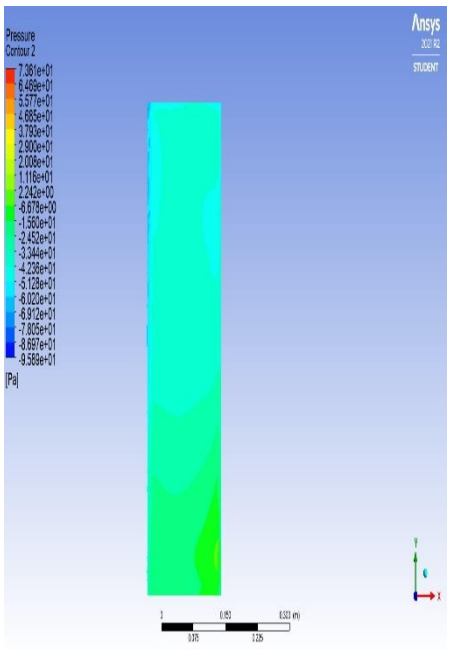

Triangle Face B

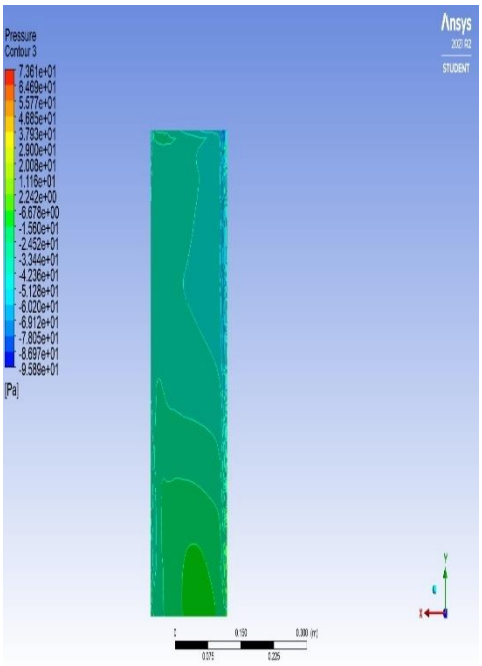

Triangle Face C

Figure 5-15 Contour Plots for different faces at 120- degree of incidence for Model 4

4. One eighty-degree contour plot

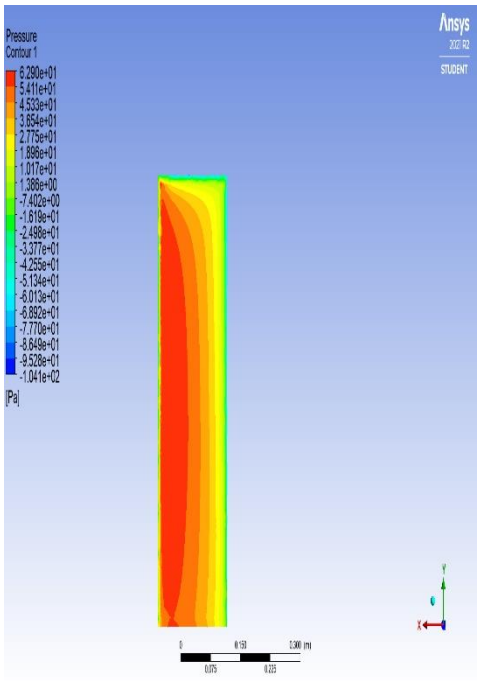

Triangle Face A

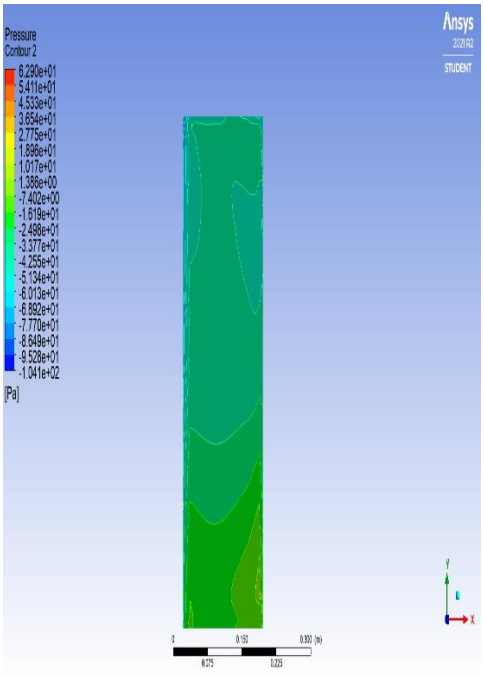

Triangle Face B

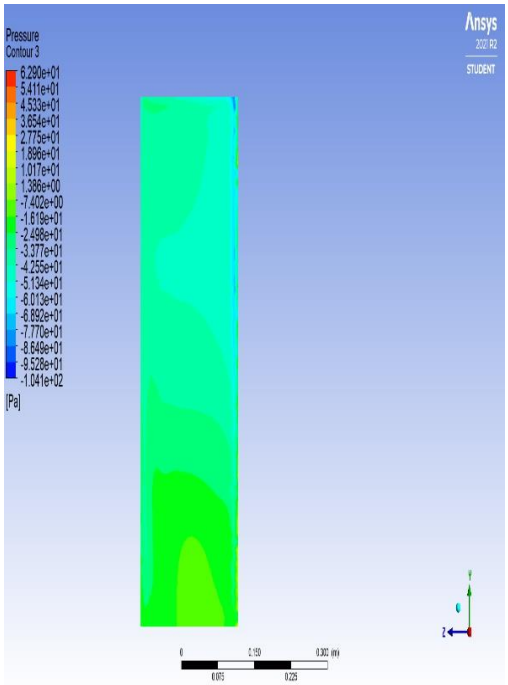

Triangle Face C

Figure 5-16 Contour Plots for different faces at 180- degree of incidence for Model 4

5.2 Velocity Distribution

The velocity variation at various faces of Buildings at different angles are as shown using contour plots.

1. **Model- 1 (375 triangle 125 circle)**

- Figure 5-17 exhibit the velocity distribution on different faces at different angles of incidence.
- At Wind velocity and pressure are at their highest on the building's windward side.
- At 0° and 180° vortex shedding is maximum and can be seen in the fig.
- At 60° and 120° vortex shedding is minimum.
- Wind velocity and pressure is varying at different angle of incidence.
- Red The red line represents the maximum wind velocity and speed, while the blue line represents the minimum wind velocity and speed.

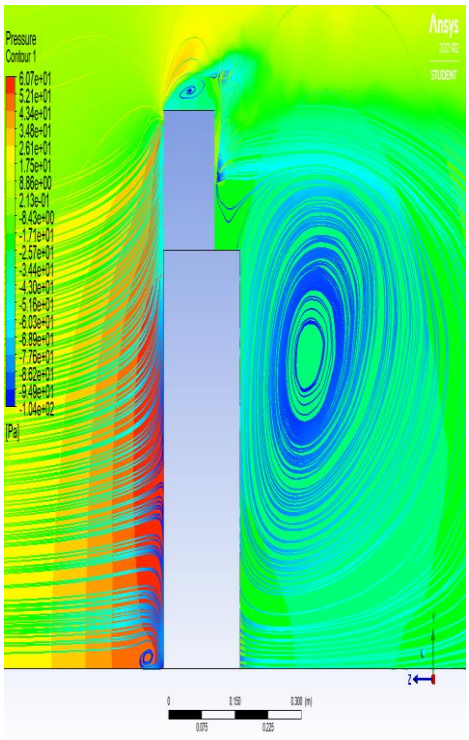

Zero-degree

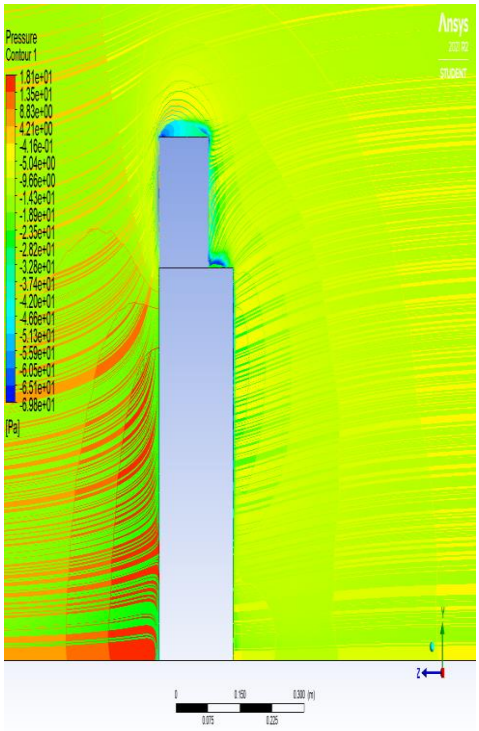

Sixty degree

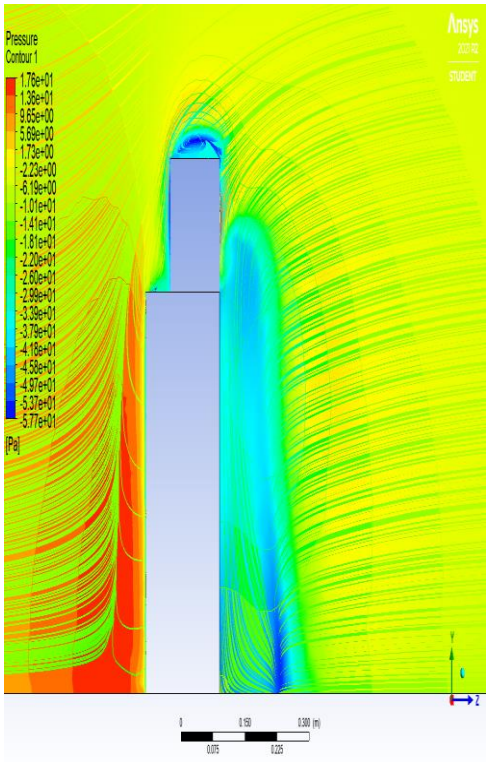

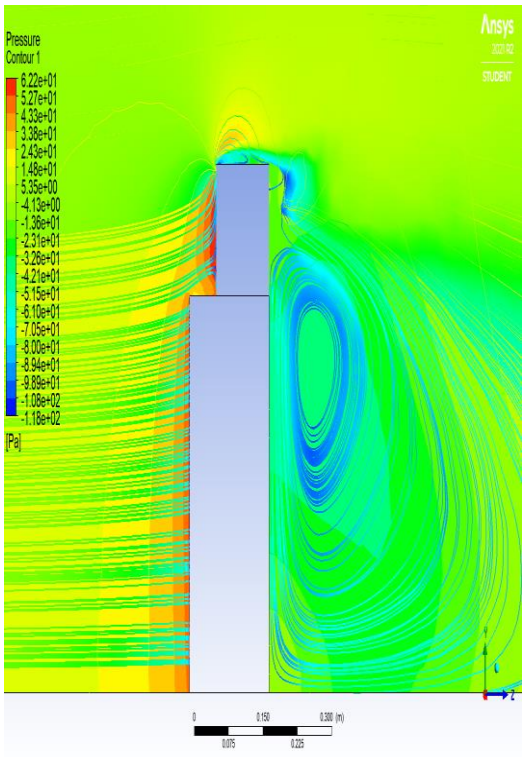

One twenty degree **One eighty degree**

Figure 5-17 Velocity Streamline Plots for different faces at different degree of incidence for Model 1

2. Model- 2 (250 triangle 250 circle)

- Figure 5-18 exhibit the velocity distribution on different faces at different angles of incidence.
- At windward face of the building wind velocity and wind pressure is maximum.
- At 0° and 180° vortex shedding is maximum and can be seen in the fig.
- At 60° and 120° vortex shedding is minimum.
- Wind velocity and pressure is varying at different angle of incidence.
- Red line shows the maximum wind velocity and wind speed whereas blue line shows minimum wind velocity and speed.

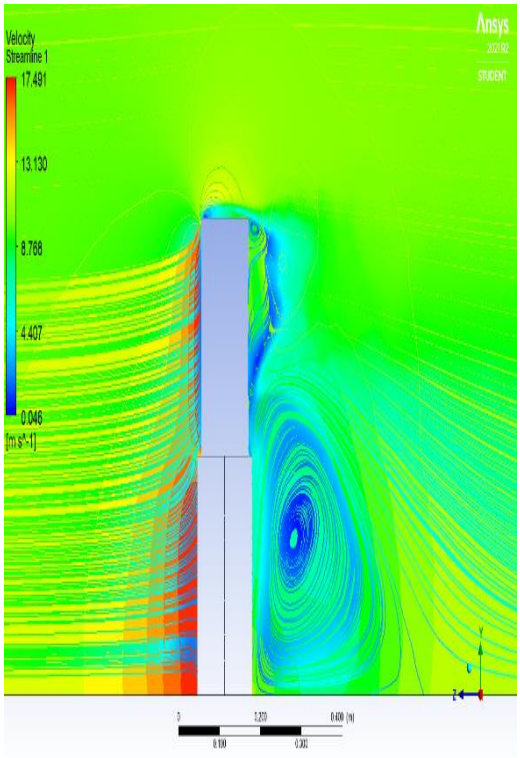

zero-degree

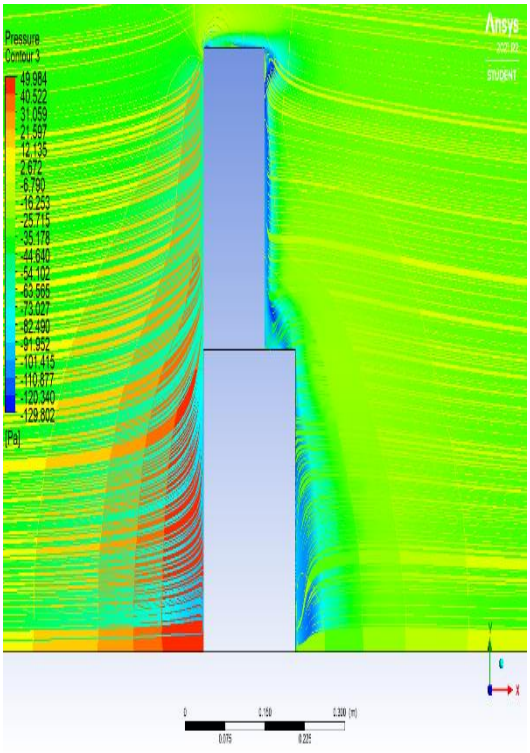

sixty degree

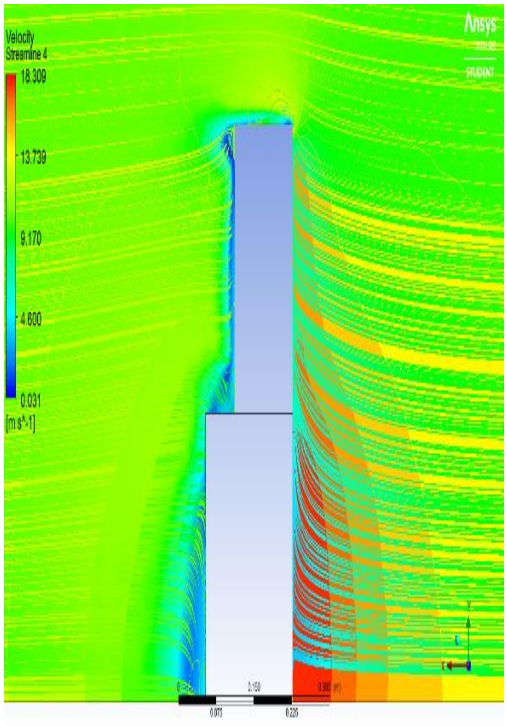

One twenty degree

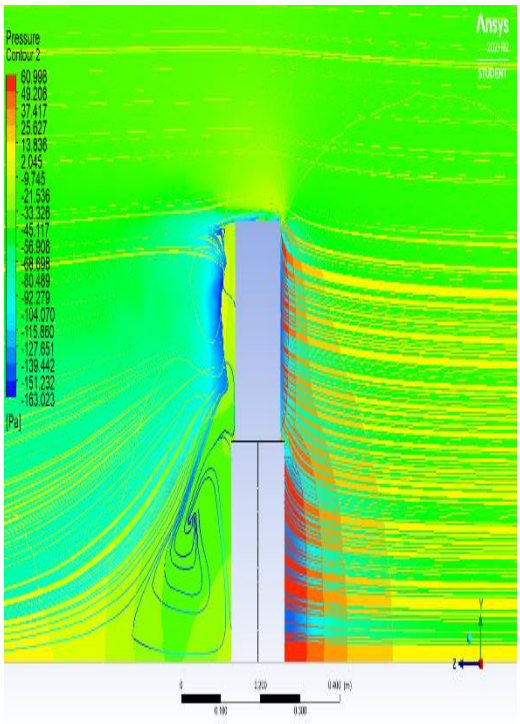

One eighty degree

Figure 5-18 Velocity Streamline Plots for different faces at different degree of incidence for Model 2

3. Model- 3 (125 triangle 375 circle)

- Figure 5-19 exhibit the velocity distribution on different faces at different angles of incidence.
- At Wind velocity and pressure are at their highest on the building's windward side.
- At 0° and 180° vortex shedding is maximum and can be seen in the fig.
- At 60° and 120° vortex shedding is minimum.
- Wind velocity and pressure is varying at different angle of incidence.
- Red line shows the maximum wind velocity and wind speed whereas blue line shows minimum wind velocity and speed.

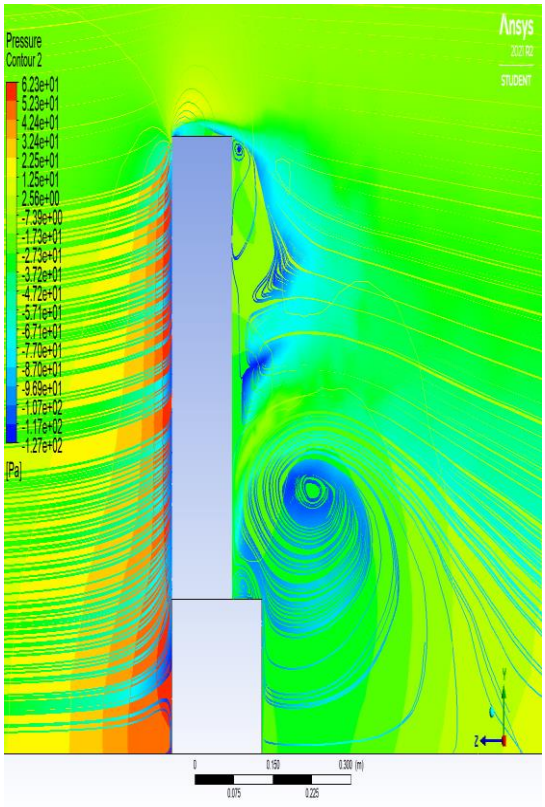

zero-degree

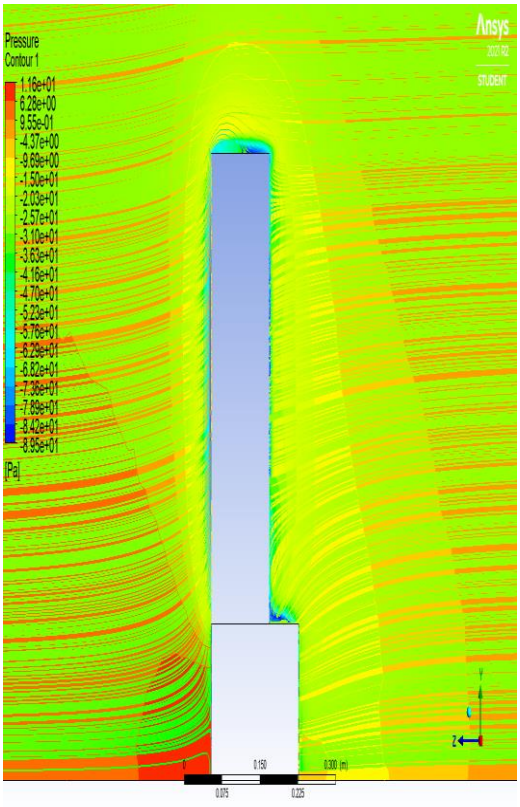

sixty degree

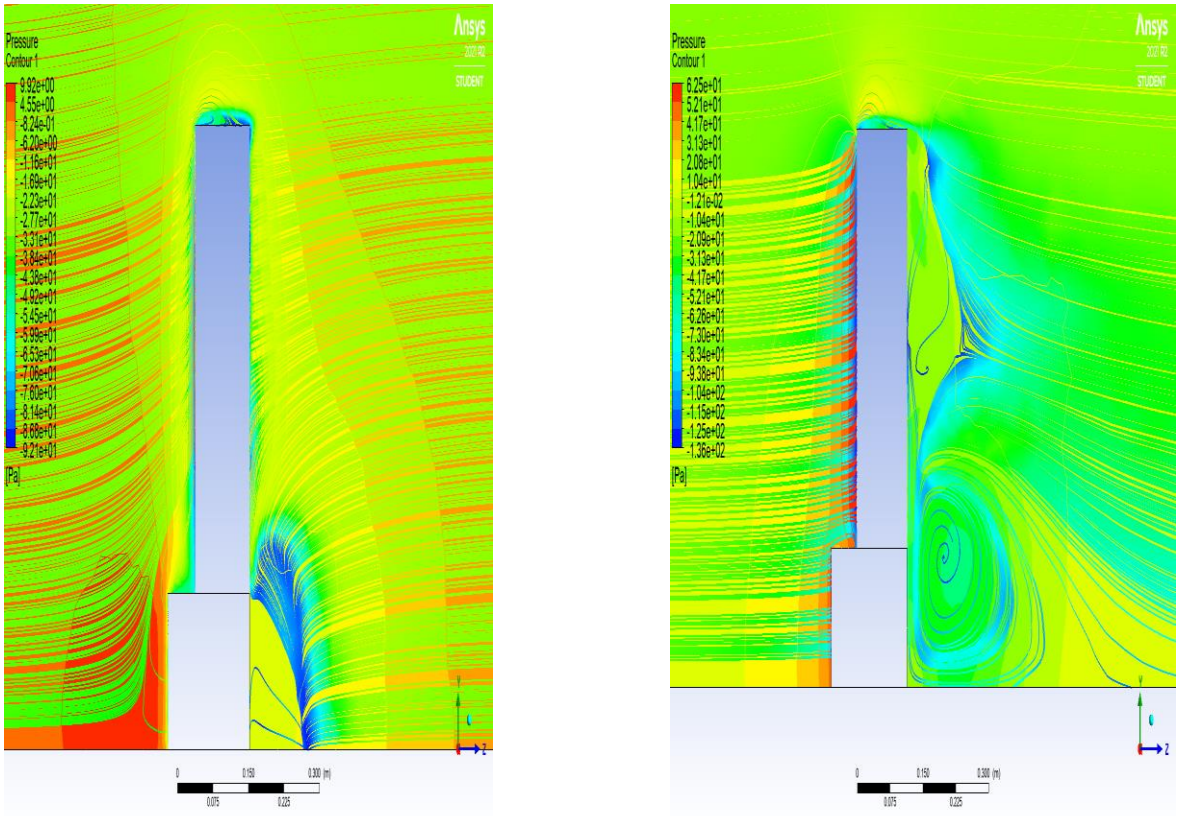

One twenty degree **One eighty degree**

Figure 5-19 Velocity Streamline Plots for different faces at different degree of incidence for Model 3

4. Model- 4 (500 triangle)

- Figure 5-20 exhibit the velocity distribution on different faces at different angles of incidence.
- At windward face of the building wind velocity and wind pressure is maximum.
- At 0° and 180° vortex shedding is maximum and can be seen in the fig.
- At 60° and 120° vortex shedding is minimum.
- Wind velocity and pressure is varying at different angle of incidence.
- Red line shows the maximum wind velocity and wind speed whereas blue line shows minimum wind velocity and speed.

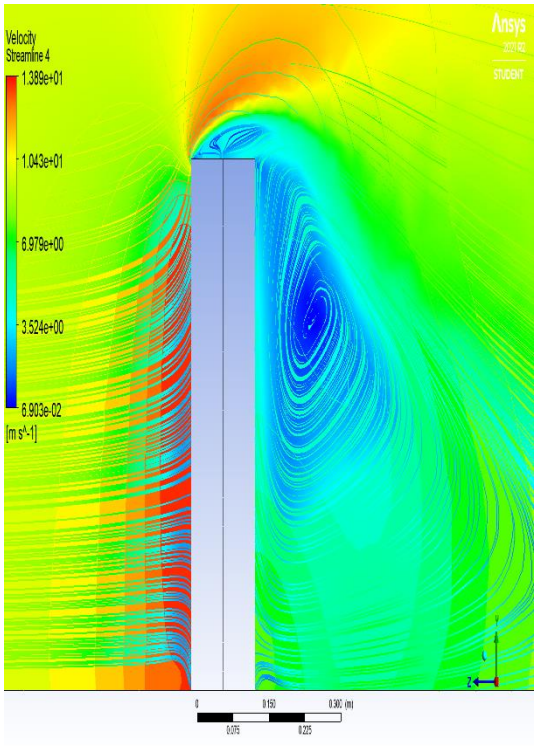

zero degree

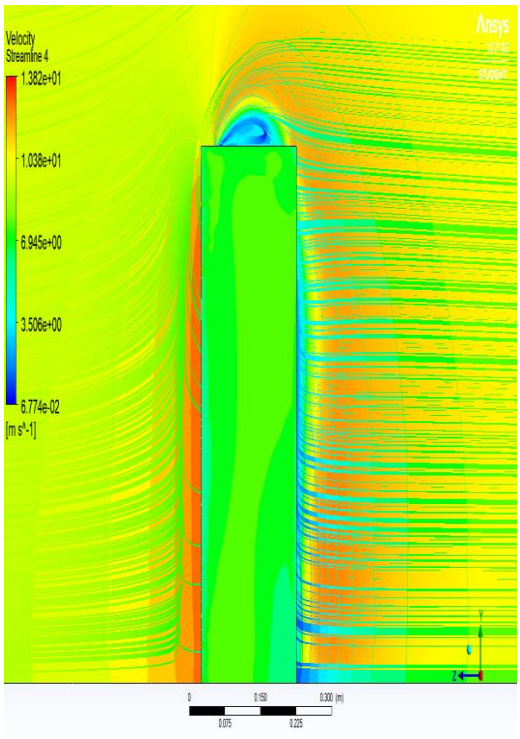

sixty degree

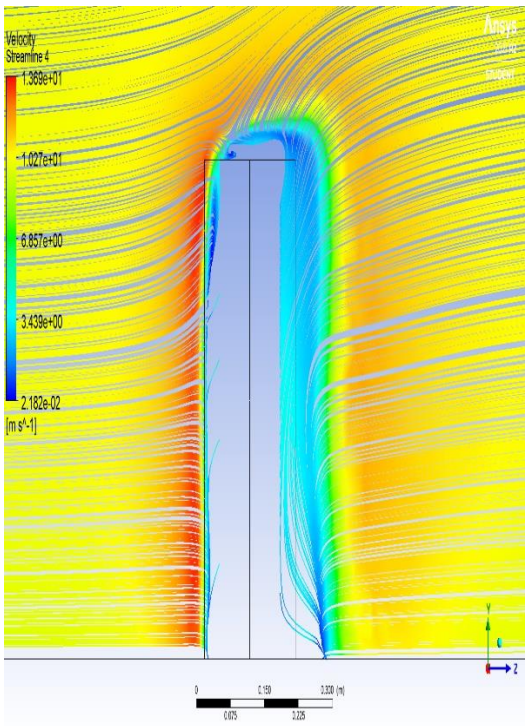

One twenty degree

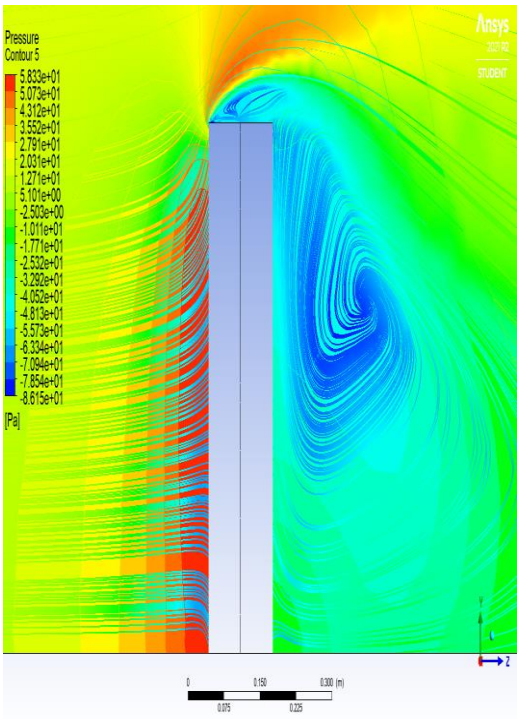

One eighty degree

Figure 5-20 Velocity Streamline Plots for different faces at different degree of incidence for Model 4

5.3 Vertical Centerline Pressure Coefficients

The curve in these figures depicts the variation in the pressure coefficient Cp value for various faces of the building as a function of height.

MODEL 1 (375 TRIANGLE 125 CIRCLE)

- The curve in these figures 5-21 to 5-27 depicts the variation in the pressure coefficient Cp value for various faces as a function of height. Therefore, the face average value of Cp for several models at various angles of incidence are evaluated.
- For faces A of the triangular building the mean face average values of Cp at 0°,60°,120° and 180°angle of attack are +.75, +0.2, -.0.3, and -0.15, respectively.
- The face average Cp values for face B at 0°, 60°, 120° and 180° are -.38, -.40, -.55, and -.28, respectively.
- The face average Cp values for face C at 0°, 60°, 120° and 180° are -.35, +.90, +.82, and -.50 respectively.

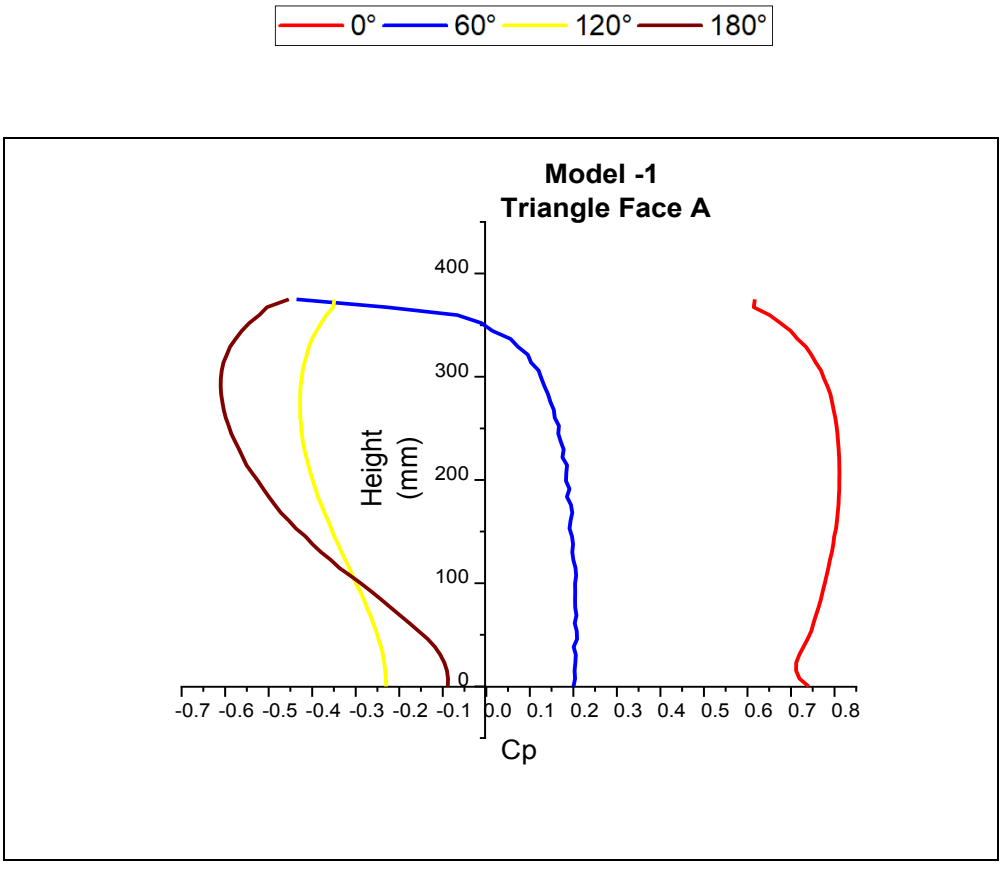

Figure 5-21 Face A pressure variation along the Centerline for all degrees of AOA of model 1

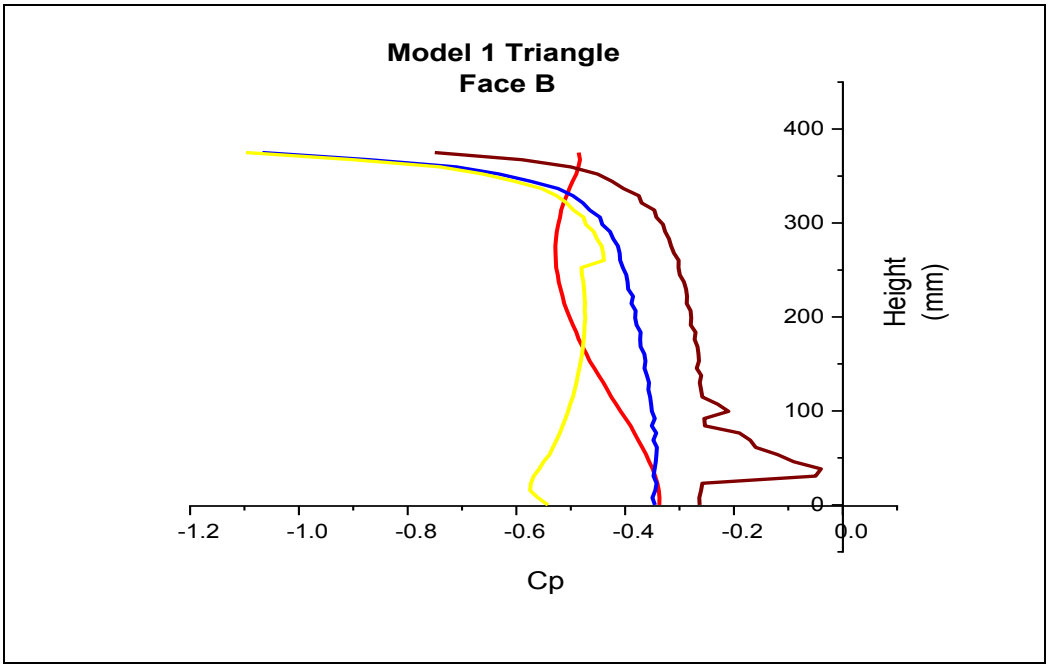

Figure 5-22 Face B pressure variation along the centerline for all degrees of AOA of model 1

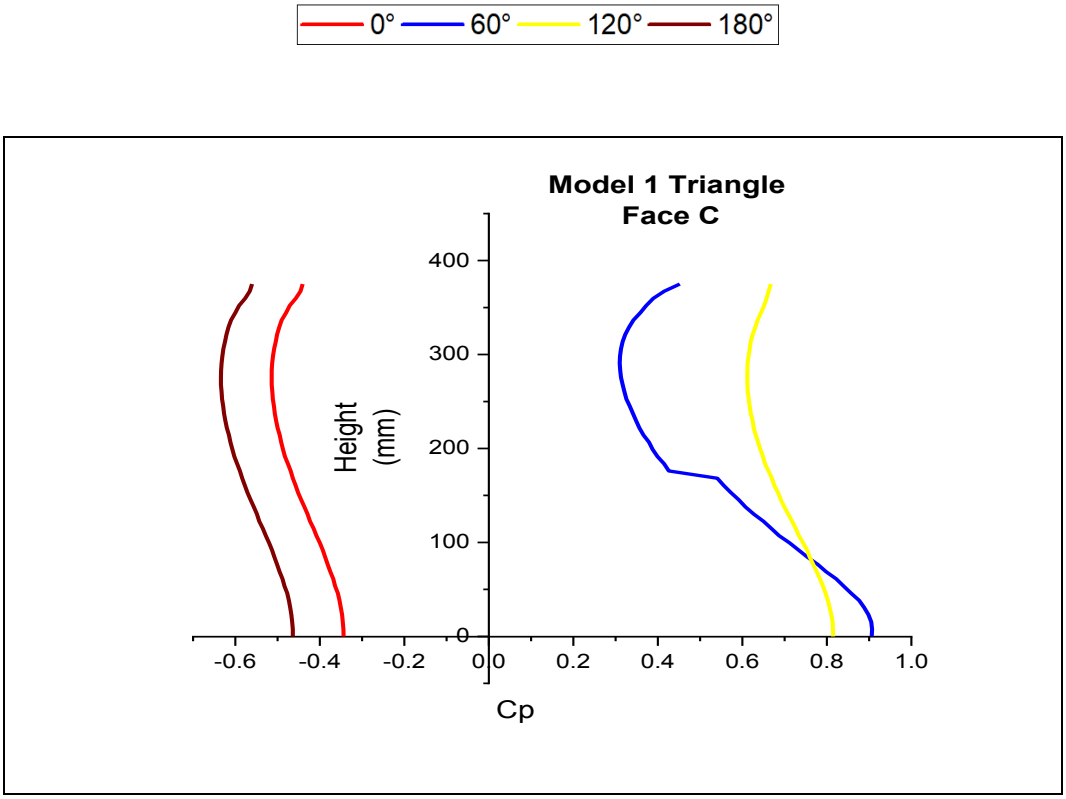

Figure 5-23 For all degrees of AOA in the model, pressure variation along the centerline for face C.

- For faces A of the circular building the mean face average values of Cp at 0°,60°,120° and 180°angle of attack are +.65, -0.28, -.0.38, and -0.39 respectively.
- For faces B of the circular building the mean face average values of Cp at 0°,60°,120° and 180°angle of attack are -1.8, -0.28, -2.3, and -2.4 respectively.
- For faces C of the circular building the mean face average values of Cp at 0°,60°,120° and 180°angle of attack are -.25, -0.22, +.0.82, and +0.80 respectively.
- For faces D of the circular building the mean face average values of Cp at 0°,60°,120° and 180°angle of attack are -2.0, +0.9, -2.2, and -2.3 respectively.

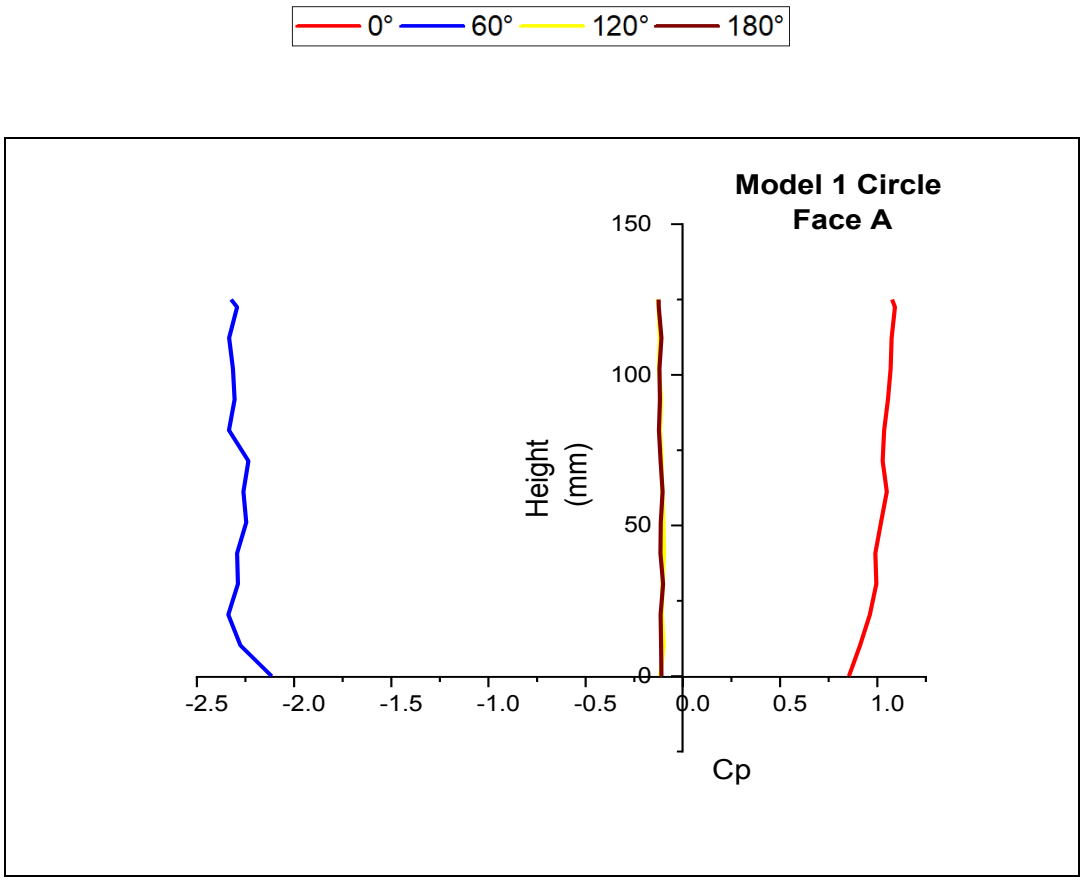

Figure 5-24 Face A pressure variation along the Centerline for all degrees of AOA of model 1

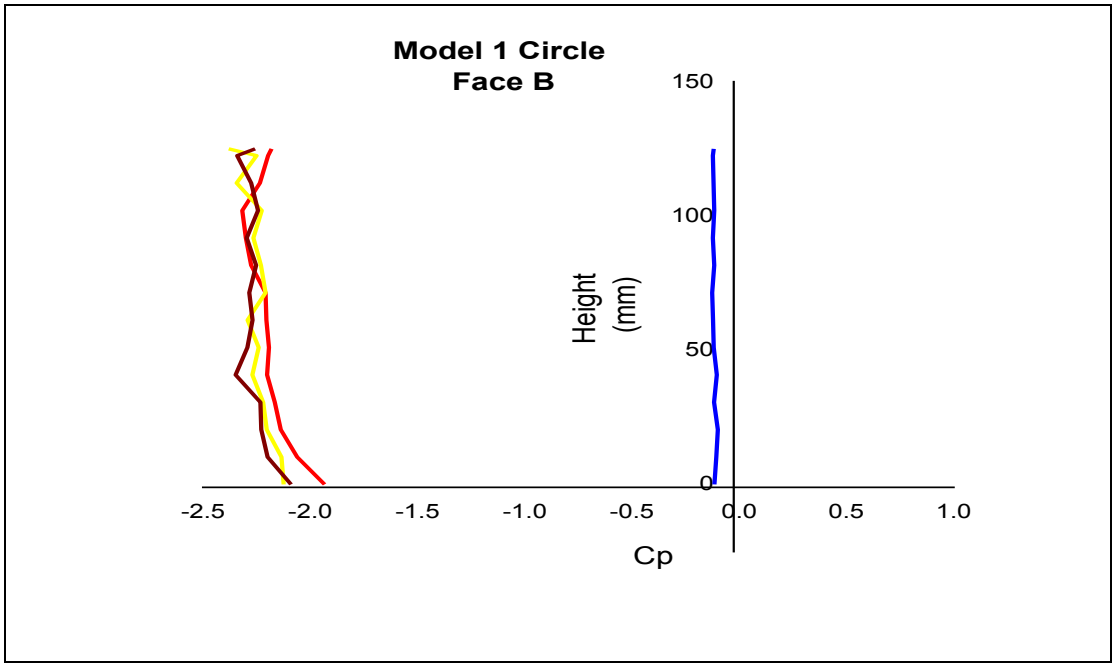

Figure 5-25 Face B pressure variation along the centerline for all degrees of AOA of model 1

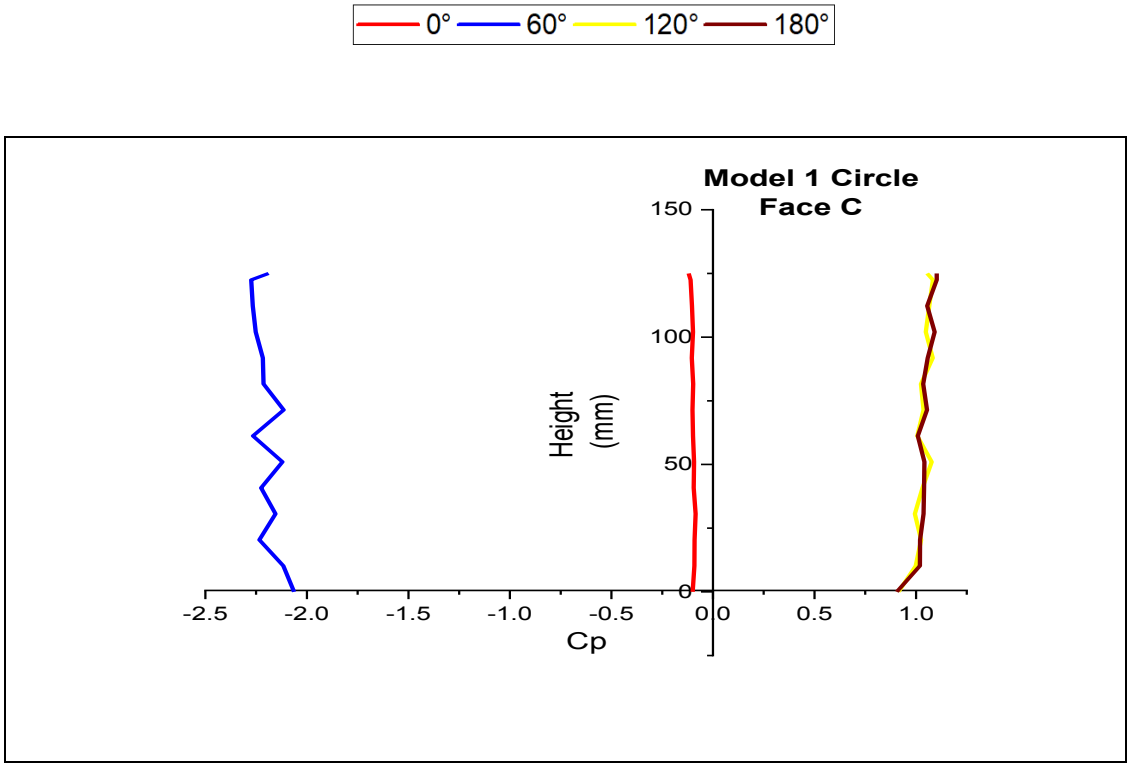

Figure 5-26 For all degrees of AOA in the model, pressure variation along the centerline for face C

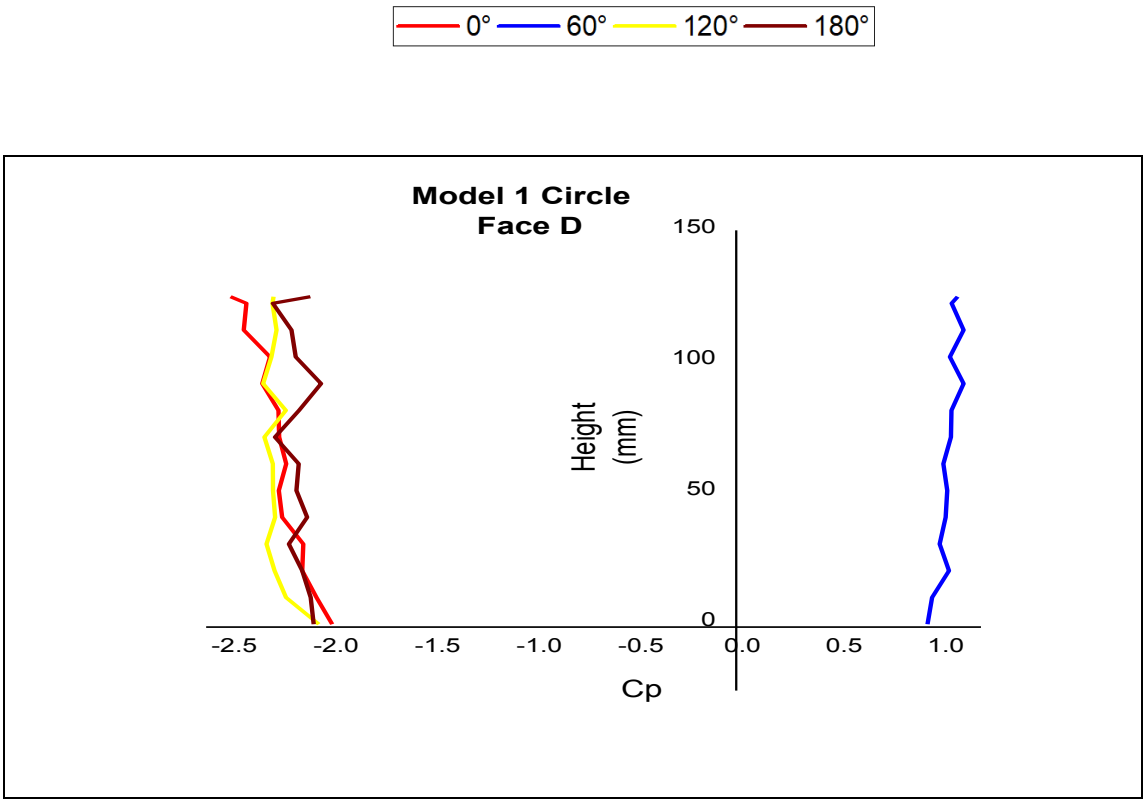

Figure 5-27 For all degrees of AOA in the model, pressure variation along the centerline for face D

MODEL 2 (250 TRIANGLE 250 CIRCLE)

- The Cp Variation along the centerline for all the faces at different angle of incidences are depicted in fig 5-28 to 5-34.
- For faces A of the triangular building the mean face average values of Cp at 0°,60°,120° and 180°angle of attack are +.78, -0.1, -.0.2, and -0.4 respectively.
- For faces B of the triangular building the mean face average values of Cp at 0°,60°,120° and 180°angle of attack are -.78, -.74, -.80, and -.72 respectively.
- For faces C of the triangular building the mean face average values of Cp at 0°,60°,120° and 180°angle of attack are -.48, +0.9, +.82, and -0.49 respectively.

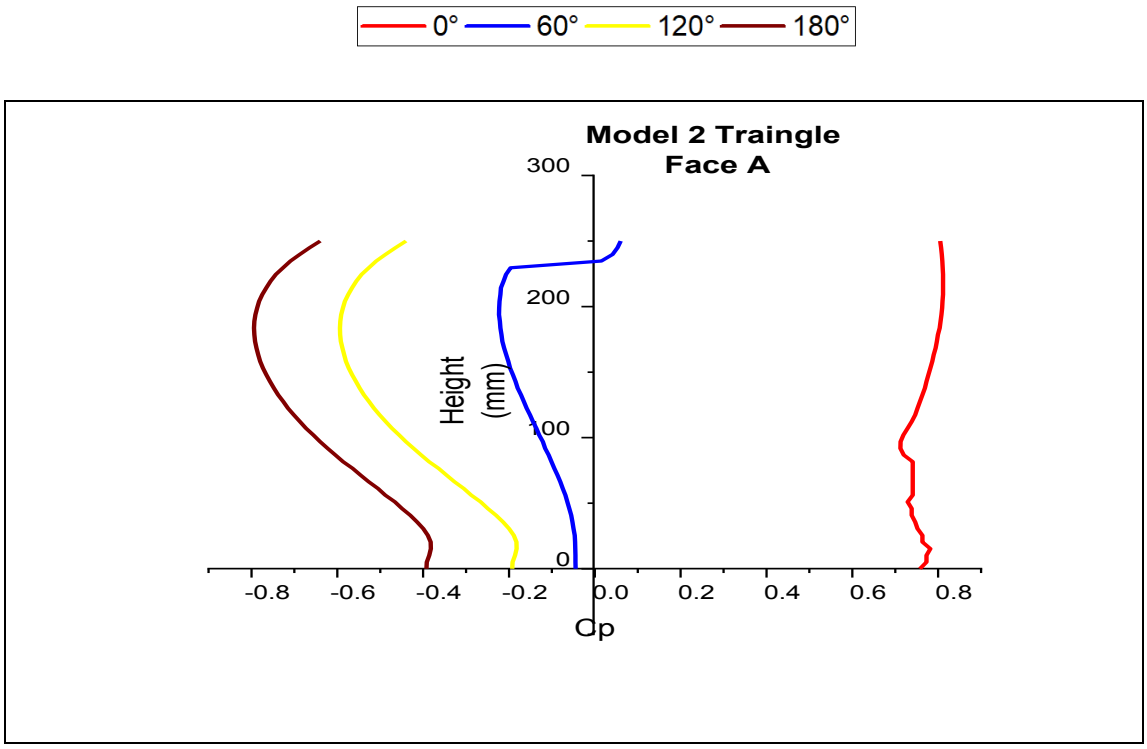

Figure 5-28 Face A pressure variation along the Centerline for all degrees of AOA of model 2

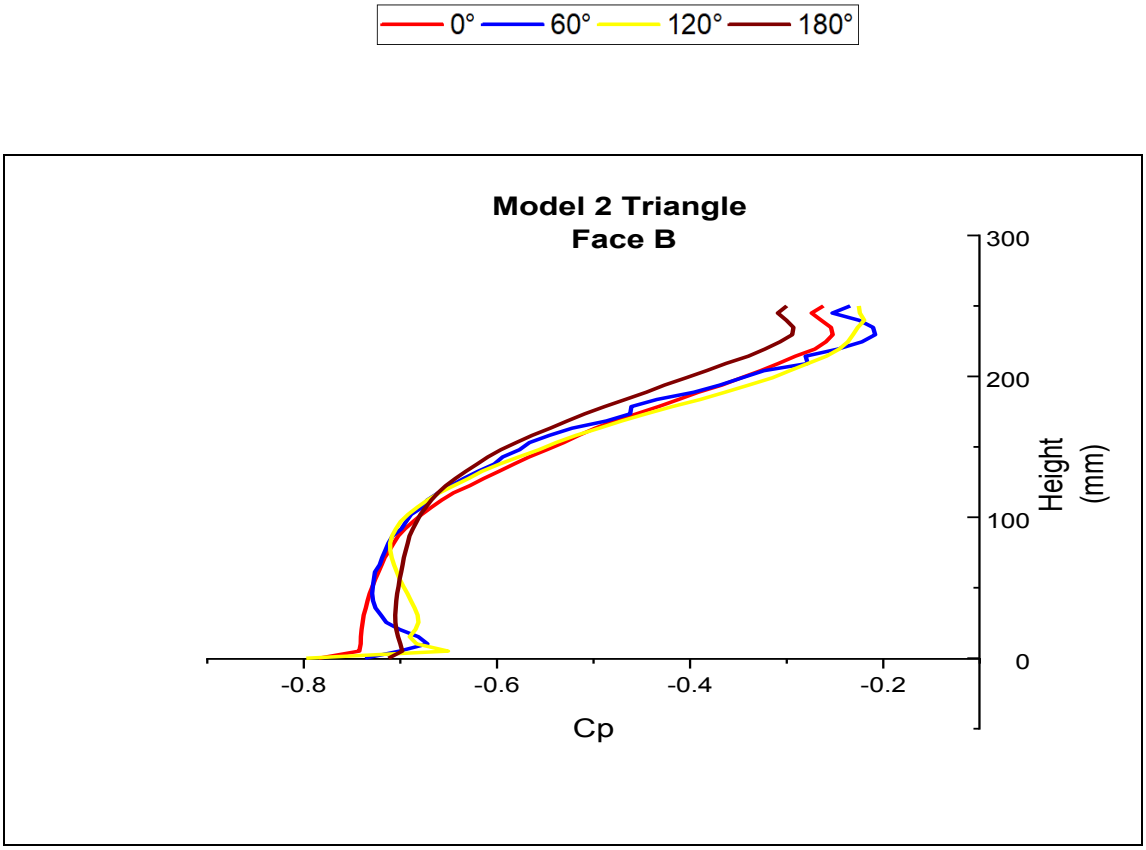

Figure 5-29 Face B pressure variation along the Centerline for all degrees of AOA of model 2

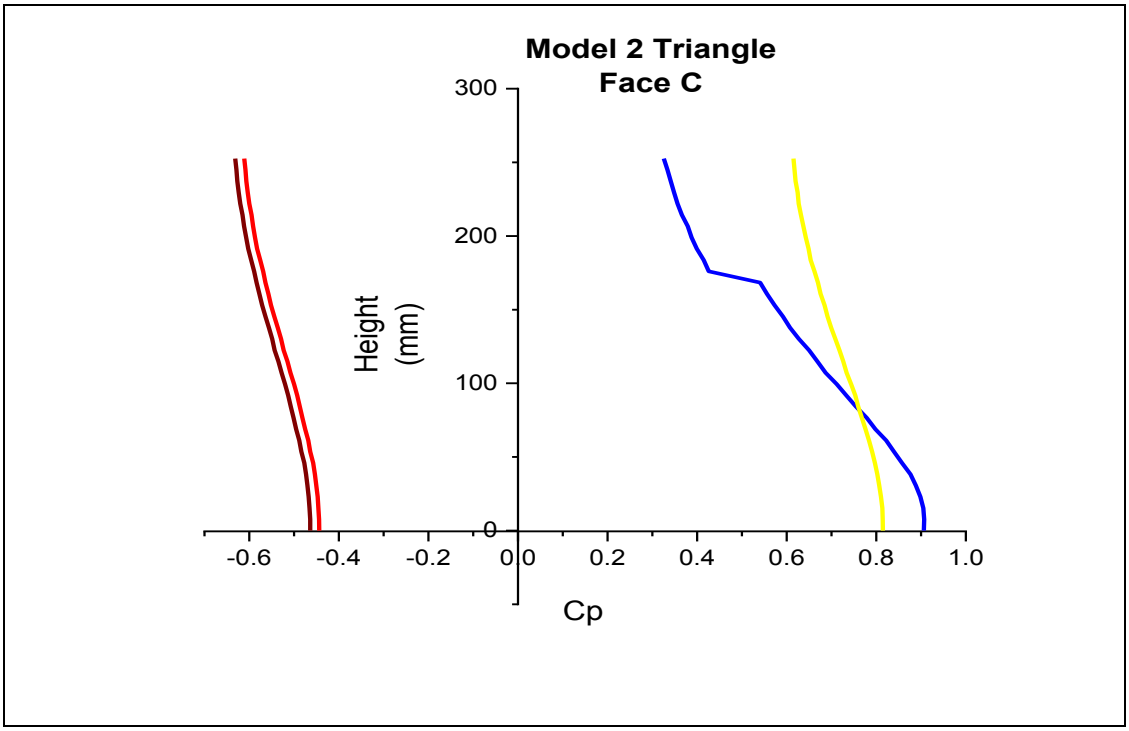

Figure 5-30 Face C pressure variation along the Centerline for all degrees of AOA of model 2

- For faces A of the circular building the mean face average values of Cp at 0°,60°,120° and 180°angle of attack are +1.2, -2.3, -0.3, and -0.2 respectively.
- For faces B of the circular building the mean face average values of Cp at 0°,60°,120° and 180°angle of attack are -2.3, -0.2, -2.2, and -2.4 respectively.
- For faces C of the circular building the mean face average values of Cp at 0°,60°,120° and 180°angle of attack are -.22, -2.25, +1.2, and +.80 respectively.
- For faces D of the circular building the mean face average values of Cp at 0°,60°,120° and 180°angle of attack are -2.5, +1.0, -2.0, and -2.25 respectively.

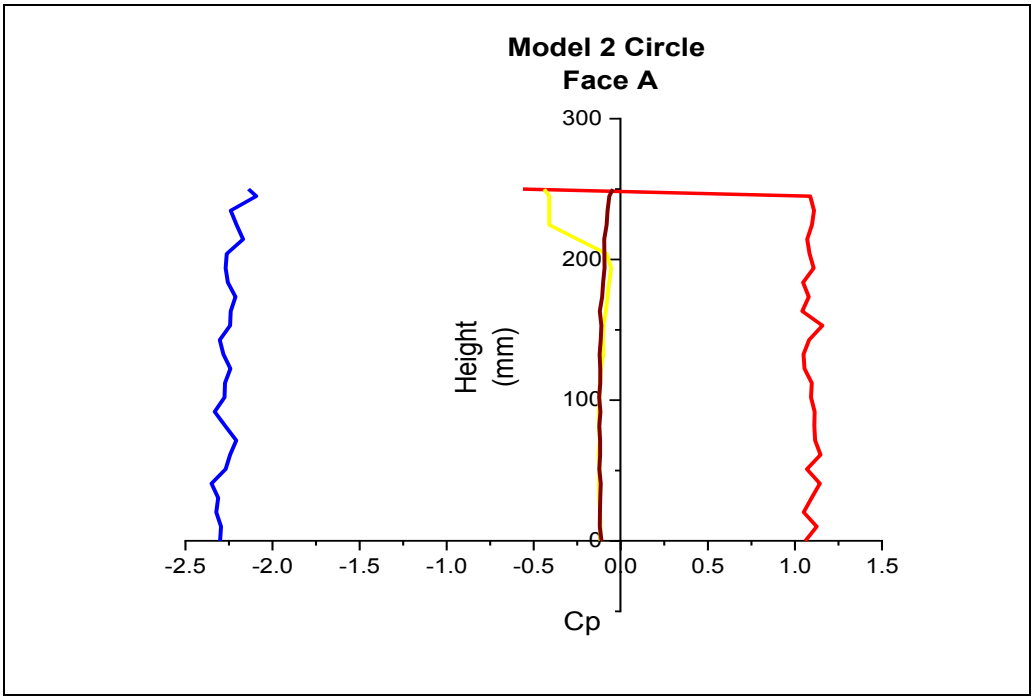

Figure 5-31 Face A pressure variation along the Centerline for all degrees of AOA of model 2

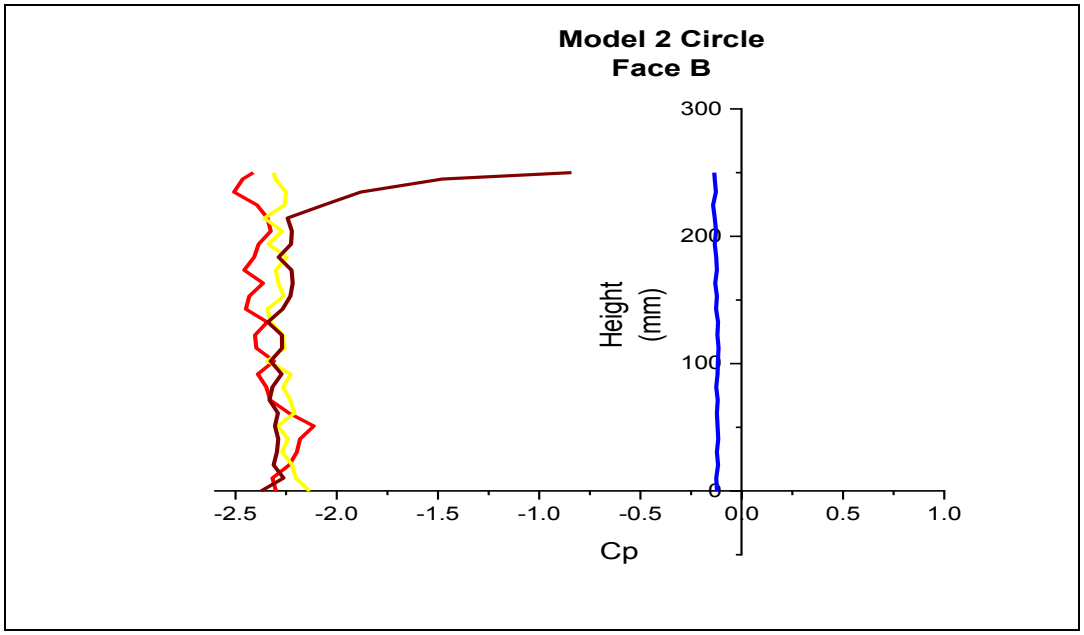

Figure 5-32 Face B pressure variation along the Centerline for all degrees of AOA of model 2

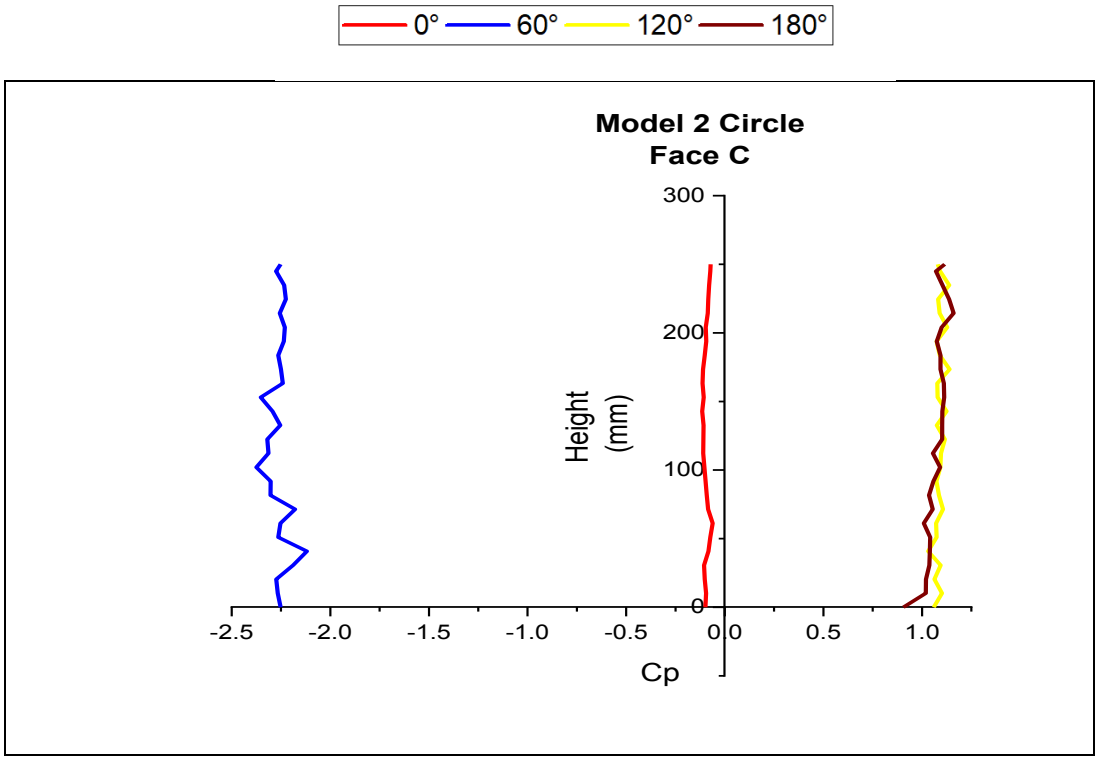

Figure 5-33 Face C pressure variation along the Centerline for all degrees of AOA of model 2

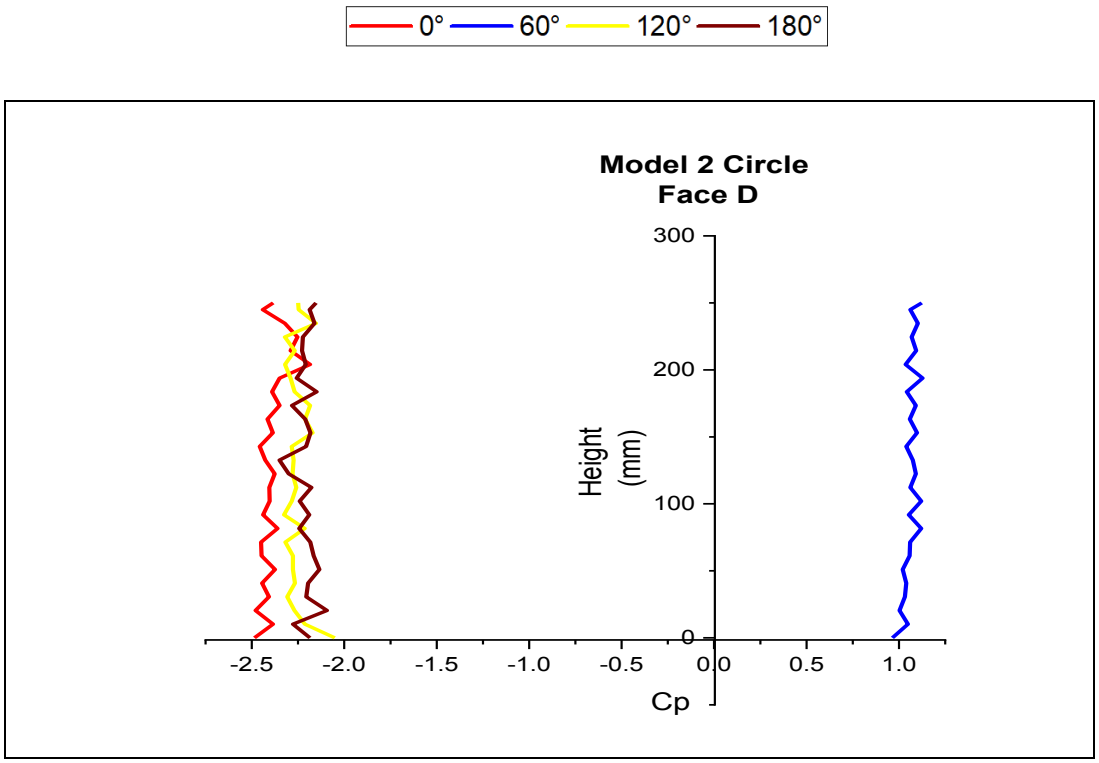

Figure 5-34 Face D pressure variation along the Centerline for all degrees of AOA of model 2

MODEL 3 (125 TRIANGLE 375 CIRCLE)

- The Cp Variation along the centerline for all the faces at different angle of incidences are depicted in fig 5-35 to 5-41.
- For faces A of the triangular building the mean face average values of Cp at 0°,60°,120° and 180°angle of attack are +.78, +0.2, -0.23, and -0.1 respectively.
- For faces B of the triangular building the mean face average values of Cp at 0°,60°,120° and 180°angle of attack are -.62, -.68, -.65, and -.69 respectively.
- For faces C of the triangular building the mean face average values of Cp at 0°,60°,120° and 180°angle of attack are -.48, +0.9, +.80, and -0.49 respectively.

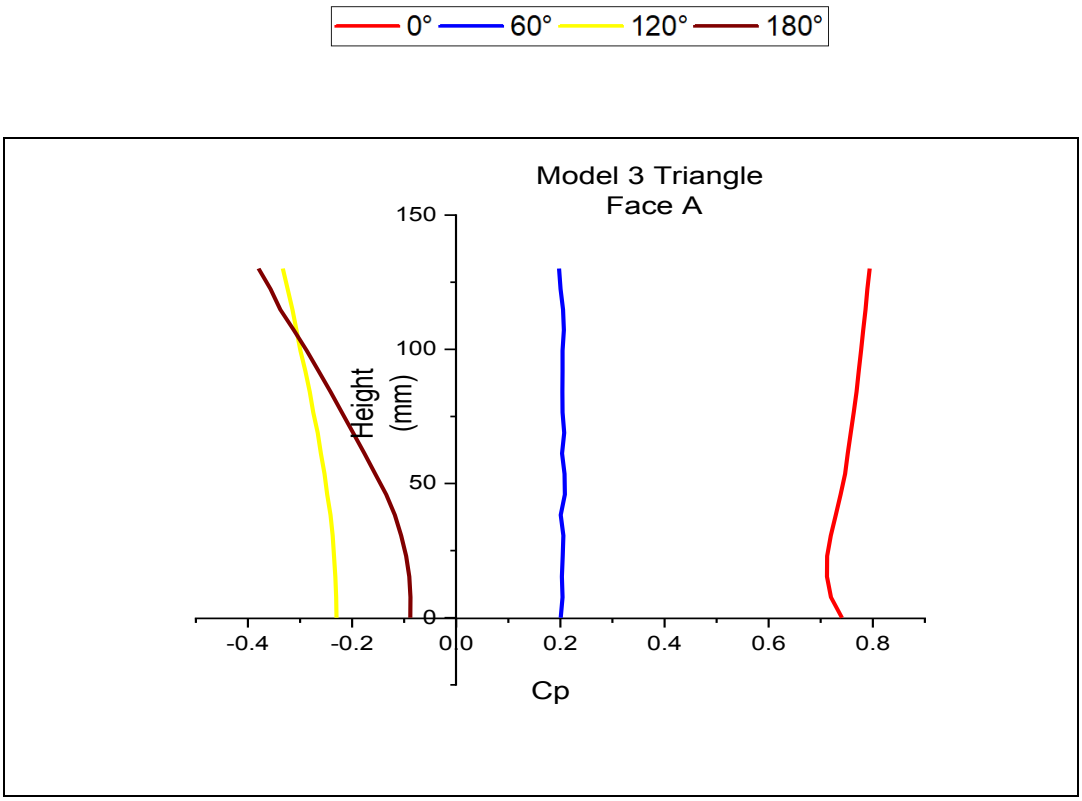

Figure 5-35 Pressure Variation along Centerline for face A for all degrees AOA of model 3

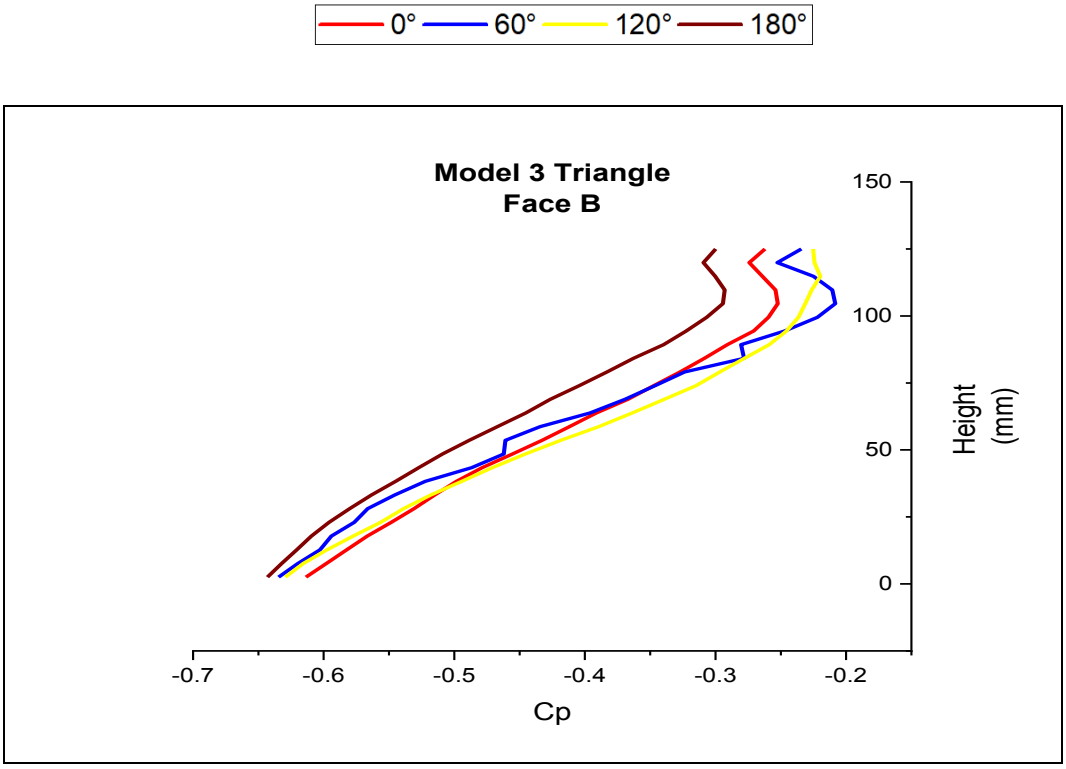

Figure 5-36 Pressure Variation along Centerline for face B for all degrees AOA of model

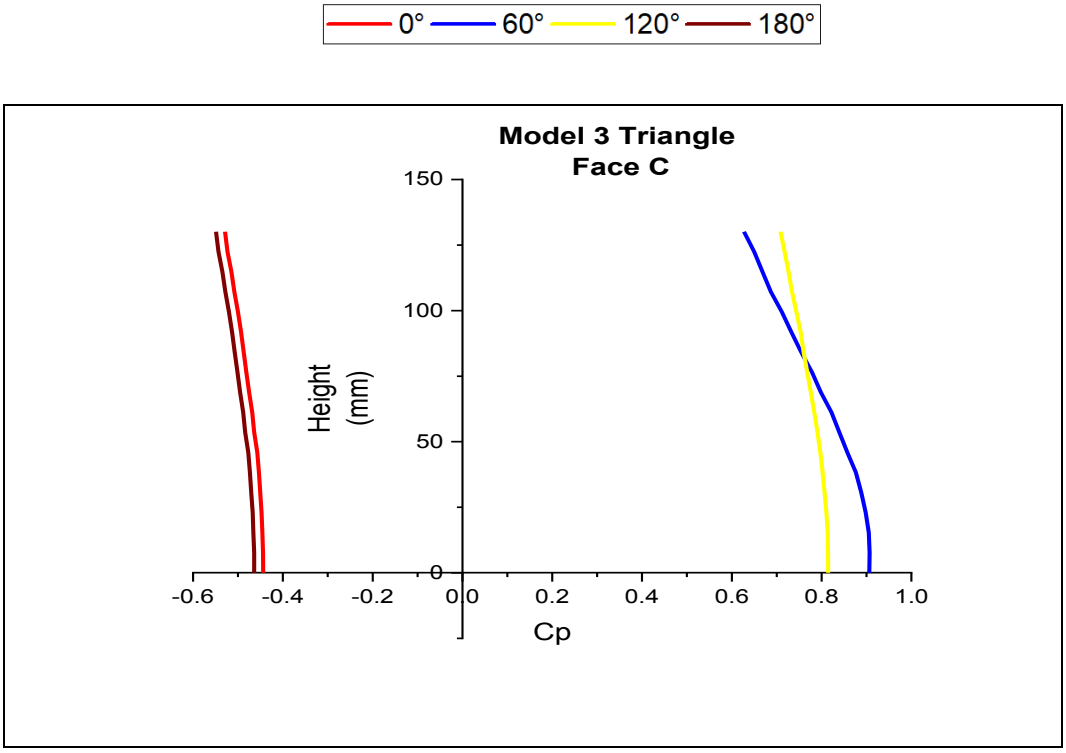

Figure 5-37 Pressure Variation along Centerline for face C for all degrees AOA of model 3

- For faces A of the circular building the mean face average values of Cp at 0°,60°,120° and 180°angle of attack are +.8, -2.2, -0.2, and -0.25 respectively.
- For faces B of the circular building the mean face average values of Cp at 0°,60°,120° and 180°angle of attack are -2.3, -.15, -2.2, and -2.0 respectively.
- For faces C of the circular building the mean face average values of Cp at 0°,60°,120° and 180°angle of attack are -0.1, -2.25, +1.1, and +.80 respectively.
- For faces D of the circular building the mean face average values of Cp at 0°,60°,120° and 180°angle of attack are -1.25, +0.9, -2.0, and +0.89 respectively.

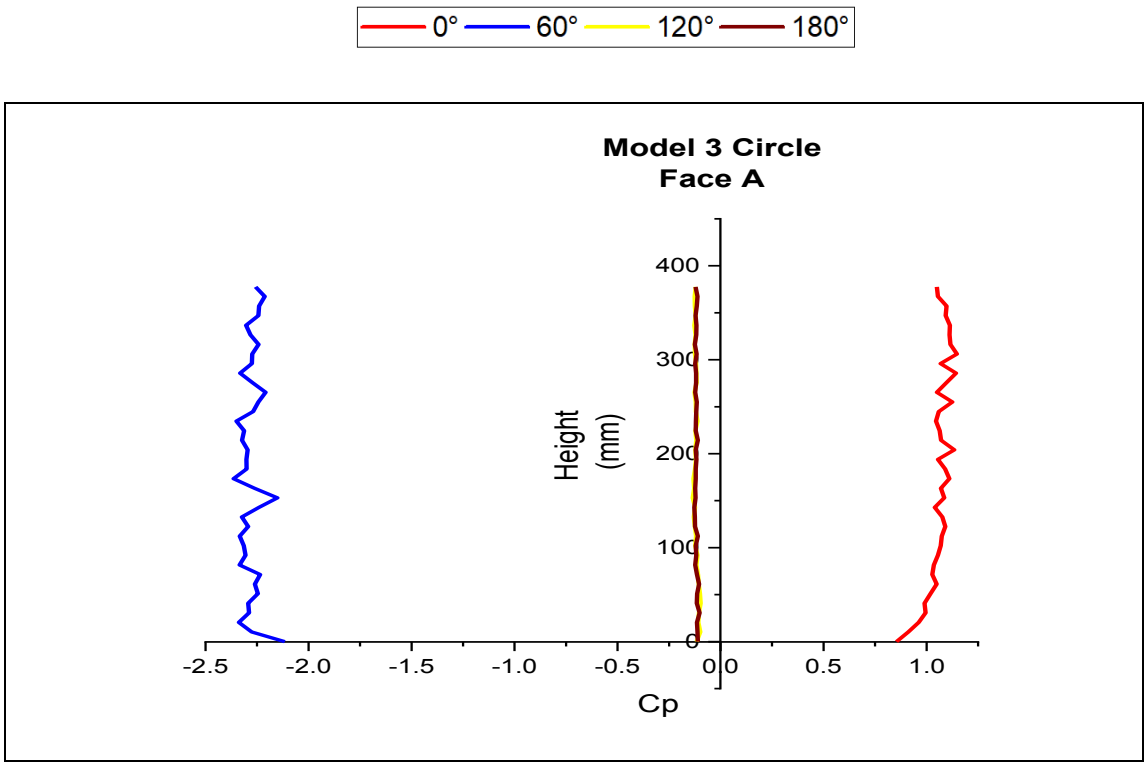

Figure 5-38 Pressure Variation along Centerline for face A for all degrees AOA of model 3

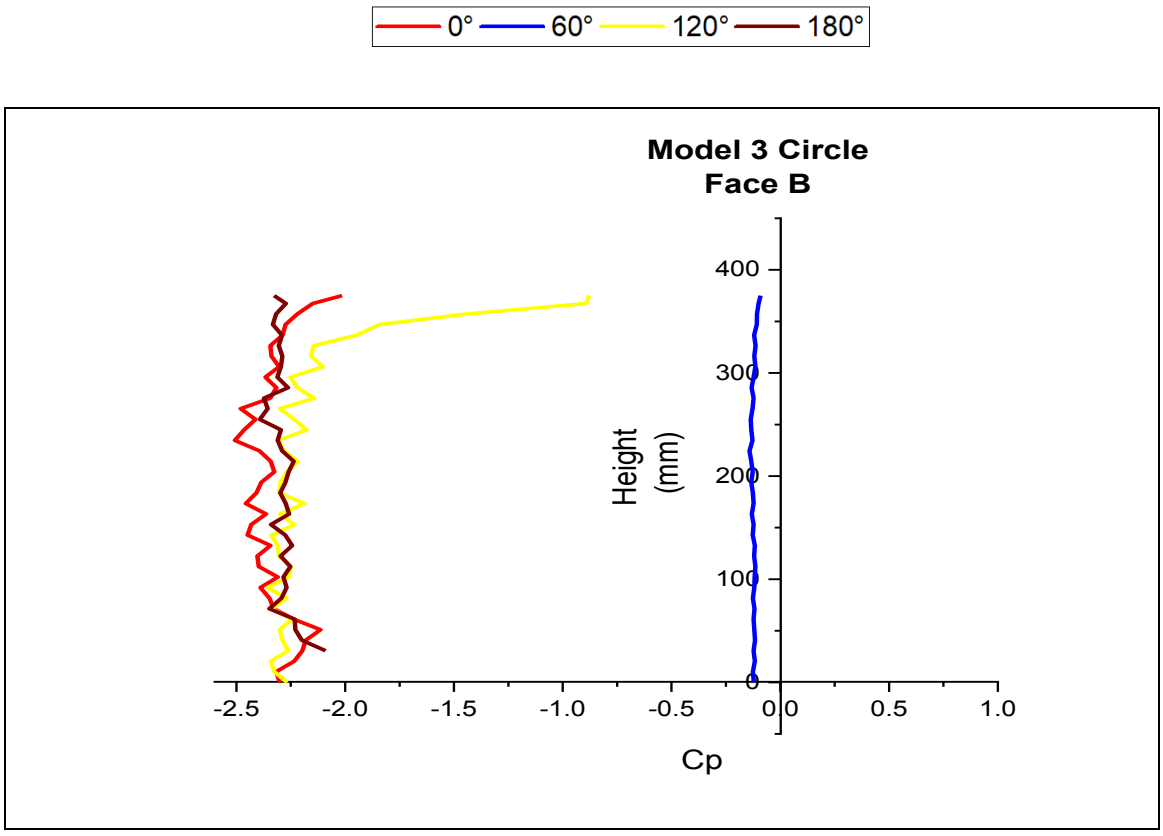

Figure 5-39 Pressure Variation along Centerline for face B for all degrees AOA of model 3

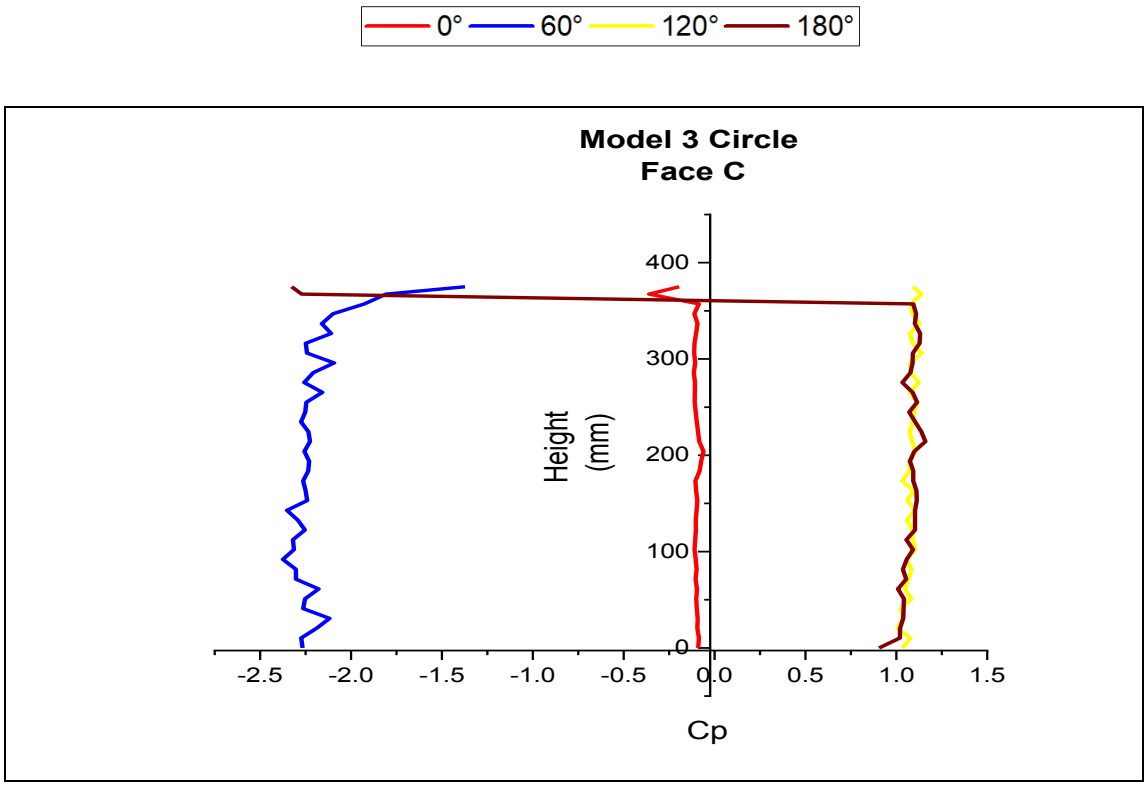

Figure 5-40 Pressure Variation along Centerline for face B for all degrees AOA of model 3

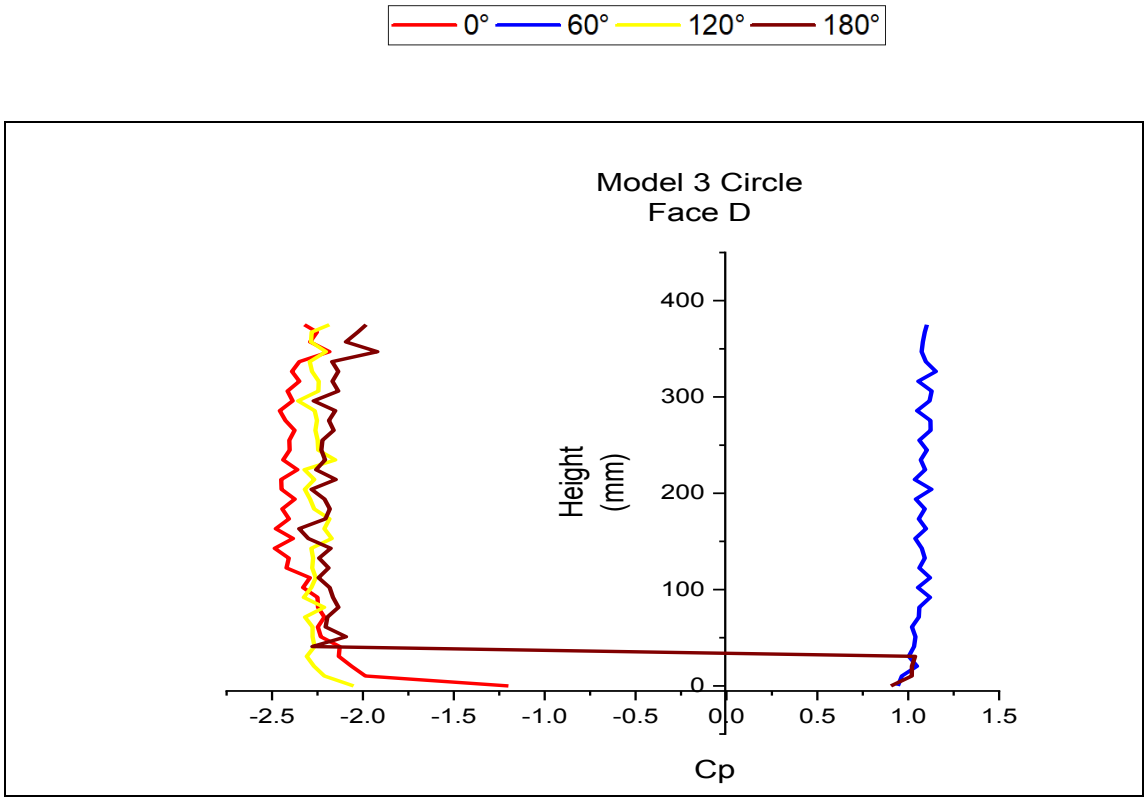

Figure 5-41 Pressure Variation along Centerline for face B for all degrees AOA of model 3

MODEL 4 (500 TRIANGLE)

- The Cp Variation along the centerline for all the faces at different angle of incidences are depicted in fig 5-42 to 5-44.
- For faces A of the triangular building the mean face average values of Cp at 0°,60°,120° and 180°angle of attack are +.80, -0.31, -0.32, and +0.81 respectively.
- For faces B of the triangular building the mean face average values of Cp at 0°,60°,120° and 180°angle of attack are -.25, -.23, -.22, and -.30 respectively.
- For faces C of the triangular building the mean face average values of Cp at 0°,60°,120° and 180°angle of attack are -.30, +0.91, +.80, and -0.20 respectively.

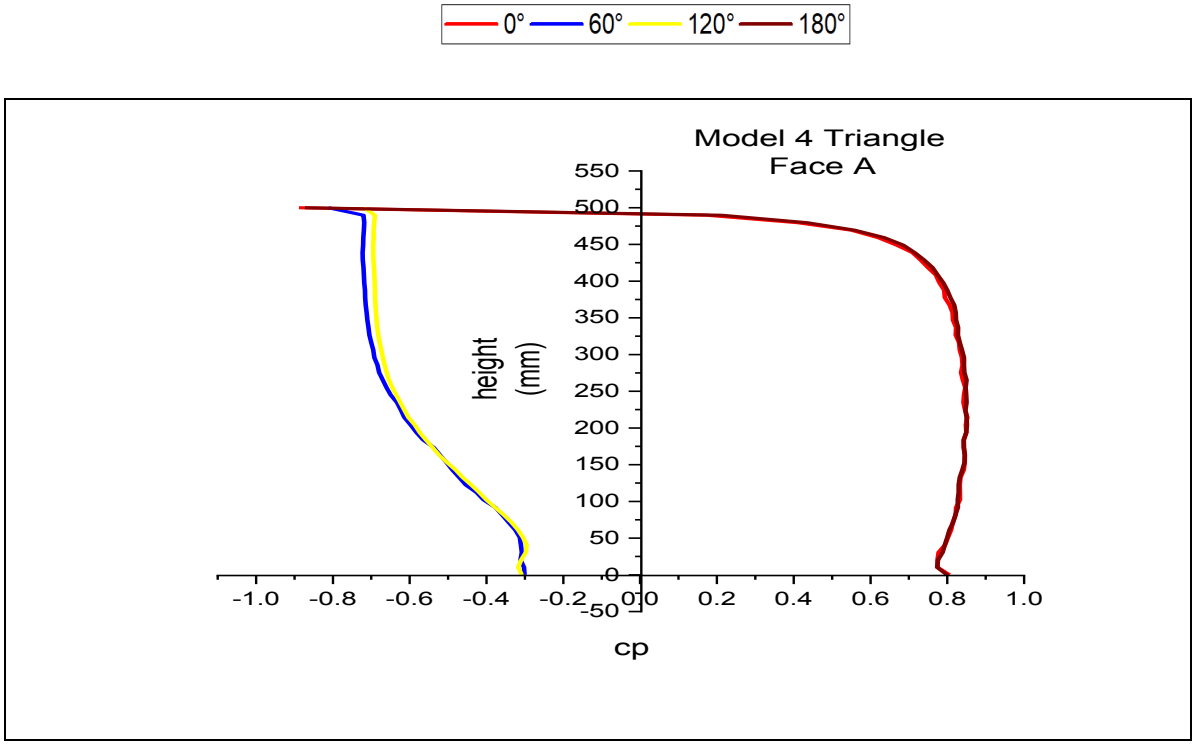

Figure 5-42 Pressure Variation along Centerline for face A for all degrees AOA of model 4

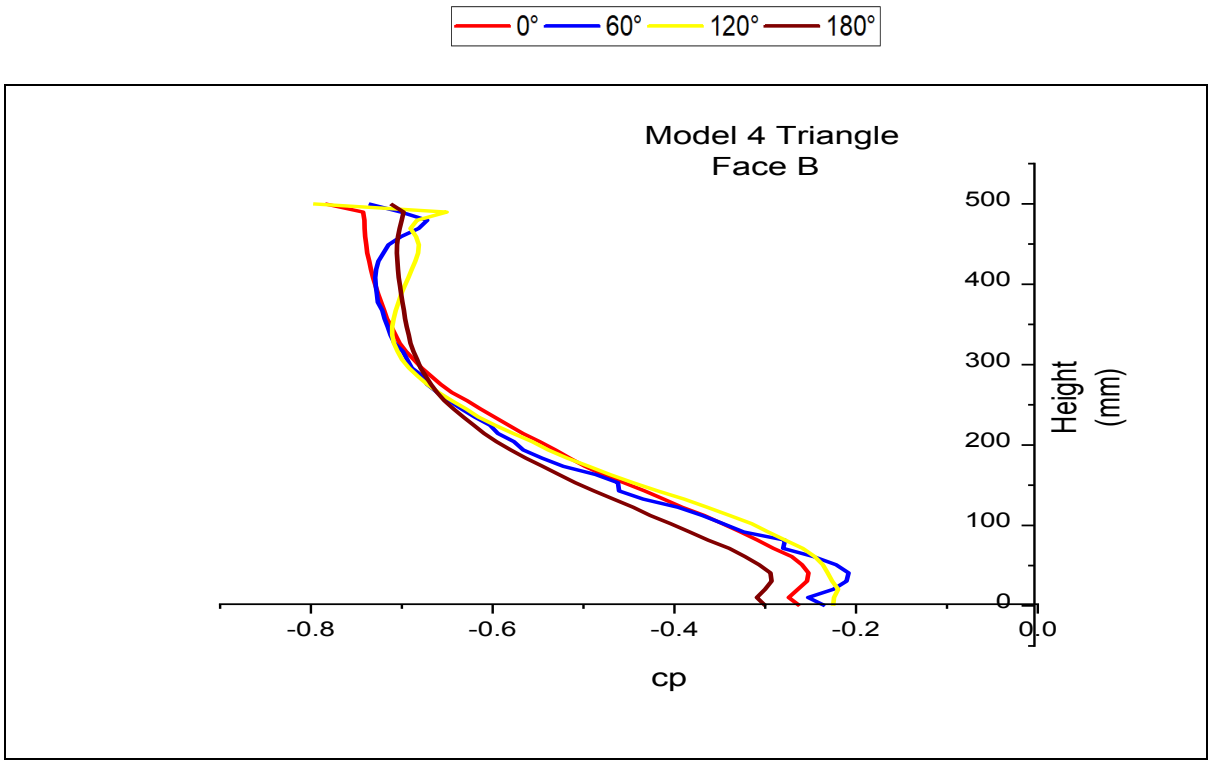

Figure 5-43 Pressure Variation along Centerline for face B for all degrees AOA of model 4

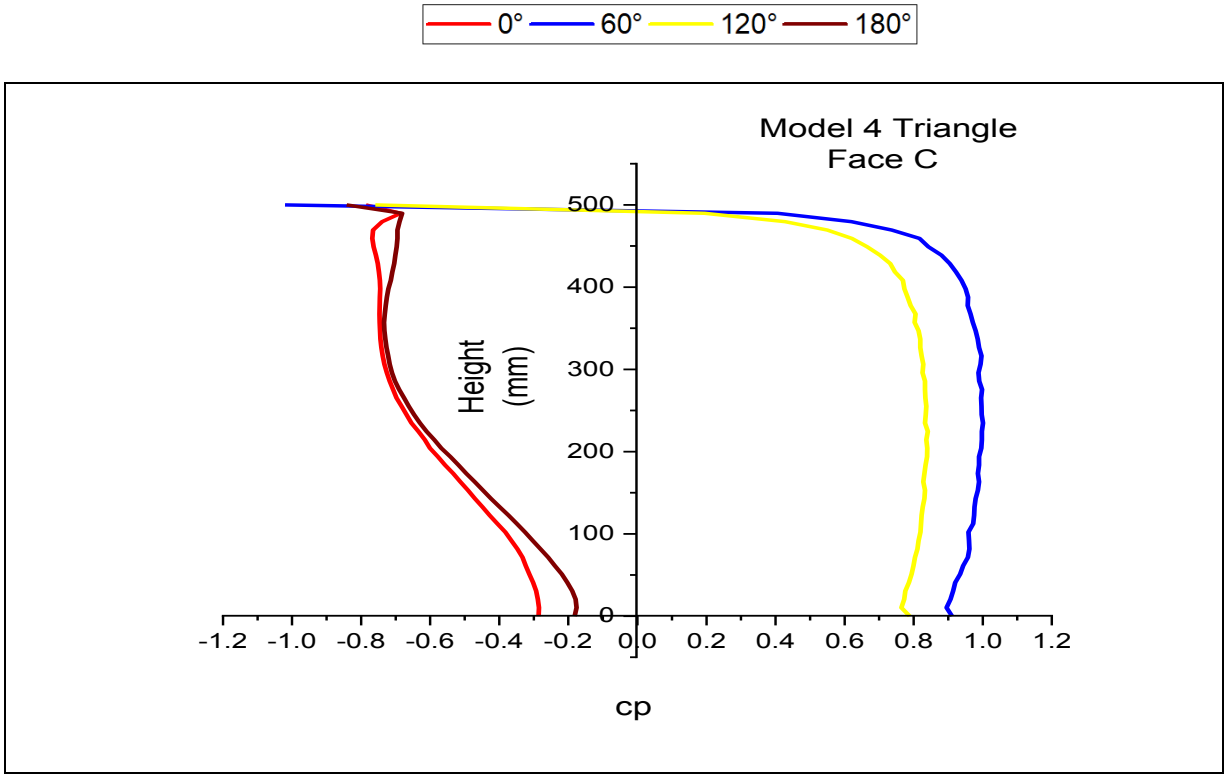

Figure 5-44 Pressure Variation along Centerline for face C for all degrees AOA of model 4

5.4 Pressure Coefficient

Model-1 375 Triangle	0°	+0.75	-0.38	-0.35
	60°	+0.20	-0.40	+.90
	120°	-0.30	-0.55	+0.82
	180°	-0.15	-0.28	-0.50
Model-2 250 Triangle	0°	+0.78	-0.78	-0.48
	60°	-0.10	-0.74	+0.90
	120°	-0.20	-0.80	+0.82
	180°	-0.40	-0.72	-0.49
Model-3 125 Triangle	0°	+0.78	-0.62	-0.48
	60°	+0.20	-0.68	+0.90
	120°	-0.23	-0.65	+0.80
	180°	-0.10	-0.69	-0.49
Model-4 500 Triangle	0°	+0.80	-0.25	-0.30
	60°	-0.31	-0.23	+0.91
	120°	-0.32	-0.22	+0.80
	180°	+0.81	-0.30	-0.20

Table 5-1 Cp for different faces for different triangular models at different angle of incidence

Building model	Angle of attack	Face A	Face B	Face C	Face D
Model-1 125 Circle	0°	+0.65	-1.80	-0.25	-2.0
	60°	-0.28	-0.28	-0.22	-0.90
	120°	-0.38	-2.30	+0.82	-2.2
	180°	-0.39	-2.40	+0.80	-2.3
Model-2 250 Circle	0°	+1.20	-2.30	-0.22	-2.50
	60°	-2.30	-0.20	-2.25	+1.0
	120°	-0.30	-2.20	+1.20	-2.0
	180°	-0.20	-2.40	+0.80	-2.25
Model-3 375 Circle	0°	+0.80	-2.30	-0.10	-1.25
	60°	-2.20	-0.15	-2.25	+0.90
	120°	-0.20	-2.20	+1.10	-2.0
	180°	-0.25	-2.0	+0.80	+0.89

Table 5-2 Cp for different faces for different circular models at different angle of inside

CHAPTER 6

CONCLUSION

The For the triangular and circular-shape buildings, the pressure contour and mean pressure coefficients models for different height ratios at 0^0 ,60^0 ,120^0 and 180^0 wind incidence angles are compared in this paper. The *k*-ε model is used to simulate the results.

The accuracy of numerical models for predicting along wind components was demonstrated in this study. The results of this research have led to a better knowledge of the aerodynamic and response properties of tall buildings with varying wind incidence angles. The computational fluid dynamics simulations in the numerical model have been shown to agree with the experimental results. On the windward face, sidewalls, and leeward face, the findings are more consistent. To obtain more convergent findings, several changes to the fluid domain and meshing must be made in models. In computer simulations, the k-e turbulence model has performed admirably. This research implies that numerical simulations for more sophisticated wind simulations can be trusted.

The major finding of this research are as follows:

- The influence of height ratios and wind orientations on wind pressure distribution and magnitude of pressure coefficients on triangular and circular building models is identified by numerical study measurement of wind pressures on building models.
- The fluctuation of pressure coefficients on the centerline is addressed and graphically displayed.
- Model height ratio has a significant impact on the amplitude and distribution of wind pressure on windward, leeward and sidewalls, of the building at different wind incidence angles.
- Changes in height ratio have little effect on the general magnitude of peak pressures and peak suctions in models with constant cross section.
- Comparison is made for numerical simulation data with various codes.

7 References

1) Nagar, S., & Ritu Raj. (2020). Experimental study of wind-induced pressures on tall buildings of different shapes. *Wind and Structures, Vol. 31, No. 5 (2020) 441-453*.
2) Ahuja, J. A. (n.d.). Effects of Side Ratio on Wind-Induced Pressure Distribution on Rectangular Buildings.
3) bailey, k. a. (1987-88). Effects of Aerodynamic Modifications of Building Shapes on Wind Induced Response of Tall Buildings.
4) Bairagi, A. M. (n.d.). Wind pressure and velocity pattern around 'N' plan shape tall building.
5) Dalui1, N. A. (n.d.). Aerodynamic analysis of pentagon-shaped tall buildings.
6) Dalui2, B. B. (n.d.). Experimental and Numerical Study of Wind-Pressure Distribution on Irregular-Plan-Shaped Building.
7) Dalui2, P. S. (n.d.). Comparison of aerodynamic coefficients of various types of Y-plan-shaped tall buildings.
8) Franke, J., & Hirsch, C. (n.d.). Recommendations on the use of CFD in wind engineering.
9) Kastner, P., & Dogan, T. (2020). Streamlining meshing methodologies for annual urban CFD simulations. *Journal of Energy and Buildings*.
10) M. Mallick, A. M. (n.d.). Modelling of Wind Pressure Coefficients on C-Shaped Building Models.
11) On the domain size for the steady-state CFD modelling of a tall building . (n.d.).
12) Pal, S., & Ritu Raj. (2021). Comparative study of wind induced mutual interference effects on square and fish-plan shape tall buildings. *Elsivier*.
13) Q.S. Li, J.Y. Fu, & Y.Q. Xiao. (n.d.). Wind tunnel and full-scale study of wind effects on China's tallest building.
14) R. Sheng a, b. L. (n.d.). Wind tunnel study of wind effects on a high-rise building at a scale of 1:300.
15) R. Sheng, L. Perret, & I. Calmet. (n.d.). Wind tunnel study of wind effects on a high-rise building at a scale of 1:300.

16) Suresh K Nagar1a, R. R. (n.d.). Experimental study of wind-induced pressures on tall buildings of different shapes.
17) R. Ahlawat and A. Ahuja, "Wind Loads on T Shape Tall Buildings," *J. Acad. Ind. Res.*, vol. 24, no. 1, p. 257922, 2015.
18) R. Ahlawat and A. K. Ahuja, "Wind loads on Y plan shape tall building," *Int. J. Eng. Appl. Sci.*, vol. 2, no. 4, p. 257946, 2015.
19) IS: 875 (2015), *Indian Standard design loads (other than earthquake) for buildings and structures-code of practice,part 3(wind loads)*. 2015.
20) ASCE: 7-10(2013), *Minimum Design Loads for Buildings and Other Structures. Structural Engineering Institute of the American Society of Civil Engineering, Reston*. 2013.
21) GB 50009-2001, *NATIONAL STANDARD OF THE PEOPLE'S REPUBLIC OF CHINA*. 2002.
22) AS/NZS:1170.2(2011), *Structural Design Actions - Part 2: Wind actions. Standards Australia/Standards New Zealand, Sydney*. 2011.
23) Hong Kong Building Department, "Code of Practice on Wind Effects in Hong Kong 2019," 2019.

LIST OF PUBLICATION

1. Srivastava, K. N., & Raj, R. (2022). Aerodynamic study of tall buildings under wind load. International Journal of Health Sciences, 6(S3), 2620–2641. https://doi.org/10.53730/ijhs.v6nS3.6142